1-1-1979

Seismic and electrical definition of sand-gravel deposits beneath clay in Essex county, Ontario.

Spiros Vergos
University of Windsor

SEISMIC AND ELECTRICAL DEFINITION OF SAND-GRAVEL DEPOSITS BENEATH CLAY IN ESSEX COUNTY, ONTARIO

by

Spiros Vergos

A Thesis
submitted to the Faculty of Graduate Studies through
the Department of Geology in Partial Fulfilment
of the requirements for the Degree of
Master of Science at the
University of Windsor

Windsor, Ontario, Canada
1979

DEDICATION

To my parents

Theodoros and Panayota Vergos

ACKNOWLEDGEMENTS

I gratefully acknowledge Dr. D.T.A. Symons for suggesting this topic of research and for his tireless reading of the thesis in manuscript. His invaluable assistance in drawing up the final draft of this thesis has been greatly appreciated. In addition I thank Dr. M. Stupavsky and Dr. M. Ballargeon for their assistance with the computer treatment of the data. I also thank Dr. D. Russel for his comments on this study.

Furthermore I express my sincere thanks to my wife Glenda who has been a constant source of encouragement through the writing of this thesis.

ABSTRACT

Sand and gravel exist in Essex County, Ontario, as para-glacial deposits beneath lake clay or glacial till. The geophysical exploration for these aggregates is becoming a necessity because of the high demand for them and of the near exhaustion of the existing supplies. Seismic velocities and electrical resistivities of clay, sand and gravel were measured at 50 sites in Essex County. The objective is to define possible relationships between these parameters.

Seismic velocities of gravel were not found to be significantly different from those of clay. Thus, the seismic refraction survey will not be an effective geophysical method in the exploration of gravel deposits in Essex County. Although the seismic velocities of sand are significantly different from those of clay, sand also cannot be routinely differentiated either because of the large dispersion in its seismic velocities.

The three sediments have significantly different electrical resistivities and relatively small dispersion in the electrical resistivities. This suggests that electrical resistivity survey would be an effective method in detecting gravel and sand deposits under the conditions existing in Essex County.

The combined analysis of the two methods does not improve the results obtained by the electrical resistivity method alone.

TABLE OF CONTENTS

ACKNOWLEDGEMENTS. v

ABSTRACT. vi

LIST OF APPENDICES. ix

LIST OF TABLES. x

LIST OF FIGURES xi

Chapter

I. INTRODUCTION. 1

1.1 Aim of the thesis. 2
1.2 Demand for sand and gravel deposits. 4
1.3 Geology. 10
1.3.i Bedrock. 10
1.3.ii Glacial geology of southwestern Ontario, Essex County. 11

II. GRAIN SIZE ANALYSIS 16

III. SEISMIC REFRACTION METHOD 20

3.1 Theory 20
3.2 Field work 23
3.2.i Instruments. 23
3.2.ii Field work 25
3.3 Data-Statistics. 26

IV. ELECTRICAL RESISTIVITY METHOD 32

4.1 Introduction 32
4.2 Previous work. 32
4.3 Theory 33
4.3.i Resistivity concept. 33
4.3.ii Concept of apparent resistivity. . . 36
4.4 Field work 37
4.4.i Electrode configuration. 37
4.4.ii Instrument used. 38
4.4.iii Galvanic voltage adjustment 38
4.5 Interpretation of the apparent resistivity results. 38
4.6 Data-Statistics. 41

V. INTEGRATED ANALYSIS 47

5.1 Introduction 47
5.2.i Seismic velocity vs grain size . . . 47

5.2.ii Discussion of the results. 52
5.3.i Resistivity vs grain size. 53
5.3.ii Discussion of the results. 57
5.4 Resistivity vs seismic velocity. . . . 61

VI. CONCLUSIONS 65

REFERENCES 67

APPENDIX I: Grain size analyses. 70

APPENDIX II: Seismic velocities 81

APPENDIX III: Apparent resistivities 114

APPENDIX IV: Derivation of equation (4.3.2) 131

APPENDIX V: Integrated analyses - Graphs 134

APPENDIX VI: Instruments used 168

LIST OF APPENDICES

APPENDIX I: Grain size analyses. 70

APPENDIX II: Seismic velocities 81

APPENDIX III: Apparent resistivities 114

APPENDIX IV: Derivation of equation (4.3.2) 131

APPENDIX V: Integrated analyses - Graphs 134

APPENDIX VI: Instruments used 168

LIST OF TABLES

		page
Table A.	List of the symbols used in the text.	xiii
Table 1.	Tonnage and $value of sand and gravel produced in Ontario.	9
Table 2.	Subdivisions of the Quaternary ice-age in southwestern Ontario	12
Table 3.	Grain size analyses results	18
Table 4.	Seismic velocities of all sites	30
Table 5.	Mean and deviation statistics for the seismic velocities.	31
Table 6.	Group correlation statistics for the seismic velocities.	31
Table 7.	Summary of the interpreted resistivity data.	45
Table 8.	Mean and deviation statistics for electrical resistivities.	46
Table 9.	Group correlation statistics for electrical resistivities.	46
Table 10.	Log ρ values for GRAVEL, SAND and CLAY. . . .	60
Table 11.	Grain size analyses for GRAVEL.	71
Table 12.	Grain size analyses for SAND.	72
Table 13.	Grain size analyses for CLAY.	73
Table 14.	Grain size plots included in Appendix I . . .	74
Table 15.	Measured travel-times and calculated seismic velocities for 26 sites	82
Table 16.	Seismic records included in Appendix II . . .	89
Table 17.	Apparent resistivity results.	115
Table 18.	Apparent resistivity. Plots included in Appendix III	122
Table 19.	Integrated analyses. Plots included in Appendix V	135

LIST OF FIGURES

		page
Figure 1.	Essex County, reference map.	5
Figure 1a.	Sample sites near Windsor.	6
Figure 1b.	Sample sites near Leamington	7
Figure 2.	Mineral aggregate utilization pattern for Ontario.	9
Figure 3.	Ice-front position at the times of Lake Whittlesey and Lake Warren	14
Figure 4.	Particle size distribution for five samples	19
Figure 5.	Ray paths of least time for two layers . . .	21
Figure 6.	Time-distance curve for two layers	21
Figure 7.	Typical record from the FS-3	24
Figure 8.	Histograms for the seismic velocities. . . .	27
Figure 9.	Generalized electrode configuration.	35
Figure 10.	Electrode arrangement for the Wenner configuration.	35
Figure 11.	Various multilayer profiles for ρ_a	40
Figure 12.	Example of apparent resistivity interpretation	40
Figure 13.	Histograms for the electrical resistivities.	43
Figure 14.	% Sand vs Velocity plot for all samples. . .	49
Figure 15.	% Sand vs log V plot for all samples	50
Figure 16.	% Gravel vs Velocity plot for SAND and GRAVEL	51
Figure 17.	% Clay vs log V plot for the CLAY group. . .	54
Figure 18.	% Gravel vs log ρ plot for SAND and GRAVEL	55

Figure 19. Regression line, second- and third-degree polynomials for % Gravel and log ρ 56

Figure 20. % Sand vs log ρ for all samples 58

Figure 21. Intervals for log ρ values. 59

Figure 22. Log ρ vs log V plot for all samples 62

Figure 23. Boundary limits of log V, log ρ for GRAVEL, SAND and CLAY 63

Figure 24. (24.1-24.6). Grain size vs cumulative percentage. 75

Figure 25. (25.1-25.24). FS-3 seismic records 90

Figure 26. (26.1-26.7). Interpretation of apparent resistivity data 123

Figure 27. Current lines from a point current source. 132

Figure 28. (28.1-28.32). Integrated analysies 136

Figure 29a. FS-3 seismograph. 169

Figure 29b. Resistivity instrument. 170

TABLE A

List of the symbols used in the text

α	electrode separation for Wenner "spread" in m
c	correlation coefficient
D.F.	degrees of freedom
F	the F-statistic
F(r's)	Roman's form factor
i	angle of incidence of a seismic wave
i_c	critical angle
I	electrical current in milliamperes
l	length in m
m	meter(s)
π	3.14
P	the two-tail significance level
r	electrode separation in m
r'	angle of refraction
ρ	resistivity in ohm-m
ρ_α	apparent resistivity in ohm-m
R	resistance in ohm
S	cross-sectional area in m^2
T	arrival time of a seismic wave
T_i	intercept time of a seismic wave
T	the T-separate statistic
V	velocity in m/sec of a seismic pulse
V	voltage in millivolts
X	shot-point - geophone distance in m
X_c	critical distance in m
Z	depth to an interface from surface in m

CHAPTER I

INTRODUCTION

Sand and gravel are important industrial resources produced in Ontario. They are used as aggregate in various types of construction together with crushed stone. New deposits are in demand because large amounts of sand and gravel are used every year, and economical deposits are being rapidly depleted.

In Essex County sand and gravel deposits are located mainly near Leamington. They are associated with the Essex moraine which was deposited during the retreat of the ice which covered the area in the Pleistocene Epoch. The sand and gravel are deposited on the sides and shoulders of the moraine by the lakes which covered Essex County after the retreat of the ice. These lakes also left shallow lacustrine clay overlying the sand and gravel deposits.

Generally the different elastic and electrical properties of clays, sands and gravels may be used to differentiate between these sediments. The objective of this study is to look for possible contrasts in seismic velocities and electrical resistivities between the clays, sands and gravels in Essex County. If favourable contrasts do exist they might be used in geophysical exploration for new sand and gravel deposits.

Seismic velocities and electrical resistivities were measured at 50 sites in Essex County over a wide range of

physical conditions of the specific sediment. Various statistical and regression computer programs were used in the search of possible relationships between the type of sediment and its seismic velocity and electrical resistivity.

1.1 Aim of the thesis

It is generally believed that the seismic velocities of clays are higher than the seismic velocities of sands and gravels. It is also believed, and justified from theory and experience, that the electrical properties of the minerals forming clays are significantly different than those of the minerals forming sands and gravels. However unexpected changes in composition or compaction might produce unexpected geophysical properties in a particular sediment.

When sand gravel deposits exist in Essex County, they usually occur beneath 1 to 3m of clay and overlie older till. The seismic velocities and the electrical resistivities of sands, gravels and clays were measured in this study to see whether or not they can be used to differentiate the above sediments.

Because the seismic velocities of the overlying clays are usually greater than those of sand and/or gravel, the latter constitutes a hidden layer using the seismic refraction method. For a given sequence of layers, a hidden layer (or low-speed layer (Dobrin, 1976)

or hidden-zone (Telford, 1977)) is defined as one that has a lower seismic velocity than the one above it. Such a bed in the sequence "will not be detectable by refraction shooting at all" (Dobrin, 1976). This is a different situation from a "blind zone" where the second layer also does not appear on the seismic record. A blind zone is a layer which is very thin and, although it has greater seismic velocity than the one above it, it is not detectable because other seismic events such as refracted waves from deeper layer interfaces mask the refracted waves from the "blind zone". This distinction between a "hidden layer" and a "blind zone" is necessary because some writers (Green, 1962 ; Griffiths, 1975 ; Hawkins, 1960 ; Morgan, 1966 ; Soske, 1959) interchange their definition.

When the seismic refraction method is used, sand or gravel hidden layers do not appear on the time-distance seismic record. The theoretical explanation will be given in chapter 3.1.

When the seismic reflection method is used only the lower interface of sand and gravel layer may give a reflection on the seismic record. When there is little or no impedance contrast between two layers, then very little or no reflected energy will return from the lower interface.

In general sands and gravels are poor electrical conductors because they are usually high in quartz content

and lack soluble salts. Clays on the other hand are much better electrical conductors because they usually contain abundant soluble salts. Thus conductivity, or its reciprocal resistivity, can also be used to differentiate sands and gravels from clays.

Fifty sites were selected (Fig. 1, 1a, 1b) at which seismic velocities and electrical resistivities were measured. A representative sample was also taken to be used for grain size analysis. The selected sites exhibited a wide range of physical conditions from "moist" to "dry" conditions. Such conditions were chosen to give a characteristic representation of the sediment response to seismic velocities and electrical resistivities as they might be encountered in the geophysical exploration for sand and gravel deposits.

The seismic velocities, electrical resistivities and grain size results were subjected to various statistical tests in an attempt to define any existing quantitative relationships.

1.2 Demand for sand and gravel deposits

The construction and paving industries are the principal consumers of sand and gravel. They require increasing tonnages of these two types of mineral aggregate each year for various types of construction in Ontario as shown in Fig. 2. Typical uses include portland-concrete aggregate, paving, highways, dams, airport runways, piers,

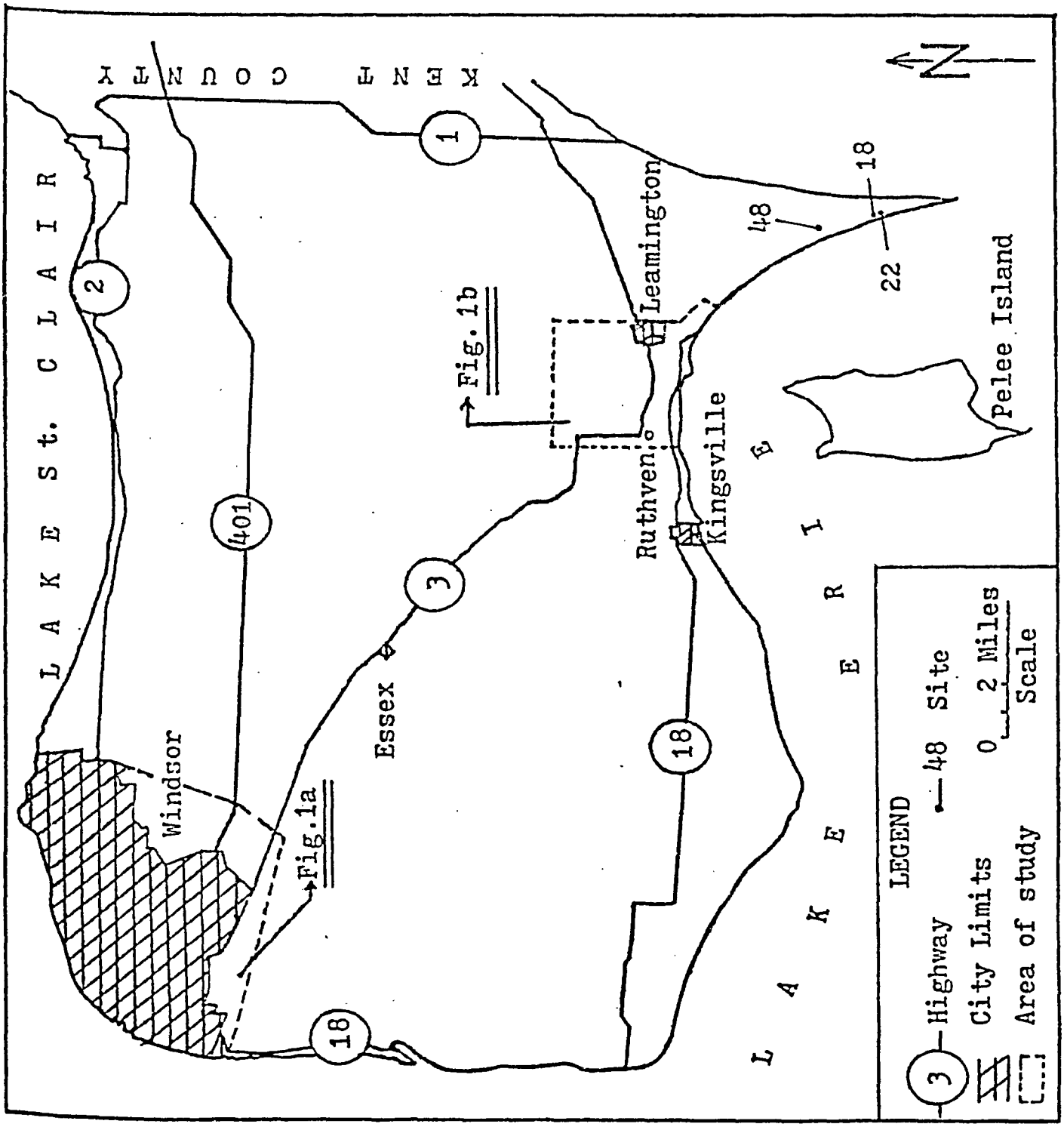

Fig. 1. Essex County reference map.

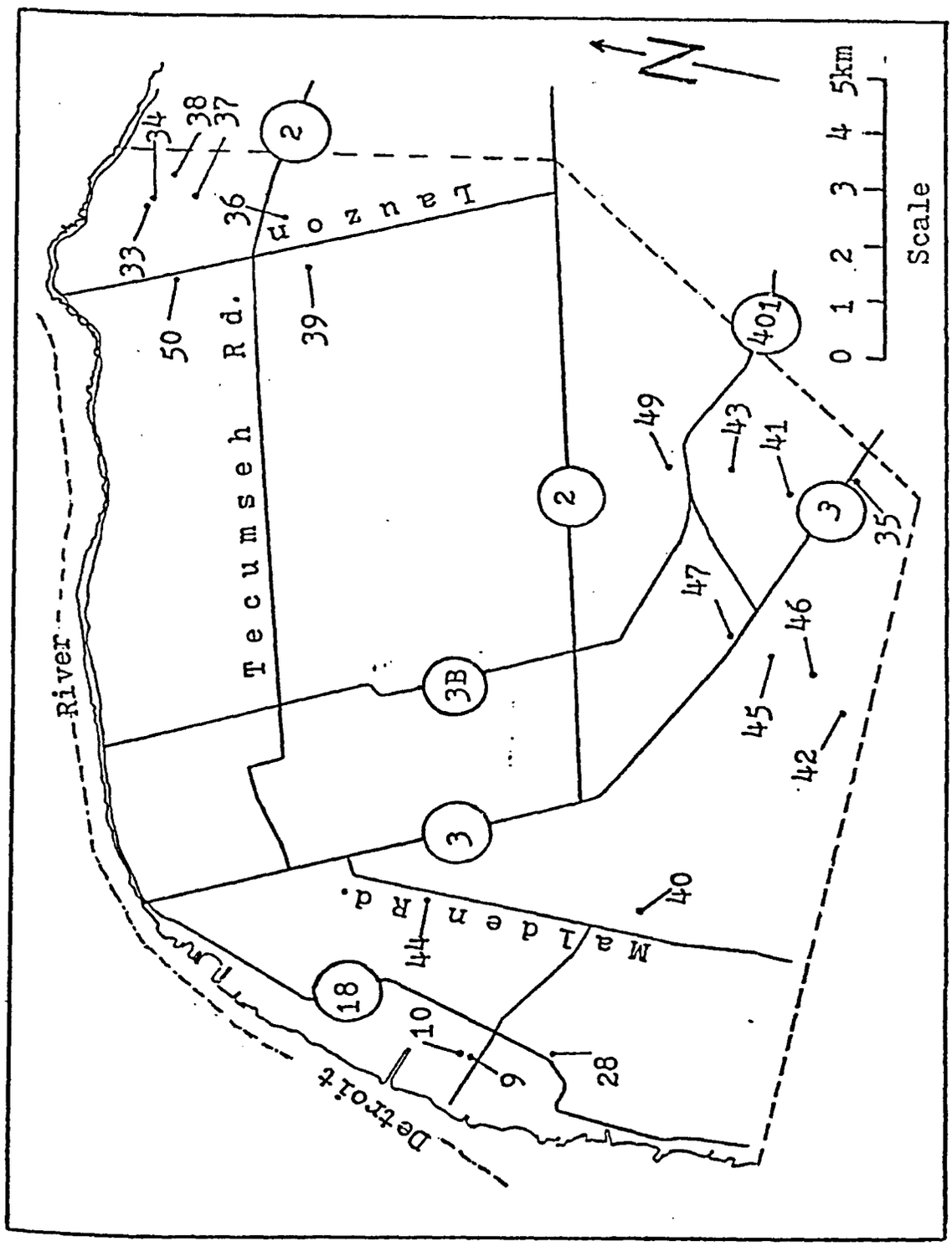

Fig. 1a. Sample sites in Windsor. Legend as in Fig. 1.

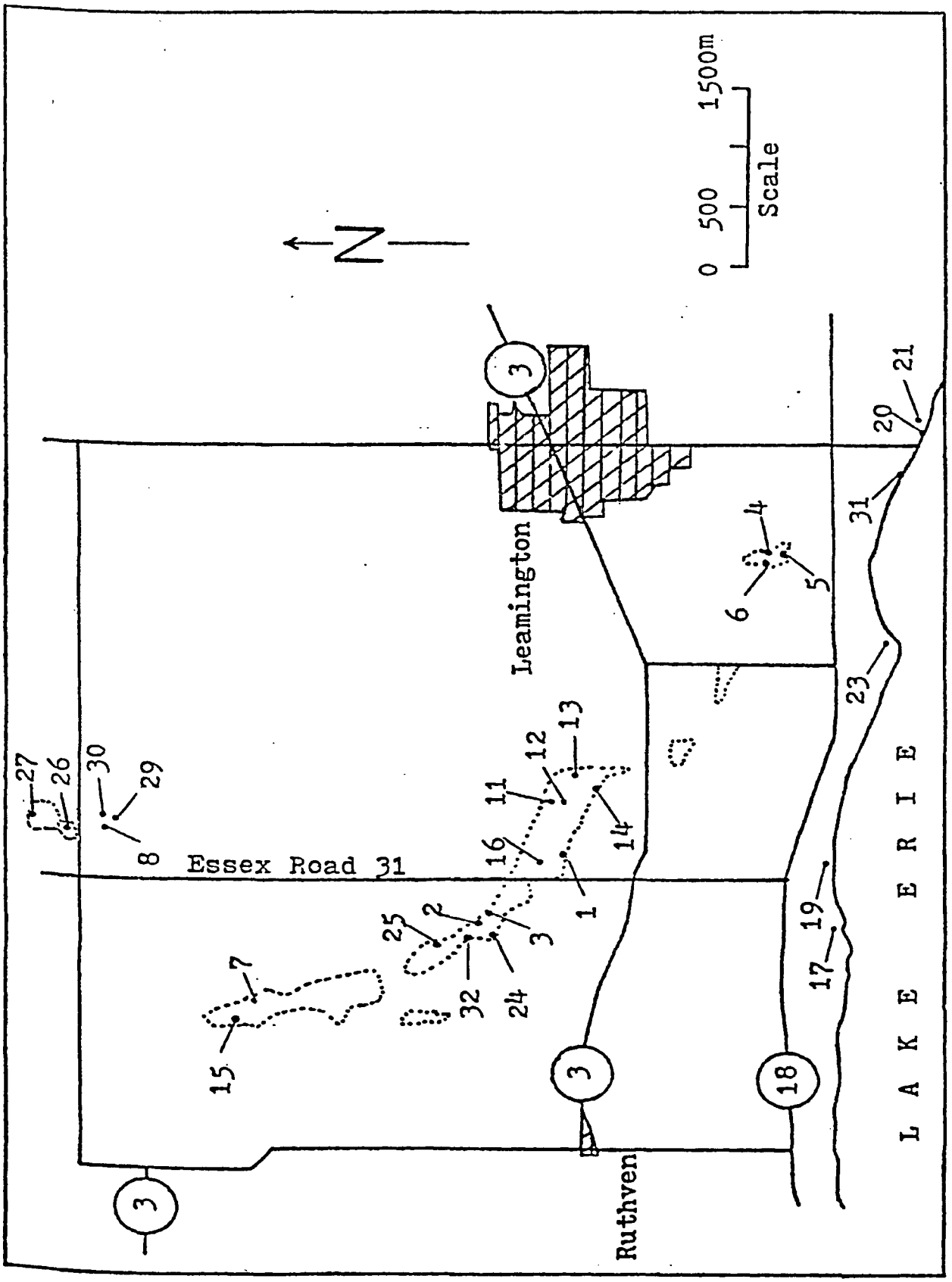

Fig. 1b. Sample sites near Leamington. Dotted lines outline sand and gravel pit boundaries. Legend as in Fig. 1.

house foundations, buildings and sewers. In the years 1974-1977, for example, sand and gravel rank second after cement among Ontario industrial mineral products (Table 1). 70.3×10^6 tons of sand and gravel were produced in Ontario with a value of 112×10^6 dollars. Thus they are of great economic importance. Demand for sand and gravel is expected to increase annually with a 55% increase projected by the year 2000 (Proctor and Redfern Ltd, 1975).

The production statistics represent an over-all picture for Ontario. However the distribution of sand and gravel deposits is not uniform. In most counties the supply is less than the demand. Thus sand and gravel is moved from one county to another or even imported from the United States of America. In either case their cost to the consumer increases.

For Essex County the total possible reserves for sand and gravel were estimated at only 253.3×10^6 tons in 1975 (Proctor and Redfern Ltd., 1975). Most of these reserves are in the southeast corner of the county near Leamington. Hence sand and gravel must be trucked about 50km to Windsor which is the most significant market in the county. Alternatively Windsor consumers use crushed aggregate from quarries around Amherstburg which are about 20km away. Aggregate reserves stood at about $3,058 \times 10^6$ tons in 1975. Finally sand and gravel or aggregate may be imported into Windsor from the United States of America. In 1975, for

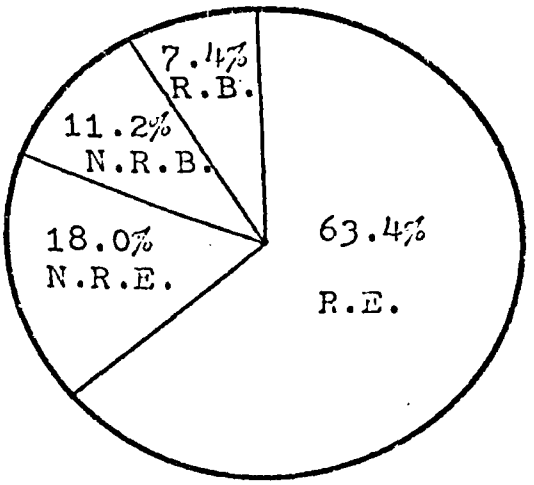

R.B.=Residential Building.
N.R.B.=Non-residential Building.
R.E.=Road Engineering.
N.R.E.=Non-road Engineering.

Fig. 2. Mineral aggregate utilization pattern for Ontario's 1971 total of 77,631,000 tons after Proctor and Redfern Ltd (1975).

Year	Tons	$ Value
1974	79,712,838	85,104,576
1975	69,705,434	95,578,927
1976	68,802,045	106,093,326
1977	70,306,817	112,400,000

Table 1. Tonnage and $ Value of sand and gravel produced in Ontario.

example, about 493,000 tons were imported with a value of $1.80 to $2.50 per ton. This compares to $0.73 per ton at the source near Leamington and Amherstburg.

Although the importance of discovering new deposits in Ontario is not questioned, "no individual deposit is necessarily mined just because it exists" (Ontario Dept. of Mines, 1975). Sterilization of large deposits has resulted because of zoning restrictions in urban areas or of development of the land for other purposes. The environmental costs must be traded off against the cost of moving sand and gravel especially by trucks. Trucking costs were at about $0.12/ton mile in Ontario in 1975 (Ontario Dept. of Mines, 1975).

1.3 Geology

1.3.i Bedrock in Essex County

The basement in Essex County is composed of Precambrian rocks of the Grenville geologic province. Overlying the basement are four flat lying Paleozoic Devonian formations: 1) the Detroit River formation composed of brown to buff limestone, dolomite and sandstone; 2) the Columbus formation composed of grey to buff sandy limestone and dolomite; 3) the Delaware formation composed of brown to buff limestone with some chert; and 4) the Hamilton formation composed of grey shale and argillaceous limestone (Geological Survey of Canada, 1958). These sediments are covered by about 30m of Quaternary drift except near Amherstburg

where the Devonian sediments come to the surface.

1.3.ii. Glacial Geology of Southwestern Ontario-Essex County

All of the known sand and gravel deposits in southwestern Ontario are associated with the Pleistocene Epoch. During this epoch large ice-sheets advanced and retreated over the area several times. The main sources for sand and gravel deposits are the resulting moraines and eskers although some spillways and kames have also produced quite large deposits.

The glacial history and deposits of southwestern Ontario have been described in detail by Chapman (1969), Hewitt (1963) and Taylor (1913). A summary of the events affecting the formation of these sand and gravel deposits follows.

There were four major cold glacial stages in the Pleistocene Epoch during which the ice advanced (Hewitt, 1963). The intervals between the ice advances were characterized by interglacial stages that were as warm or even warmer than the present climate. These subdivisions of the Quaternary ice age are shown in Table 2. Economic pre-Wisconsinan sand and gravel deposits are very rare in Ontario and "they can be disregarded when describing the surface features" (Chapman, 1969).

C^{14} dating studies on plant remains (Goldthwait, 1973) have established that the Wisconsin ice-sheet had

PERIOD	EPOCH	GLACIAL STAGES	INTERGLACIAL STAGES
QUATERNARY	HOLOCENE		Recent
	PLEISTOCENE	Wisconsinan	
			Sangamonian
		Illinoian	
			Yarmouthian
		Kansan	
			Aftonian
		Nebraskan	

Table 2. Subdivisions of the Quaternary ice age in southwestern Ontario.

covered all of southern Ontario by 20,000 years ago. This area remained under the ice until about 14,000 years ago. With the subsequent retreat of the ice, large meltwater streams left sand and gravel in deposits such as the Waterloo kame accumulation and the Orangeville moraine. The ice melted progressively to the north.

One of the recessional moraines left during the retreat was Essex moraine. This moraine was first described by Taylor (1913) as "extending from Detroit southwestward through Essex to the high knoll west of Leamington, and being a low broad ridge of till, very smooth and with such gentle slopes as to be quite inconspicuous to the eye as a ridge".

By about 13,000 years ago Lake Whittlesey covered all of southwestern Ontario (Fig. 3). This lake left a prominent shoreline in southwestern Ontario which is preserved as beach deposits lagging around the Essex moraine. These deposits have been sources for sand and gravel such as the Erie Sand and Gravel deposit (e.g. sites 1, 11, 12, 13, 14, 16 in Fig. 1b). Most of Essex County was under water during the life of this lake.

The next prominent lake was Lake Warren which also covered most of southwestern Ontario (Fig. 4). It also left sand and gravel beach deposits on the shoulders of the Essex moraine such as the deposit operated by Kennette Co. lot 1 concession IV, Mersea township, Essex (e.g.

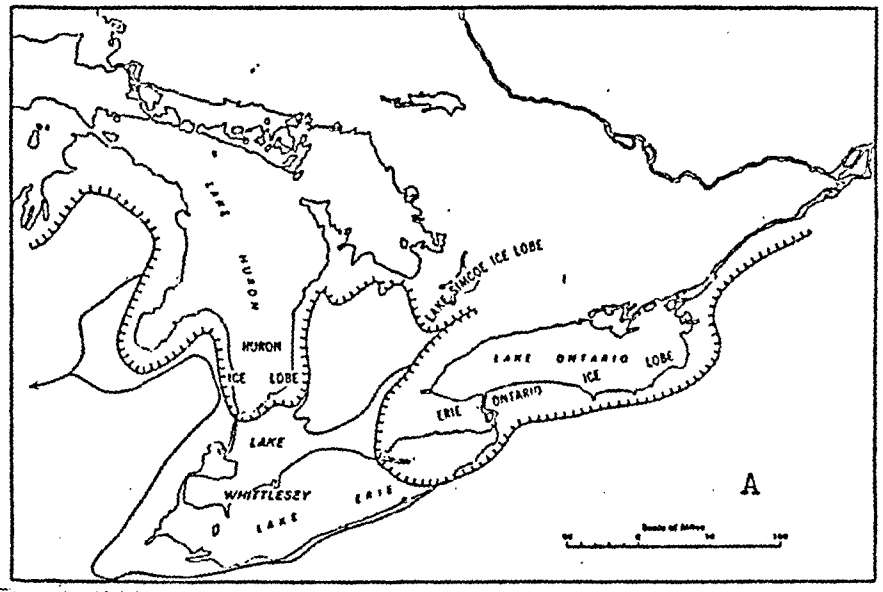

Fig. 3. Ice-front position at the time of :
A) Lake Whittlesey, and B) Lake Warren;
after Hewitt (1963).

sites 2, 24, 25, 32).

Leverett and Taylor (1915) have recognized one more successor lake in the County, namely Lake Grassmere, at about 15m lower altitude. They consider the gravel bar on the crest of the moraine to be "a Grassmere storm beach".

All of these lakes left beach deposits around the sides and the shoulders of the Essex moraine. Thus the moraine is bounded by sand and gravel except at its highest point just north of Ruthven where it is composed entirely of till.

The Essex till plain (Chapman, 1969) was deposited under the ice. Lake Whittlesey and Lake Warren failed to leave any deep stratified beds on the till plain (Chapman, 1969). The plain was smoothed by shallow deposits of lacustrine clay from the lakes which settled in the depressions while the knolls were being lowered by wave action.

CHAPTER II

GRAIN SIZE ANALYSIS

At each site a 2 to 3kg sample was taken at a depth of about 0.4m below the surface. A representative subsample of 600-700g was then split from it using the quartering method. This subsample was used for the grain size analysis. The cumulative percentage of gravel, sand and clay were then calculated.

The Wentworth classification was used to define the percentage of sand, gravel and clay contained in the samples because it is "the classification commonly accepted by geologists" (Bates, 1969). Thus the dividing line between sand and gravel was set at the 2mm diameter sieve size and between sand and clay at the 0.074mm diameter sieve size, i.e. #10 and #200 in the U.S. Sieve series respectively. It must be noted though that different limiting diameters are often assigned to sand and gravel by highway departments, engineering organizations and various other government agencies.

The first 32 samples of Table 3 contain less than 1% silt or clay and so were divided into two groups. The GRAVEL group includes samples with ≥50% of the particles of ≥2mm size while the SAND group includes samples with >50% of the particles between 2mm and 0.074 mm in size. In Table 3 the numerical values of the "% gravel" and "% sand" have been rounded off to the closest integer ex-

cluding the <1% clay.

The remaining 18 samples consist of silt and clay with >50% of the particles finer than 0.074mm. These samples form the CLAY group. The field term CLAY is used for the silt and clay fraction that overlies the sand and gravel deposits in Essex County. The exact percentages of silt (between 0.074mm to 0.005mm) and clay (less than 0.005 mm) varies from 60-100% with sand constituting the remaining 40-0%. The clay fraction of similar deposits in the Windsor area varies from 20-80% with an average value of about 40% (Wilkinson, 1978).

The results of the grain size analyses are shown in weight percentages on Table 3. Fig. 4 shows a graphical representation of particle size plotted against cumulative percentage for five typical samples.

GRAVEL			SAND			CLAY		
Site #	% gravel	% sand	Site #	% sand	% gravel	Site #	% clay	% sand
1	52	48	16	99	1	33	85	15
2	62	38	17	78	22	34	78	22
3	60	40	18	82	18	35	68	32
4	52	48	19	98	2	36	66	34
5	56	44	20	98	2	37	68	32
6	56	44	21	99	1	38	68	32
7	56	44	22	70	30	39	79	21
8	56	44	23	88	12	40	84	16
9	52	48	24	97	3	41	62	38
10	50	50	25	84	16	42	61	39
11	52	48	26	68	32	43	66	34
12	66	34	27	82	18	44	61	39
13	70	30	28	99	1	45	73	27
14	68	32	29	97	3	46	75	25
15	62	38	30	95	5	47	90	10
			31	99	1	48	92	8
			32	95	5	49	79	21
						50	63	37

Table 3. Grain-size analyses for samples from 50 sites in Essex County.

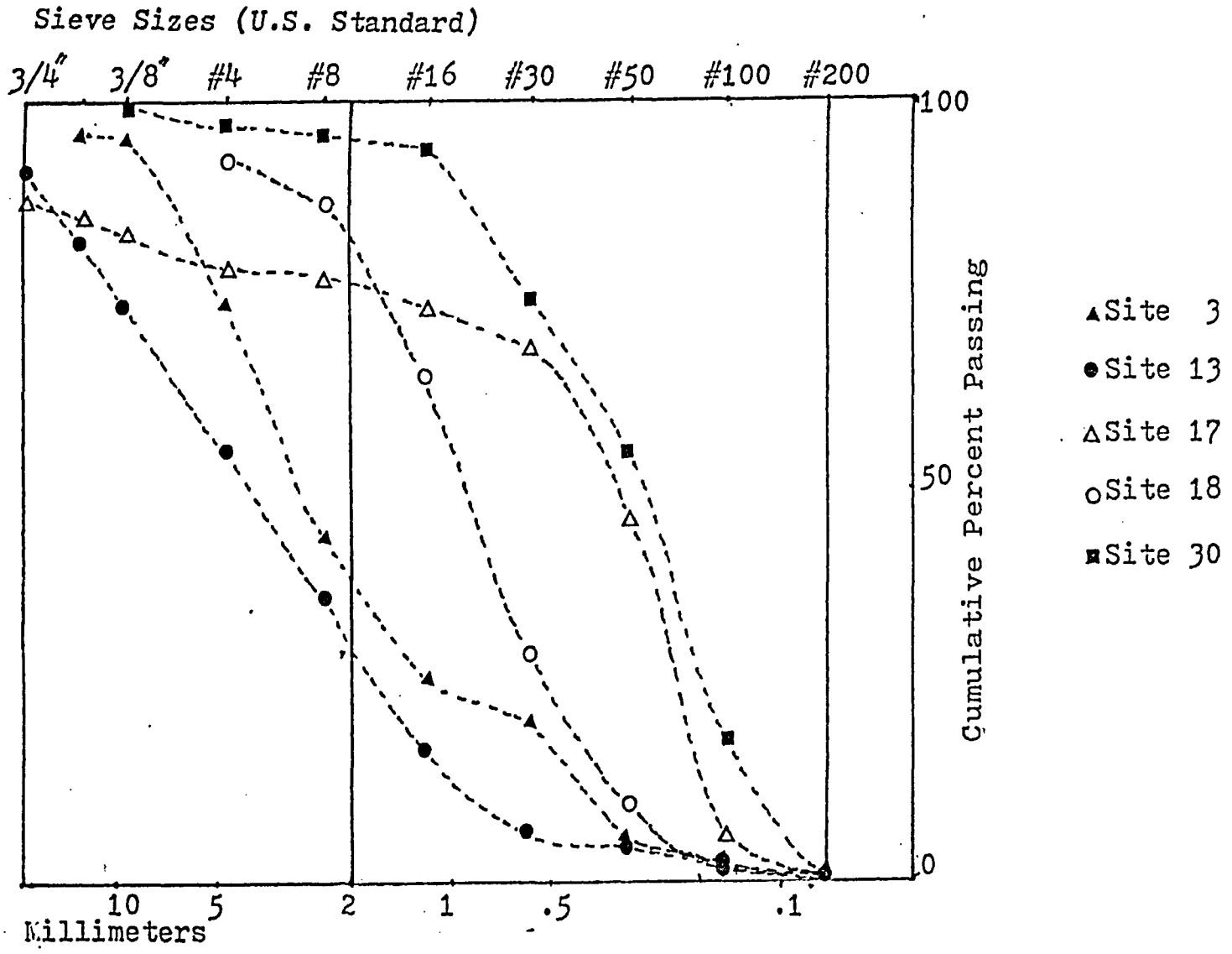

Fig. 4. Particle size against cumulative percentage for five samples.

CHAPTER III

SEISMIC REFRACTION METHOD

3.1 Theory

The seismic refraction method of prospecting generally uses waves generated at surface although subsurface sources may be used in some oil exploration or submarine studies. These waves are produced by various methods ranging from a simple sledge hammer to powerful explosives.

In this study the energy source was a sledge hammer striking a metallic plate on surface.

First consider the case where the subsurface consists of two media with uniform elastic properties and separated by a horizontal interface at depth Z (Fig. 5). Let the velocity of the longitudinal seismic wave be V_1 in the upper layer and V_2 in the lower layer with $V_2 > V_1$. Suppose that a seismic wave is generated at point A on the surface. This wave radiates out from point A in all directions as an expanding hemispherical front in the homogenous upper layer. Once the radius of the front becomes relatively large then the front can be treated as a plane. Lines perpendicular to the wave front represent the direction of propagation and are called "paths" or "rays". In Fig. 5 fronts are represented by these "rays".

When the seismic wave generated at A reaches the interface at point B_1 with an incident angle (i), some

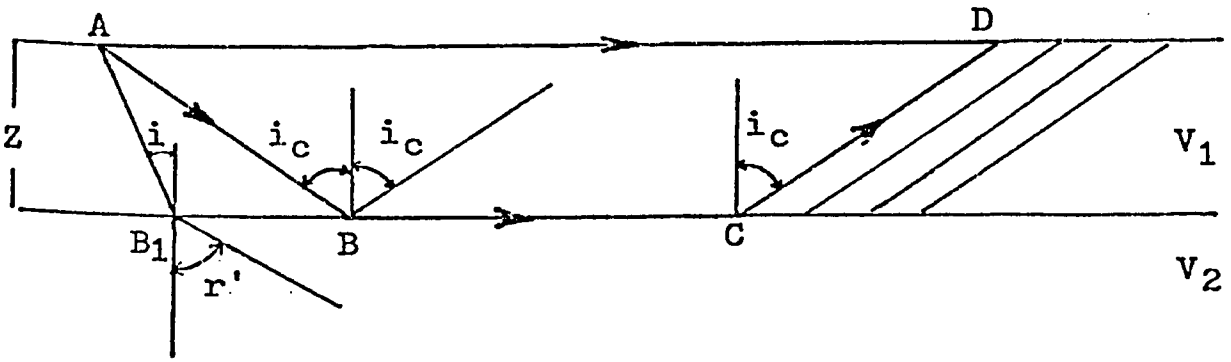

Fig. 5. Ray paths of least time for two layers separated by a horizontal interface at depth Z. The remaining symbols are given in the text.

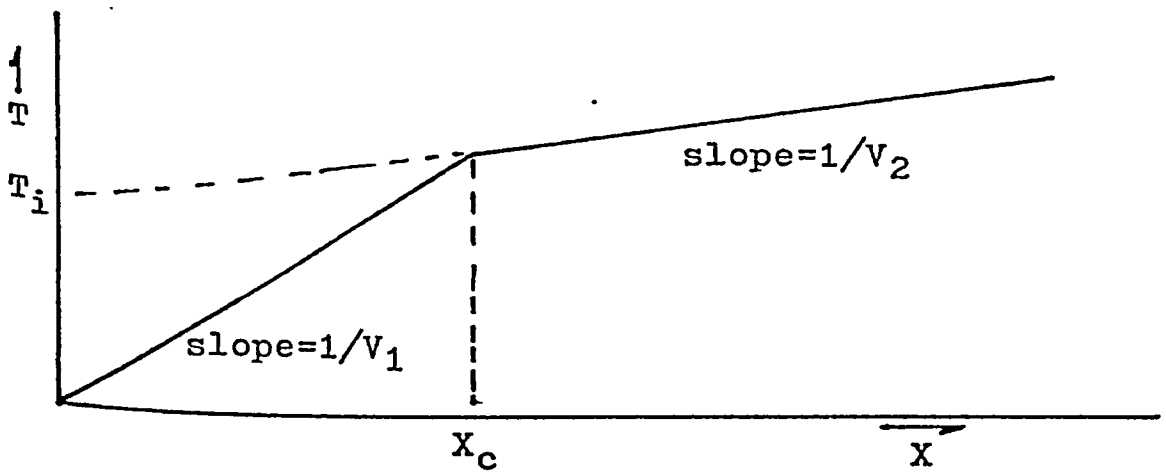

Fig. 6. Time-distance curve for two layers separated by a horizontal interface at depth Z. T is the arrival time of the first energy pulse of a wavefront at distance X from the source. The remaining symbols are given in the text.

of its energy is reflected back to surface. The rest of its energy refracted into the lower medium at an angle (r´) which satisfies Snell's law:

$$\frac{\sin(i)}{\sin(r')} = \frac{V_1}{V_2} \qquad (3.1)$$

In the special case where r´ = 90° equation (1) gives

$$i_c = \sin^{-1}(V_1/V_2) \qquad (3.2)$$

This angle (i_c) is called the critical angle. At i_c the incident wave is refracted along the interface and travels in the lower layer at a velocity V_2. At any point C the wave is subjected to Huygen's principle and is refracted back upwards into the upper layer. According to Huygen's principle every point on a wave front is the source of a new wave that also travels out from the point in spherical shells. Consequently all points on the interface are sources of new waves, and some of their energy travels towards the surface. The energy leaving C at the angle i_c is then detected first at point D.

At any point on surface between A and D the wave travelling directly through the first layer will arrive first at a detector. This happens because the path AD is sufficiently shorter than ABCD to compensate for the lower V_1 velocity. At point D the travel times of both direct wave travelling through the upper layer and the refracted wave travelling along the path ABCD are equal. Beyond

point D the refracted wave travels faster and arrives first at the detector. The distance AD is called the critical distance (X_c).

Fig. 6 is an illustration of the time-distance curve for the case of a detector moved out to well beyond Point D. The slopes of the two linear segments are equal to the inverse of the layer velocities, i.e. $1/V_1$ and $1/V_2$. The intercept time (T_i) is where the $1/V_2$ segment projects to the time axis.

When $V_1 > V_2$, then from equation (3.1) $r < i$ so that it is impossible to refract a wave along the interface. In this case all energy is refracted into second layer at a steeper angle than the incident angle. Thus that interface does not show on the time-distance curve. This is the hidden layer case which obviously cannot be solved using the refraction method alone.

3.2 Field Work

3.2.i Instruments Used

Two instruments were used in the course of collecting the field data. The Soiltest R-117B Seismic Timer is a small, portable, self-powered instrument. It records only the time required by the first pulse of energy to travel from the shot point to the single geophone. The Huntec FS-3 Seismograph, (Appendix VI), is also a portable and self-powered instrument. It records automatically on a special paper (Fig. 7) not only the first arrivals but

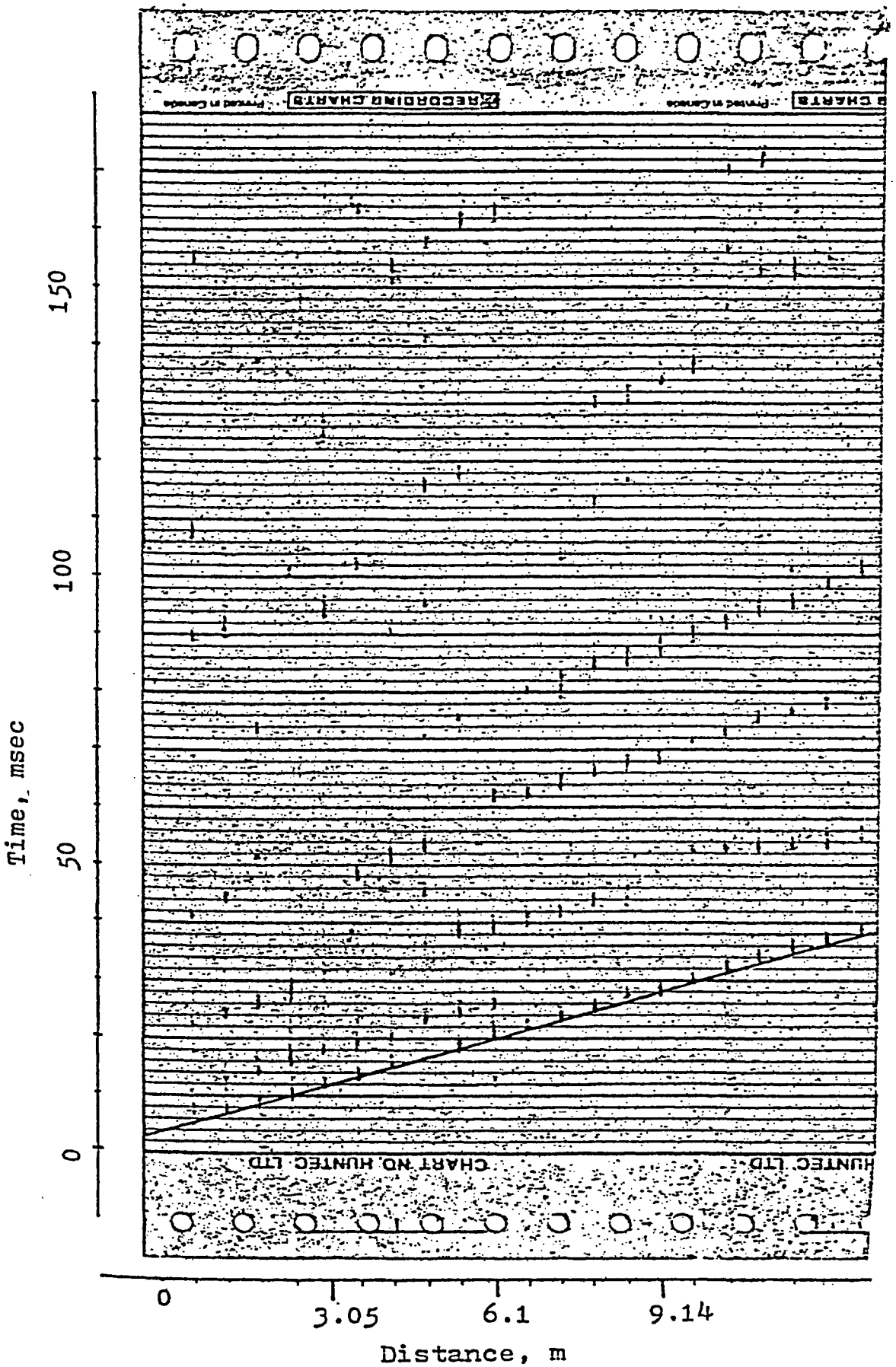

Fig. 7. Typical seismic record from the FS-3 seismograph.

also any subsequent arrivals that come to its two geophones, thereby yielding more information about the subsurface condition. A special correlator admits to the recorder only those events which are coincident in both geophones to decrease spurious "noise" events.

The source of energy for both instruments is a sledge hammer striking a metallic plate.

3.2.ii Field Work

Sites were selected such that the seismic velocities could be correlated to specific sediment type and to represent wide range of physical conditions (i.e. dry and wet samples). Clay seismic velocities were measured near construction sites or ditches. Sand and/or gravel seismic velocities were measured near "faces" of sand-gravel pits. The gravel sites were usually above water level. Some sand sites were on the beach. Their seismic velocities refer to water saturated beach sands (i.e. sites 17, 20, 22, 23).

When the R-117B Timer was used, the geophone was placed on the survey line. When the FS-3 Seismograph was used, the two geophones were placed symmetrically about the survey line. Both instruments are shown in Appendix VII.

The starting distance X was 0.6m (2 ft.). It was increased by increments of 0.6m up to 5m. Distances up to 10m were occasionally used.

3.3 Data-Statistics

The seismic velocities of the three groups (Table 4) were analyzed statistically using the BMDP3D computer program (Fu and Douglas, 1977). It provides mean and deviation statistics (Table 5) as well as group correlation statistics (Table 6). The group correlations are made by using the "Student's t-test" which provides the t-statistic, and the variance test which provides the F-statistic. The t-statistic tests the null hypothesis that the means of two groups are equal. In contrast to conventional t-tests (Kennedy, 1964) the assumption made here is that the variances of the two groups are not equal. In addition, the degrees of freedom can be non-integer numbers (Armitage, 1971). The F-statistic tests the null hypothesis that the variances of two groups are equal. The histograms for the seismic velocities of the three groups are shown in Fig. 8. Although the distributions of the seismic velocities depart from a normal distribution the t-test can be applied for the comparison of the three groups because for all but small samples "the p-values for the t-test are not greatly affected by moderate departures from normality" (Armitage, 1971).

Three possible pairs were compared in this study, namely GRAVEL versus SAND, GRAVEL versus CLAY and SAND versus CLAY. The following conclusions can be drawn based on the computed statistics.

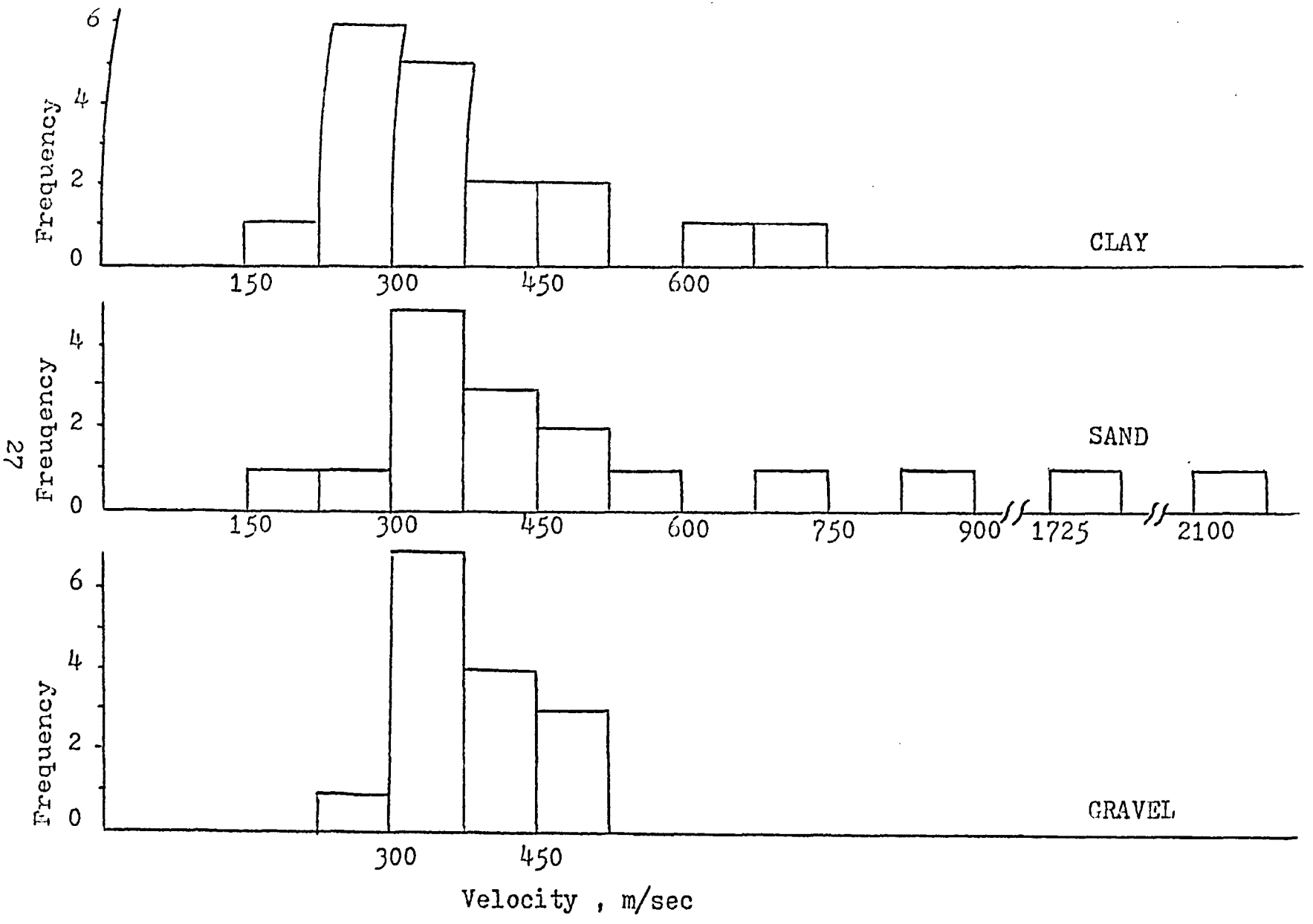

Fig. 8. Frequency distribution of the seismic velocities in the three groups GRAVEL, SAND and CLAY.

1. The SAND group of samples shows the highest mean velocity but it also has the highest standard deviation.

2. There is a very small difference between the mean velocities of the GRAVEL and CLAY groups. The interesting point is that, statistically, the GRAVEL velocities are slightly higher than the CLAY velocities.

3. The t-statistic for the GRAVEL-SAND pair is -1.98. For 16.4 degrees of freedom, the corresponding significance level is 0.065 or 6.5%. Therefore the hypothesis that the mean velocities of the GRAVEL and SAND groups are equal is rejected at the 93.5% confidence level. Thus the seismic velocities of the SAND group are statistically different from those of the GRAVEL group.

4. The t-statistic for the GRAVEL-CLAY pair is 0.62. For 23.8 degrees of freedom the corresponding significance level is 0.542 or 54.2%. This means that we can reject the hypothesis that the mean velocity of the two groups are equal at the 45.8% confidence level and accept that their mean velocities are the same at the 54.2% confidence level. Therefore the seismic velocities of the GRAVEL group are not significantly different from those of the CLAY group.

5. The t-statistic for the SAND-CLAY pair is 2.1. For 18 degrees of freedom the corresponding significance level is 0.051 or 5.1%. This, again suggests that the mean velocities of the SAND and CLAY groups are statisti-

cally different at the 94.9% confidence level.

6. The F-statistic gives similar results to those from the T-test i.e. the CLAY and GRAVEL groups are similar in that they have relatively small standard deviations whereas the SAND group differs from them in that it has a relatively large standard deviation.

In summary the GRAVEL and SAND pair and the SAND and CLAY pair have seismic velocities significantly different while the GRAVEL and CLAY pair does not.

The exploration meaning of these statistical results will be discussed in Chapter 5.

GRAVEL		SAND		CLAY	
Site #	Velocity (m/sec)	Site #	Velocity (m/sec)	Site #	Velocity (m/sec)
1	365.8	16	1764.5	33	277.1
2	343.2	17	2133.6	34	641.6
3	312.4	18	391.7	35	234.4
4	281.3	19	853.4	36	268.2
5	435.2	20	365.8	37	329.9
6	348.1	21	320.6	38	218.8
7	457.2	22	1463.0	39	328.0
8	487.7	23	548.6	40	228.9
9	435.2	24	381.0	41	391.4
10	426.7	25	369.4	42	304.8
11	335.3	26	270.7	43	484.3
12	370.0	27	304.8	44	522.4
13	474.0	28	217.6	45	406.3
14	406.3	29	731.5	46	735.5
15	365.8	30	426.7	47	232.2
		31	304.8	48	361.8
		32	461.8	49	341.4
				50	290.2

Table 4. Seismic velocities for GRAVEL, SAND and CLAY in Essex County.

	Velocity in m/sec.		
	GRAVEL	SAND	CLAY
MEAN	389.6	665.3	366.2
STANDARD DEVIATION	61.6	571.2	145.4
STANDARD ERROR	16.2	138.5	34.3
MAXIMUM	487.2	2133.6	735.5
MINIMUM	281.3	217.6	218.8

Table 5. Mean and deviation statistics for velocity for the GRAVEL, SAND and CLAY groups.

	GRAVEL vs SAND	GRAVEL vs CLAY	SAND vs CLAY
T	-1.98	0.62	2.1
P	0.065	0.542	0.051
D.F.	16.4	23.8	18.0
F	85.92	5.57	15.42
P	0.000	0.062	0.000
D.F.	16 , 14	17 , 14	16 , 17

Table 6. Group correlation statistics for velocity.T is the T-separate statistic.P is the two-tail significance level.D.F. are the degrees of freedom and F is the F-statistic.

CHAPTER IV

ELECTRICAL RESISTIVITY METHOD

4.1 Introduction

Electrical prospecting uses measurements of the electrical properties of rocks to study the structure and composition of those layers which are sufficiently shallow to be exploited by man. Electrical prospecting was used as early as 1720 by Gray-Wheeler (Jakosky, 1955). It makes use of three fundamental properties of rocks: i) the resistivity, ii) the electrochemical activity with respect to electrolytes in the ground, and iii) the dielectric constant.

Electrical resistivity measurements were used in this study. The theory and results are presented in this chapter.

4.2 Previous Work

The electrical resistivity method has been used successfully in delineating sand and gravel deposits in the past because they have very different resistivities than clays. It works because "most buried gravel and sands are covered and surrounded by clay, ground moraine and flood silt" (Kurtenacker, 1934).

Kurtenacker (1934) has described briefly the use of the resistivity method for reconnaissance and detailed quarry surveys. In a more detailed paper, Moore (1944)

described the application of the resistivity method to the location of sand and gravel deposits. He found that a very satisfactory correlation existed when the resistivity results were compared with the test-boring results. He also emphasized that these good results were obtained more quickly and cheaply than by drilling.

An empirical method for interpreting electrical resistivity data collected over a gravel deposit was described by Jacobson (1955). He produced an isopach map of overburden based on the resistivity data and compared it to a map produced from drilling results. He found that the two maps showed a high degree of correlation and that a mathematical relation could be established relating the apparent resistivity to the overburden thickness.

Other authors have also reported case histories of several prospects where the electrical resistivity method was successfully used (Johnson, 1959 ; Wilcox, 1944 ; Moore, 1945 ; Moore, 1950). The common conclusion is that the much less conductive sand and gravel deposits can be outlined accurately beneath clay when the resistivity method is used.

4.3 Theory

4.3.i Resistivity concept

The electrical resistivity (ρ) of any material is defined as the resistance between opposite faces of a

cylinder of unit length (1) having a cross-section of unit area (S). The resistivity is expressed by the formula:

$$\rho = \frac{RS}{1} \qquad (4.3.1)$$

where R is the resistance of this cylinder.

Depending on the units of S, 1, and R it follows that the resistivity units will be in ohm-m, ohm-ft, or ohm-cm with ohm-m being the most common measure.

Let us now consider the case of a thick homogenous layer with resistivity ρ. The resistivity of this layer is measured by feeding a current I into the ground, through two current electrodes (C_1 and C_2) and measuring the potential between two points using two potential electrodes (P_1 and P_2) (Fig. 9). The geometric arrangement in which the four (or sometimes more) electrodes are put into the ground is referred to as "electrode configuration" or "spread".

It can be shown (see Appendix IV) that the potential V at any point P some distance α from a point current source is given the formula:

$$V = \frac{I\rho}{2\pi\alpha} \qquad (4.3.2)$$

The potentials at P_1 due to C_1 and C_2 (Fig. 9) are calculated and added together to find the total potential. The same procedure is applied to P_2. By subtracting the

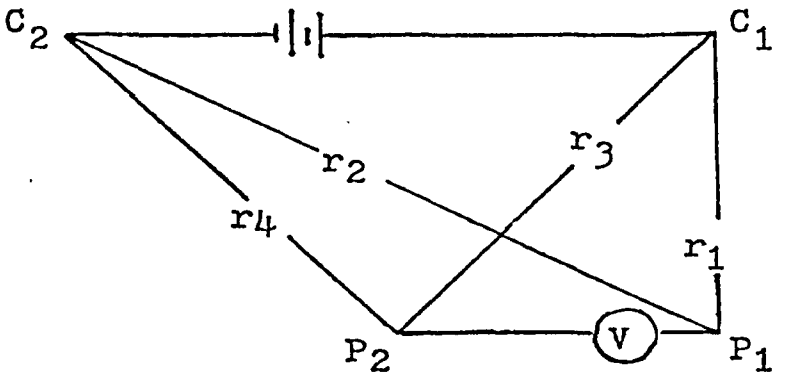

Fig. 9. A generalized electrode configuration.

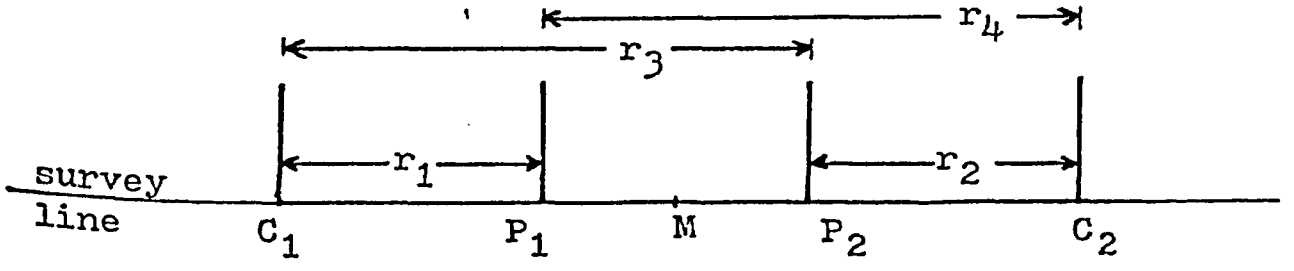

Fig. 10. Electrode arrangement using the Wenner method.

two potentials we obtain the desired potential difference, taking into account the fact that the current at C_2 has a negative sign. The general form of this potential difference is

$$V = \frac{I\rho}{2\pi} F(r's) \qquad (4.3.3)$$

where F(r's) is the "Roman's form factor". It is a simple function of the interelectrode distances:

$$F(r's) = \left(\frac{1}{r_4} - \frac{1}{r_2} \right) - \left(\frac{1}{r_3} - \frac{1}{r_1} \right)$$

Solving the equation (4.3.3) for ρ we get:

$$\rho = \frac{2\pi V}{I} \cdot \frac{1}{F(r's)} \qquad (4.3.4)$$

4.3.ii Concept of apparent resistivity

In the proceeding theory (4.3.i) the solid under consideration was assumed to be homogenous and isotropic. In this case the resistivity calculated from equation (4.3.4) will be constant for any current and any electrode arrangement. However, when dealing with inhomogenous material the ratio (V/I)/F(r's) will change resulting in different values for ρ for each electrode spacing. Thus the measured quantity is the "apparent resistivity"(ρ_α). The measured resistivity does not represent the true resistivity of the material but rather it is a function of the region where measurements are taken as well as a function of the elec-

trode configuration employed. This measured resistivity will either rise above or fall below the true resistivity of the particular material due to anomalous "pseudofocussing effects within the material. It is not an average value; it is a diagnostic value and it equals the true resistivity only if the material is homogenous.

4.4 Field work

4.4.i Electrode Configuration

The Wenner configuration was used in collecting the field data. At each of the 50 sites all four electrodes are spread out on the survey line (Fig. 10). The outer electrodes are the current electrodes C_1 and C_2. The inner potential electrodes P_1 and P_2 are used to measure the potential drop between them. M is the midpoint between P_1 and P_2. All four electrodes are moved out symmetrically about this midpoint. The interelectrode distances C_1P_1, P_1P_2 and P_2C_2 are kept equal always, and are designated by "α". The values of α were 1.52, 0.914, 0.762, 0.609, 0.304 and 0.15m. They correspond to 5.0, 3.0, 2.5, 2.0, 1.5, 1.0 and 0.5 ft. Equation (4.3.4) solved for the Wenner configuration gives:

$$\rho_\alpha = \frac{2\pi\alpha V}{I} \qquad (4.4.1)$$

The apparent resistivities were calculated from the measured I and V using this equation.

4.4.ii Instrument used

The R-50 Stratameter (Appendix VI) was used to collect the field data. It is a direct current device and consists of two units: the power or transmitting unit, and the measuring or receiving unit. It is a self powered instrument that can be recharged. An auxilliary voltmeter (type: Avometer EA-113) was used for voltage readings exceeding the range of the receiving unit.

4.4.iii Galvanic Voltage Adjustments

Galvanic voltage is the voltage shown on the receiver unit from natural electric currents in the ground. It must be measured before any current is fed into the ground.

When the R-50 was used the galvanic voltage was automatically "zeroed out". When the auxiliary voltmeter was used, a positive or negative correction was added to the measured value.

4.5 Interpretation of the Apparent Resistivity Results

For each site and for every electrode separation α, an apparent resistivity was calculated using equation (4.4.1). All the results are listed in Appendix III.

The interpretation of the results is based on the curve matching method. A field curve was constructed by joining all the field data for a particular site and by comparing with a set of theoretical master curves.

The master curves are constructed as follows:

Telford et al. (1976) show that the equation relating the apparent resistivity ρ_α and the true resistivity ρ_1 for the Wenner configuration has the form:

$$\rho_\alpha = \rho_1 (1+4D_w) \qquad (4.5.1)$$

where

$$D_w = \sum_{m=1}^{\infty} k^m \left[\frac{1}{\{1+(2mz/\alpha)^2\}} - \frac{1}{\{4+(2mz/\alpha)^2\}} \right]$$

where

$$k = \frac{\rho_2-\rho_1}{\rho_2+\rho_1}$$

and $$m = 1, 2, .. \infty$$

The master curves can now be prepared with dimensionless coordinates by dividing ρ_α by ρ_1. The ratios ρ_α/ρ_1 are plotted against α/z on a double logarithmic paper. This makes the size and shape of the curves independent of the measurement units. Such a set of master curves includes the standard collection of two-layer curves for $\rho_1>\rho_2$ and for $\rho_2>\rho_1$. The three- (and sometimes four-) layer curves cover a wide range of resistivity and layer thickness values. The three-layer master curves can be grouped into four types, as illustrated in Fig. 11. The four-layer curves can be grouped into eight types identified by a combination of the three-layer designations. For example, a type HK curve corresponds to the combination:

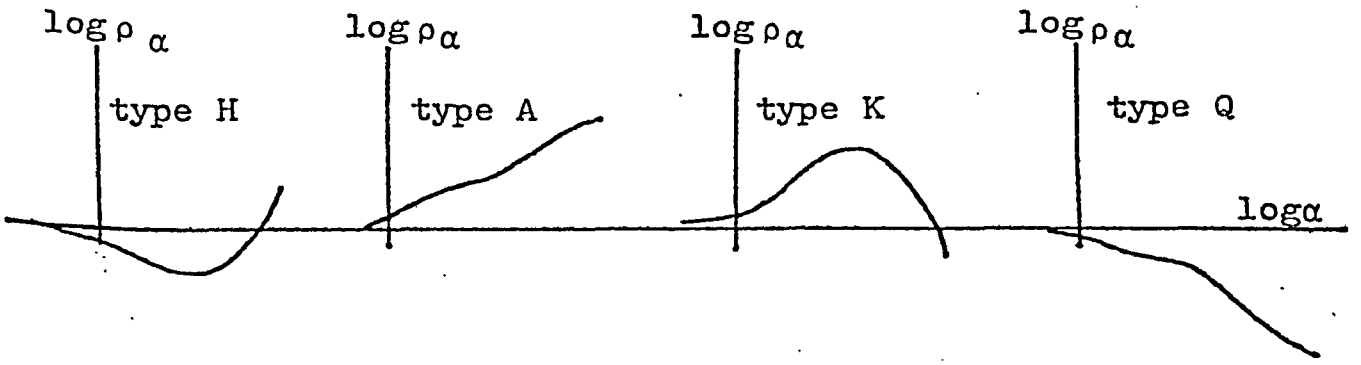

Fig. 11. Various types of multilayer profiles for ρ_α after Keller and Frischknecht (1966).

Type H : $\rho_1 > \rho_2 < \rho_3$ Type A : $\rho_1 < \rho_2 < \rho_3$

Type K : $\rho_1 < \rho_2 > \rho_3$ Type Q : $\rho_1 > \rho_2 > \rho_3$

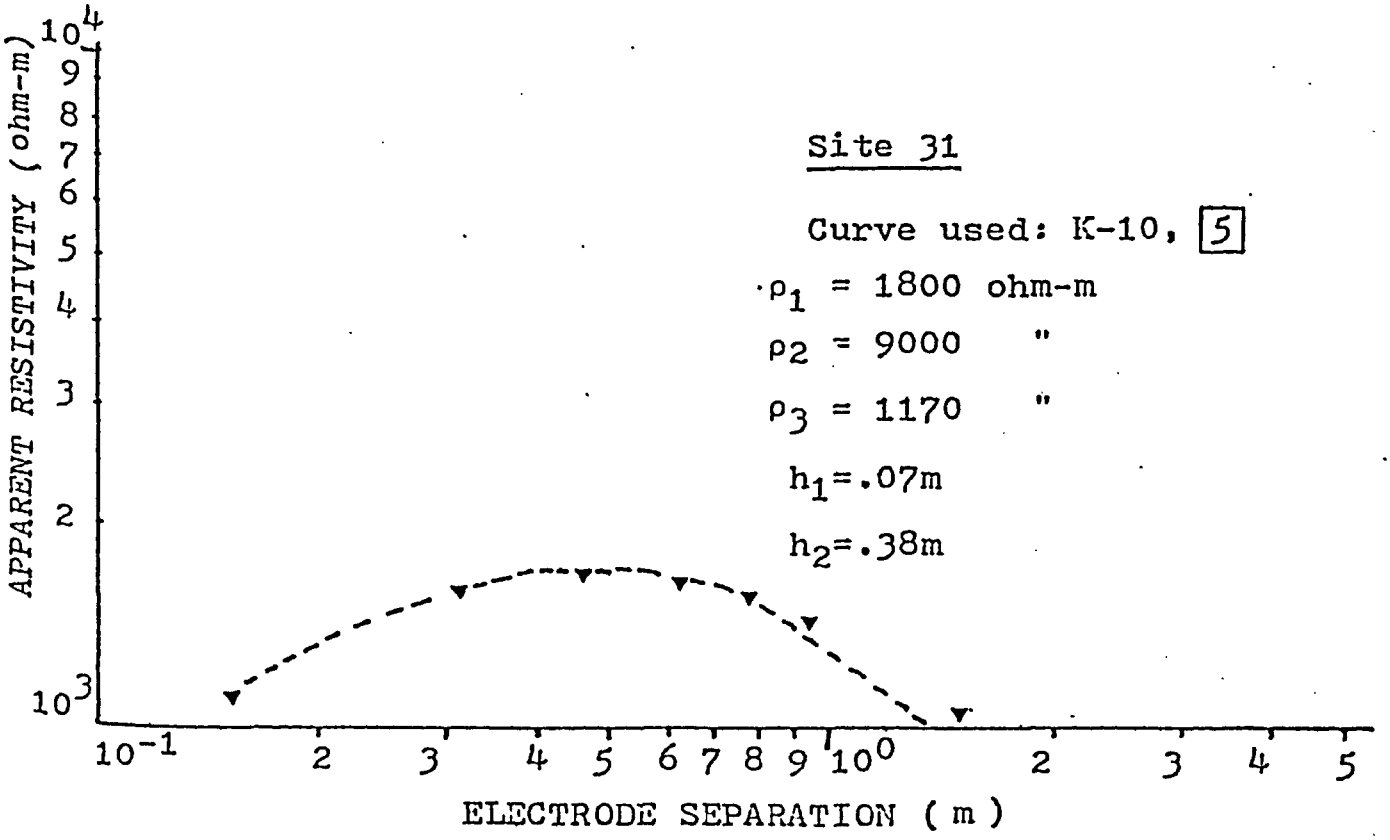

Fig. 12. Representative example of apparent resistivity interpretation.

$\rho_1 > \rho_2 < \rho_3 > \rho_4$, etc. A field curve can now be superimposed on various master curves until a satisfactory fit is obtained. Each one of the master curves has a "cross" where $(C_1C_2)/2 = 1$ and $\rho_1 = 1$. One or more "resistivity marks" refer to the numbered index marks appearing on the vertical axis of the master curve. After the satisfactory fit is found, the coordinates of the master curve "cross" are marked on the sheet where the field data are plotted. These coordinates will yield the true resistivity and the thickness of the particular layer. The resistivity marks will yield the ratios ρ_2/ρ_1, ρ_3/ρ_1, etc. Thickness ratios are recorded on each of the master curves providing estimations of D_2/D_1, D_3/D_2 etc. Further detailed instructions on the use of the master curves can be found in Orellana and Mooney (1966).

The master curves published by Orellana and Mooney (1966) were used for the interpretation of the resistivity results. The results are shown on Table 7. A representative example of field data interpretation is shown on Fig. 12.

4.6 Data - Statistics

As with the seismic velocities the BMDP3D computer program (Fu and Douglas 1977) was used for the statistical analysis of the resistivity results. The last column of Table 7 contains the resistivity values which were used for statistical analysis. These resistivity values were con-

sidered to be the most representative for the corresponding site because they correspond to its thickest section. The histograms of the electrical resistivity in the three groups are shown on Fig. 13. The results of the statistical analyses are shown on Tables 8 and 9. Based on these results the following conclusions can be drawn:

1. The GRAVEL group of samples shows the highest mean electrical resistivity but it also has the highest standard deviation.

2. There are quite large differences between the mean electrical resistivities of the GRAVEL, SAND and CLAY groups.

3. The t-statistic for the GRAVEL-SAND pair is 3.72. For 14.4 degrees of freedom, the corresponding significance level is 0.002 or 0.2%. Therefore the hypothesis that the electrical resistivities of the GRAVEL and SAND groups are the same is rejected at the 99.8% confidence level. Thus the electrical resistivities of the GRAVEL group are statistically different than those of the SAND group.

4. The t-statistic for the GRAVEL-CLAY pair is 4.24. For 14 degrees of freedom, the corresponding significance level is 0.001 or 0.1%. Therefore these two groups are also statistically different at the 99.9% confidence level. Thus the electrical resistivities of the GRAVEL group are statistically different than those of the CLAY group.

5. The t-statistic for the SAND-CLAY pair is 4.3. For 16.1 degrees of freedom, the corresponding signifi-

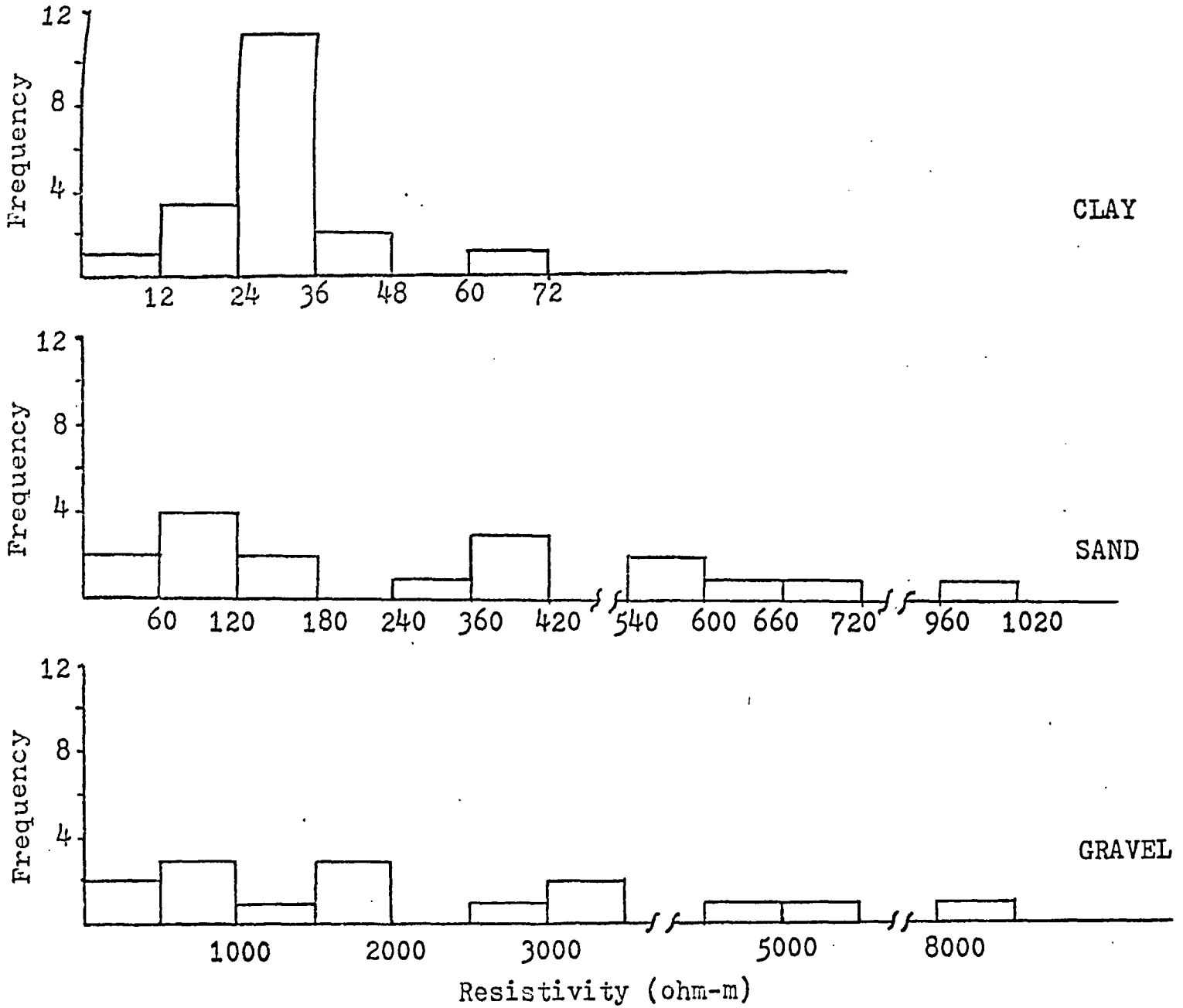

Fig. 13. Frequency distribution of the electrical resistivities in the three groups GRAVEL, SAND and CLAY

cance level is 0.001 or 0.1%. As with the other pairs of groups, the electrical resistivities of the SAND group are statistically different than those of the CLAY group at the 99.9% confidence level.

6. The F-statistic gives similar results to those of the T-test i.e. the variances of the three groups are significantly different at the 100% confidence level when examined in pairs.

Site	ρ_1	h_1	ρ_2	h_2	ρ_3	h_3	ρ_4	ρ	
1	65.5	.13	655.3					655.3	
2	823.0	.12	1234.4					1234.4	
3	1219.2	.12	1828.8	.25	877.8	1.13	5486.4	5486.4	
4	381.0	.04	7620.0	.12	2118.4	1.13	8473.4	8473.4	
5	1127.8	.18	5638.8	.35	2819.4			2819.4	
6	2255.5	.07	4511.0					4511.0	
7	951.0	.13	3328.4					3328.4	
8	195.1	.06	243.8					243.8	
9	21.0	.05	841.2					841.2	
10	155.4	.06	31.1	.06	777.2			777.2	
11	411.5	.23	1645.9					1645.9	
12	249.9	.08	374.9	.41	50.0			374.9	
13	381.0	.10	381.0	2.25	1905.0			1905.0	
14	381.0	.15	1905.0					1905.0	GRAVEL
15	42.7	.10	213.4	.80	1733.4	1.0	3474.7	3474.7	
16	97.5	.10	490.1	.50	63.4			63.4	
17	164.6	.07	823.0	.22	107.0			107.0	
18	312.4	.46	62.5	11.43	312.4			312.4	
19	457.2	.04	685.8					685.8	
20	146.3	.23	585.2					585.2	
21	155.5	.30	621.8					621.8	
22	390.1		585.2	.80	78.0			78.0	
23	195.1	.12	39.0	.12	975.4			975.4	
24	231.6	.15	2316.5	.44	329.2			329.2	
25	54.9	.15	548.6	.64	137.2			137.2	
26	270.7	.06	381.0	.13	114.3			114.3	
27	310.9	.19	777.2	.56	124.4			124.0	SAND
28	67.1	.43	26.8					26.8	
29	214.9	.09	139.6	.18	43.0			43.0	
30	27.4	.08	548.6					548.6	
31	548.6	.08	2743.2	.38	356.6			356.6	
32	85.3	.08	298.7					298.7	
33	1.8	.06	6.4					6.4	
34	6.9	.08	17.4					17.4	
35	7.9	.06	27.7					27.7	
36	11.6	.05	17.4	.24	28.9			28.9	
37	32.0	.05	6.4	.10	32.0			32.0	
38	29.6	.05	5.9	.10	29.6			29.6	
39	6.4	.09	22.4					22.4	
40	6.5	.05	16.4	.77	65.5			65.5	
41	11.6	.06	40.5					40.5	
42	115.8	.03	173.7	.10	6.4	.21	25.6	25.6	
43	12.5	.04	29.1					29.1	
44	8.5	.08	85.3	.13	17.1			17.1	
45	10.7	.10	37.2					37.2	
46	9.0	.14	31.5					31.5	
47	8.2	.06	28.8					28.8	
48	6.1	.07	30.5					30.5	
49	8.0	.15	32.1					32.1	
50	5.3	.06	26.7					26.7	CLAY

Table 7. Summary of the interpreted resistivity data. ρ_i and h_i are the resistivity (ohm-m) and thickness (m) of the i^{th} layer, where i=1, 2 ... n.

	Resistivity in ohm-m		
	GRAVEL	SAND	CLAY
MEAN	2511.7	318.1	29.3
STANDARD DEVIATION	2270.1	276.7	11.9
STANDARD ERROR	585.1	67.1	2.8
MAXIMUM	8473.4	975.4	65.5
MINIMUM	243.8	26.8	6.4

Table 8. Mean and deviation statistics for the resistivities of the GRAVEL, SAND and CLAY groups.

	GRAVEL vs SAND	GRAVEL vs CLAY	SAND vs CLAY
T	3.72	4.24	4.30
P	0.002	0.001	0.001
D.F.	14.4	14.0	16.1
F.	67.29	****	538.11
P	0.000	0.0	0.000
D.F.	14 , 16	17 , 14	16 ,17

Table 9. Group correlation statistics for resistivity.

Abbreviations as in Table 6.

**** : value not computed - out of range.

CHAPTER V

INTEGRATED ANALYSIS

5.1 Introduction

The search for useful statistical relationships between the seismic velocities, the resistivities and the grain size of the samples was done using the BMDP6D computer program (Chasen, 1977). It displays one variable against another variable in a scatter plot. The variables are seismic velocity (V), resistivity (ρ), log V, log ρ, "% gravel", "% sand" and "% clay".

Each site was first considered as belonging to one population. Thus the relationships between the measured quantities can be seen and group distinctions can be made on the same plot. Separate plots were also drawn for each group separately. A total of 44 plots were thus drawn by computer and the most important ones are presented here. The remaining plots can be found in Appendix V.

5.2.i Integration of Seismic Velocity and Grain Size Data

It was shown in Chapter 3.3 that there is a significant difference between the velocities of the GRAVEL-SAND groups and SAND-CLAY groups. No significant difference exists between the velocities of the GRAVEL-CLAY groups. These data mean that a single seismic velocity value, measured on top on an unknown sediment cannot determine the sediment grain size.

Fig. 14 shows graphically that no distinction can be made between the three groups based on the seismic velocity. It is a plot of velocities against the percentage of sand. The percentage of sand was chosen so that all the samples could be represented on the same graph. The two regression lines are:

$$(1) \quad \% \text{ Sand} = 0.025V + 40.99$$

$$(2) \quad V = 3.95(\% \text{ Sand}) + 266.4$$

with correlation coefficient c = .313.

Thus it becomes clear that: 1) very poor correlation exists between the % Sand and the velocity, and 2) there is so much overlap of the velocities of the three groups that it is impossible to differentiate between them using only the seismic velocity. The same picture is obtained when the % Sand is plotted against log V (Fig. 15).

When the GRAVEL and SAND groups are compared and the seismic velocities are plotted against % Gravel (Fig. 16), a conclusion of limited value can be drawn, namely, that it is probable that if the seismic velocity measured over a sand and gravel deposit is greater than 560m/sec then the % gravel is less than 30%.

No relationship exists within the CLAY group between the percentage of clay and the seismic velocities (Fig. 17). The correlation coefficient is very low: c = -.088. This suggests that seismic velocities in clays are not controlled

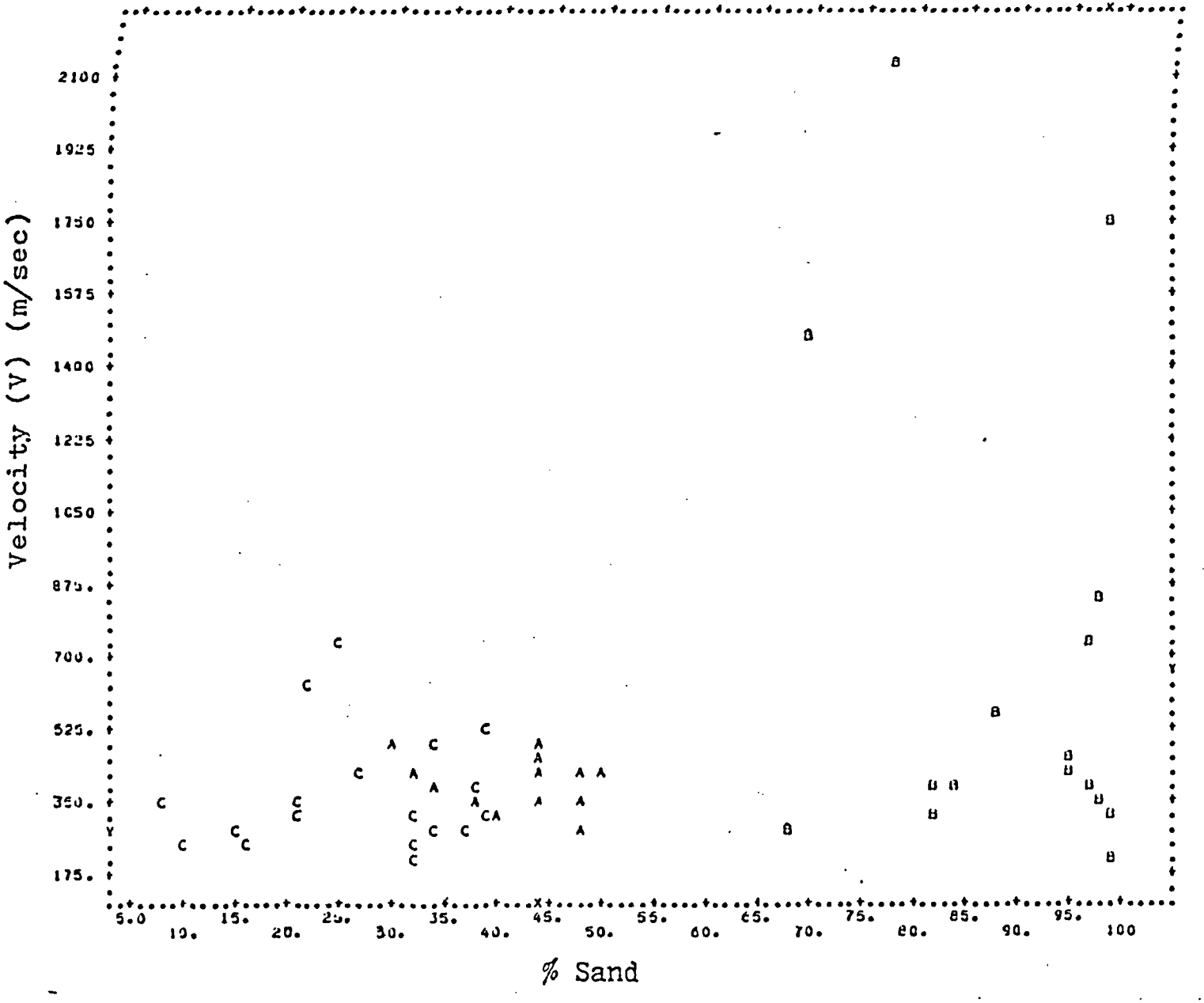

Fig. 14. % Sand - Velocity plot. All samples included. N=50. A, B and C designate the GRAVEL, SAND and CLAY samples respectively. X's and Y's show where the two regression lines (i.e. X=bY+a and Y=bX+a) intersect the frames of the plot.

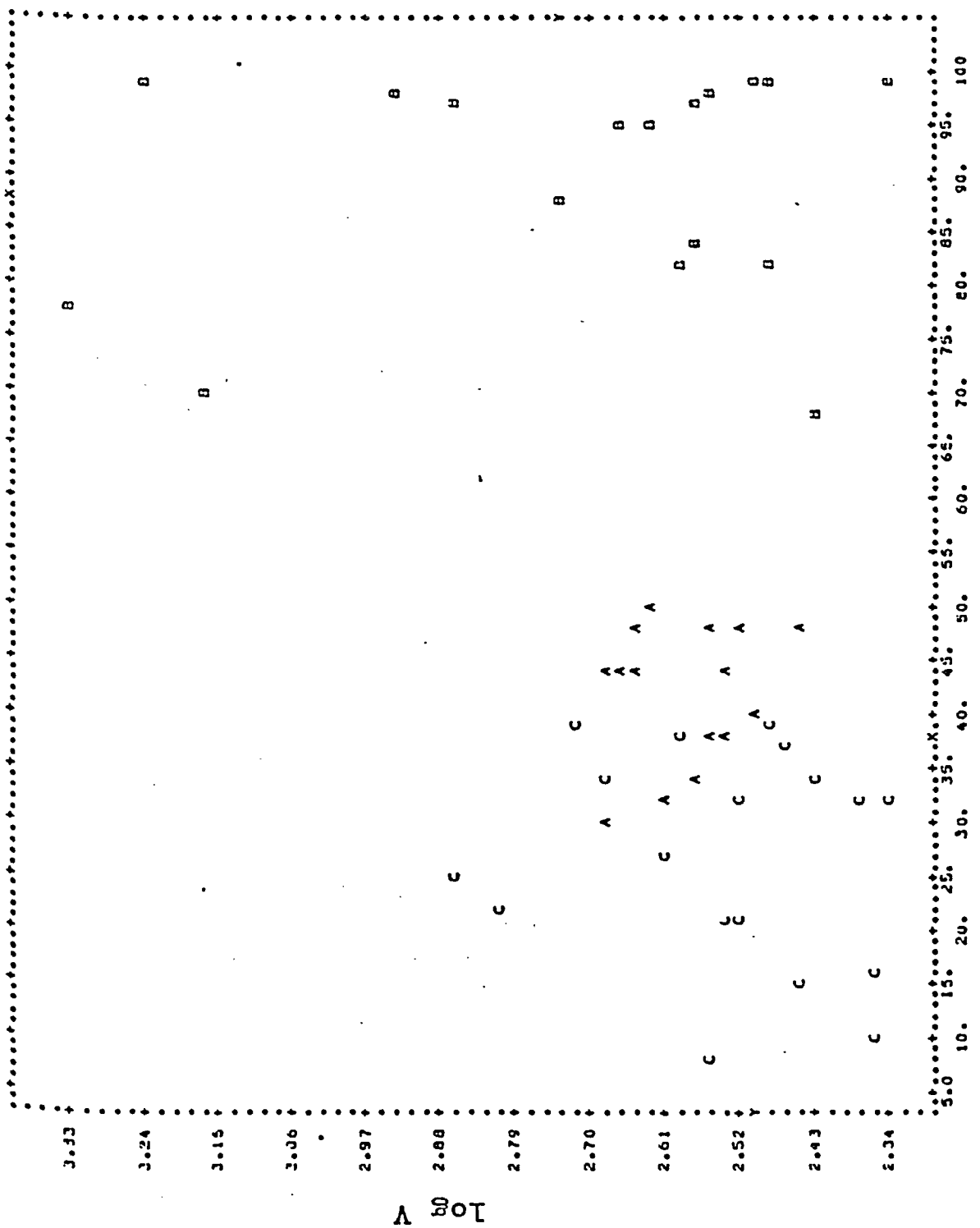

Fig. 15. % Sand-log V plot. All samples included. N=50. A, B, C as in Fig. 14.

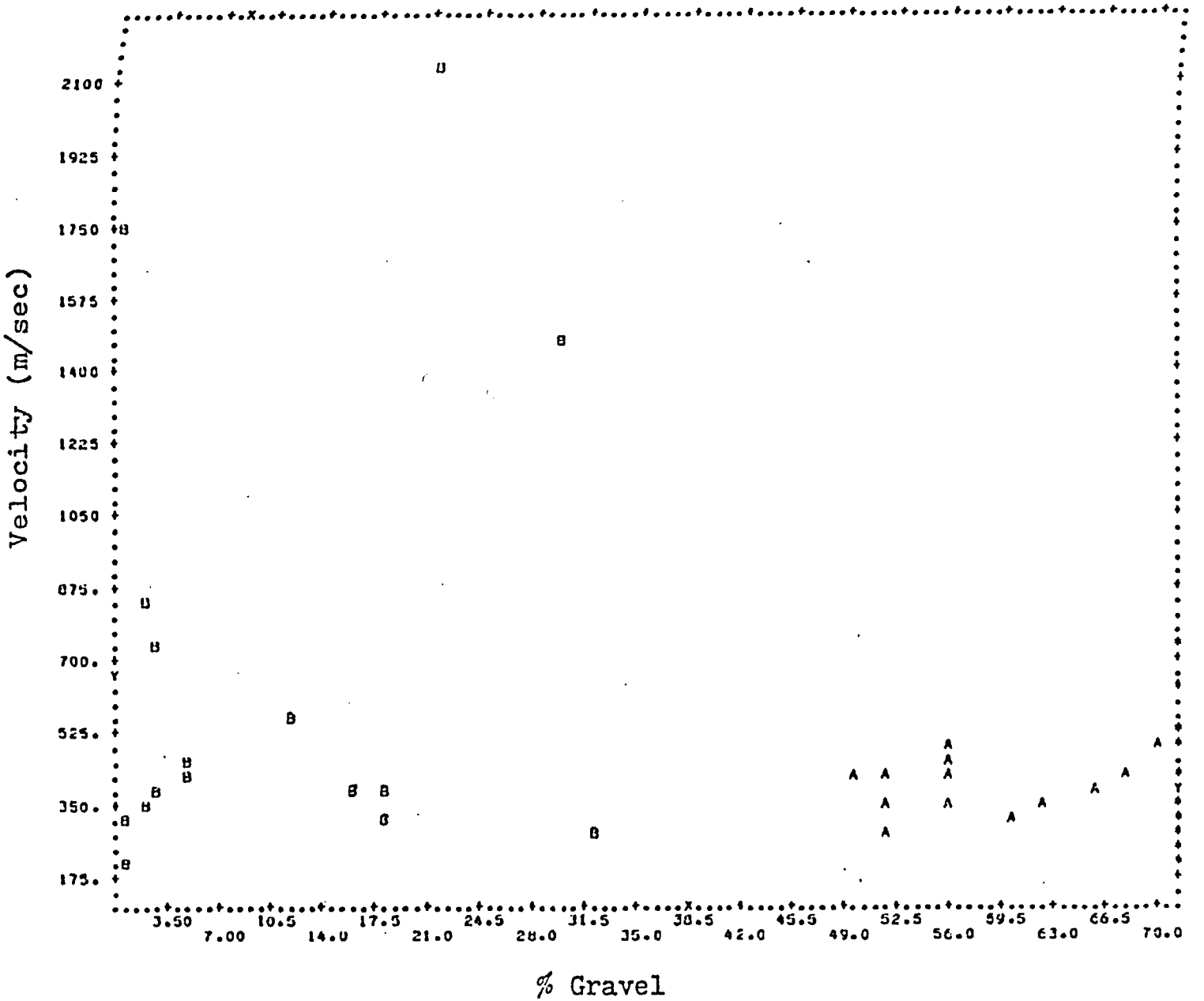

Fig. 16. % Gravel - Velocity plot. There are 32 samples from the SAND and GRAVEL groups. A, B, C as in Fig. 14.

by the percentage of contained clay.

5.2.ii Discussion of the Results

Locating near surface sand and gravel deposits with seismic methods is basically a small-scale investigation. Therefore "the difference between the theoretical assumptions on which the method is based and the actual physical conditions of the field experiments may become so pronounced, that unreliable and meaningless results are obtained" (Burke, 1967). Such conditions include: 1) the inhomogeneity of the drift especially for its section close to the surface, and 2) the degree of consolidation of the drift. These problems, together with the difficulty of generating simple seismic body waves, can lead to significant errors in a small scale investigation, thereby restricting the use of seismic prospecting for sand and gravel. This study illustrates this problem. It is apparent that a representative seismic velocity cannot be assigned a specific type of drift. Unfortunately a significant overlap of seismic velocities exists between the clays and the sand and gravels of Essex County. The overlap is more pronounced in the case of the CLAY and GRAVEL groups.

Thus it is concluded that the seismic refraction method will not differentiate the overlying CLAY from the underlying SAND and GRAVEL deposits and, consequently, the depth to the interface cannot be estimated.

This conclusion agrees with results from other similar small-scale, investigations especially when the thicknesses of the first layer is less than about 3m (10 ft.), and with what Burke, (1967), wrote: "it is usually impossible to predict, or impracticable to measure variations in thickness of this order". It should be mentioned that his conclusion was referring to an even more favourable situation where the velocity of the first layer was 300m/sec and the velocity of the second layer was 1525m/sec.

5.3.i Integration of Electrical Resistivity and Grain Size Data

Fig. 18 is a "% gravel" against log ρ plot. Thus the GRAVEL and SAND group samples can be compared on a single plot. The first degree regression equation has the form:

$$\text{"\% gravel"} = 25.91 \log \rho - 38.2$$

The correlation coefficient of c = 0.642 is the highest among all the various equations. Second- and third-degree polynomials were also calculated to obtain a better approximation. Their graphical solutions are shown on Fig. 19. Because of the dispersion of the data none of the three equations can predict accurately the "% gravel" when the resistivity is given. The important conclusion of the above plot though is that if the resistivity is greater than 1000 ohm-m then the "% gravel" is more than 50%.

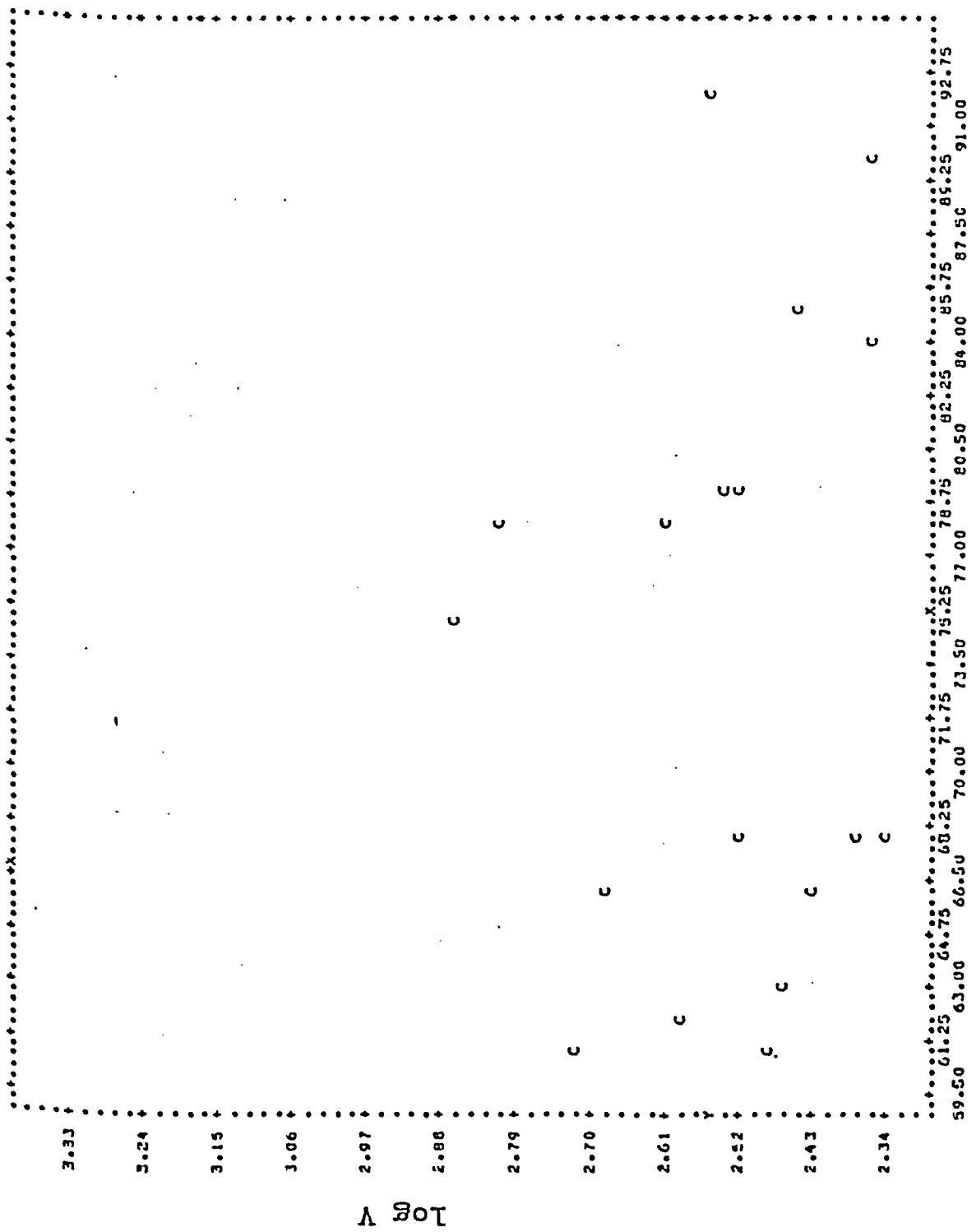

Fig. 17. % Clay - log V plot. There are 18 samples included representing the CLAY group. A, B, C as in Fig. 14.

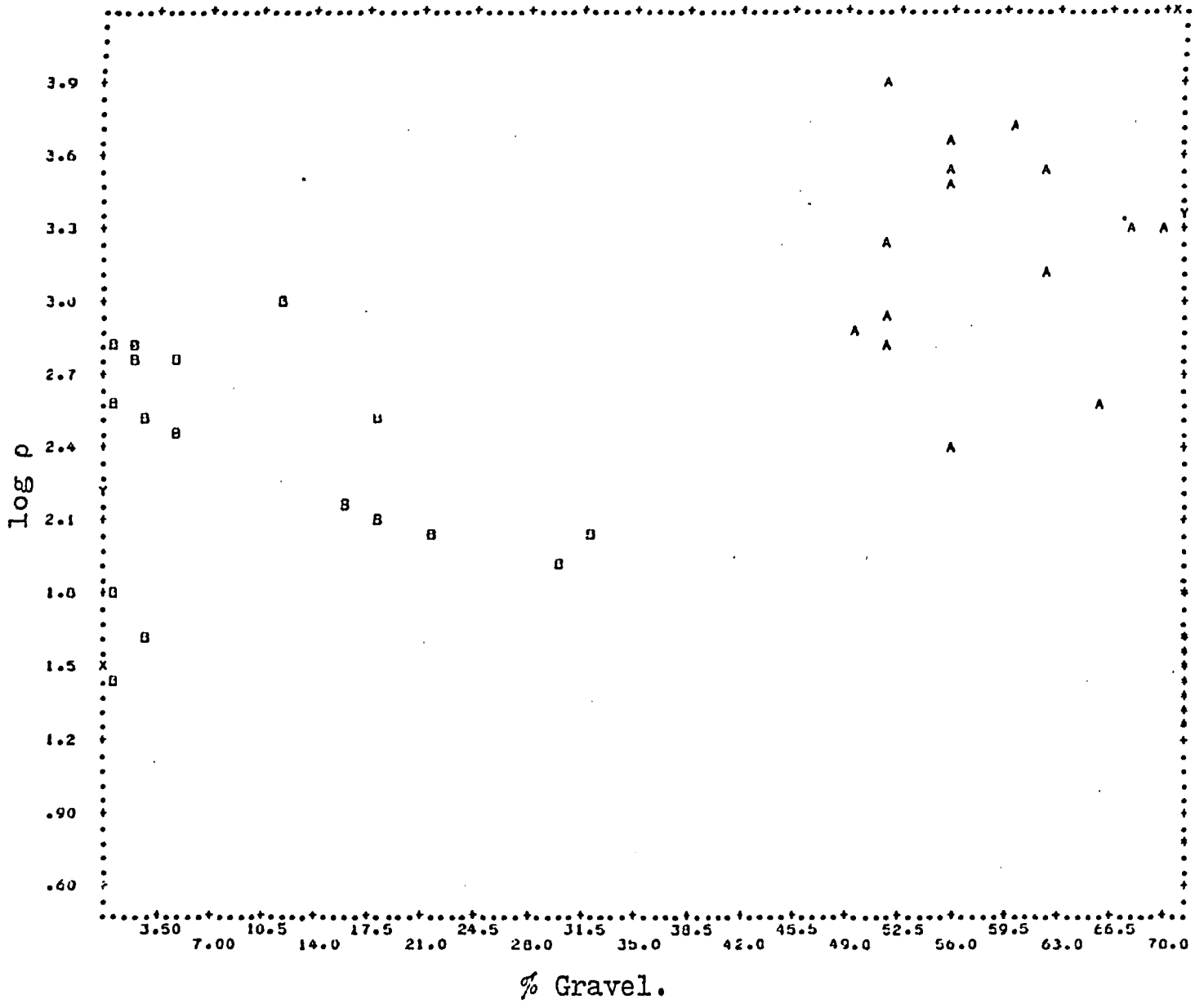

Fig. 18. % Gravel - log ρ plot. There are 32 samples from the SAND and GRAVEL groups. A, B, C as in Fig. 14.

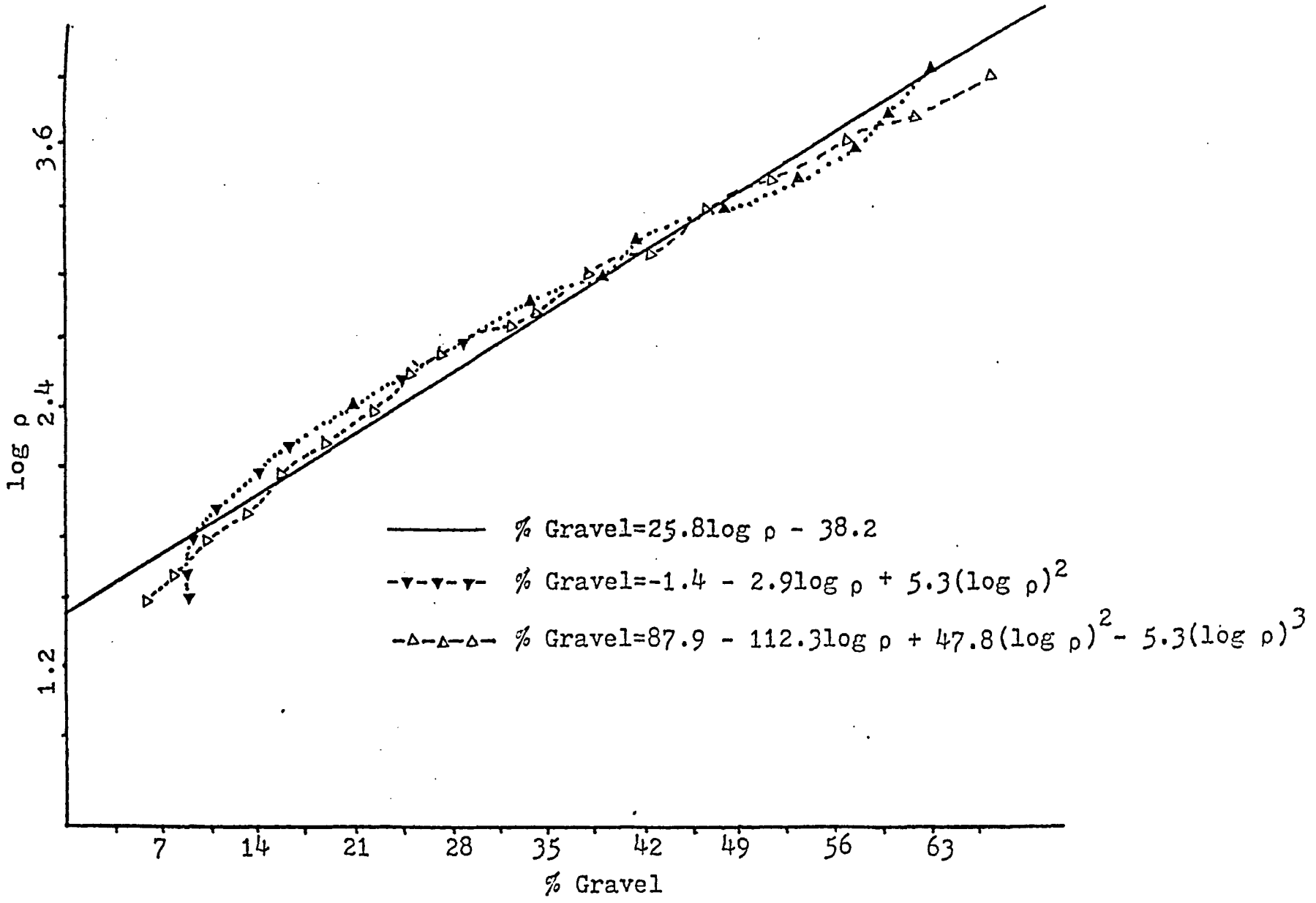

Fig. 19. Regression line and graphical solution of second and third degree polynomials.

When all the groups are compared together, the "% sand" is the only common parameter. Thus, the relationship between "% sand" and resistivity can be shown on a single plot, for all the samples. This is done on Fig. 20 which is a "% sand" versus log ρ plot. It is by far the best plot for showing the resistivity differences between the three groups. The CLAY group has generally lower resistivities than the other two groups. The overlap with two samples from the SAND group cannot be considered significant. It is attributed to moist samples.

Using this plot resistivity intervals can be established into which different materials are expected to fall. This is shown on Fig. 21 and it is summarized in Table 10.

5.3.ii Discussion of the results

It has been found that the resistivities of clays are lower than those of sand and gravel. Two factors must explain the difference in conductivity between these sediments: 1) the presence and salinity of water, and 2) the high content of quartz in sand and gravel.

Clay, sand and gravel are all porous. However, the porosity of clay is higher than that of sand and gravel. Therefore there are more ions in the pore fluids of clay than of sand and gravel. In addition to that, clays saturated with water will be surrounded by a film of partially mobile ions which will migrate under a potential

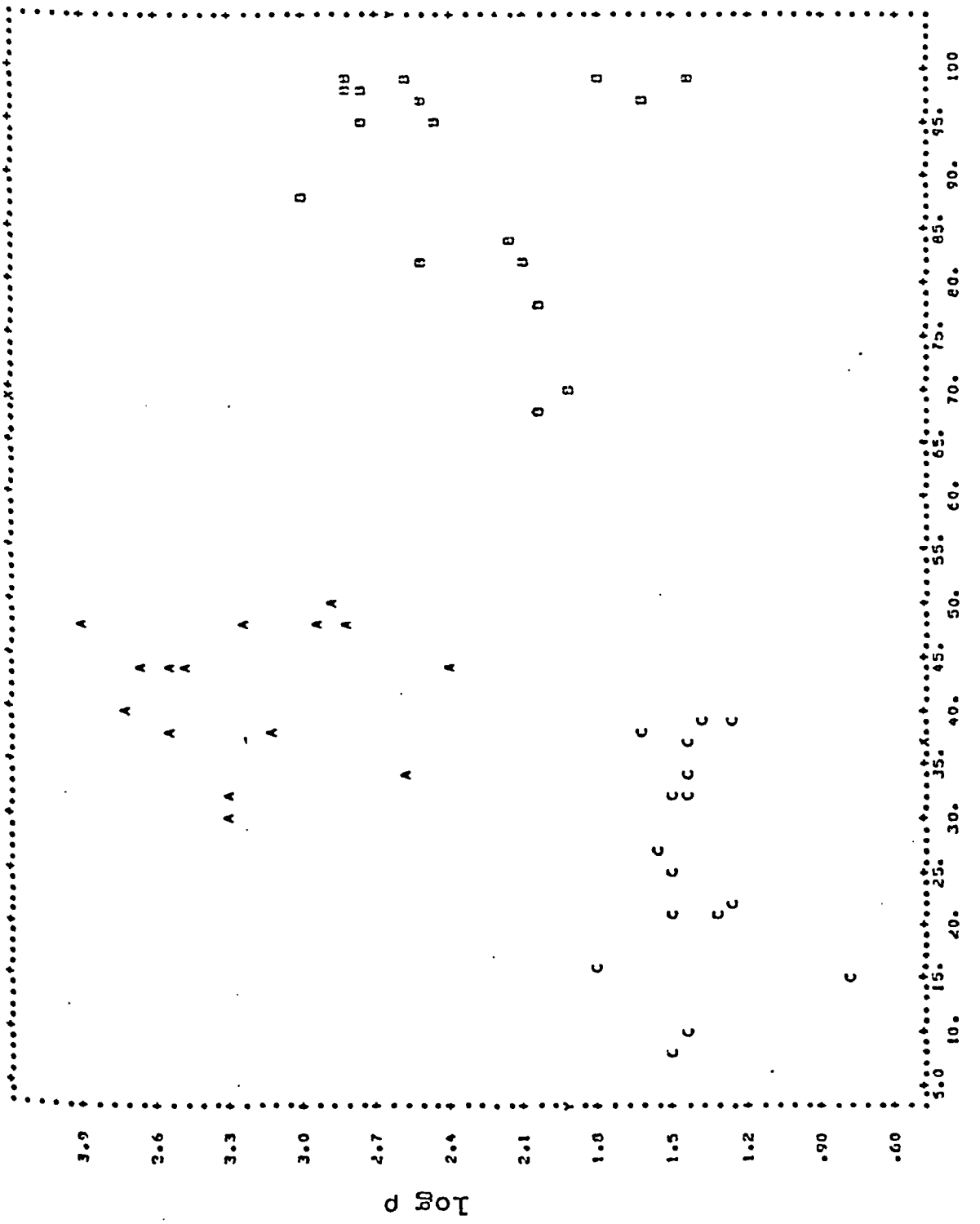

Fig. 20. % Sand - log ρ plot. All samples included. N=50. A, B, C as in Fig. 14.

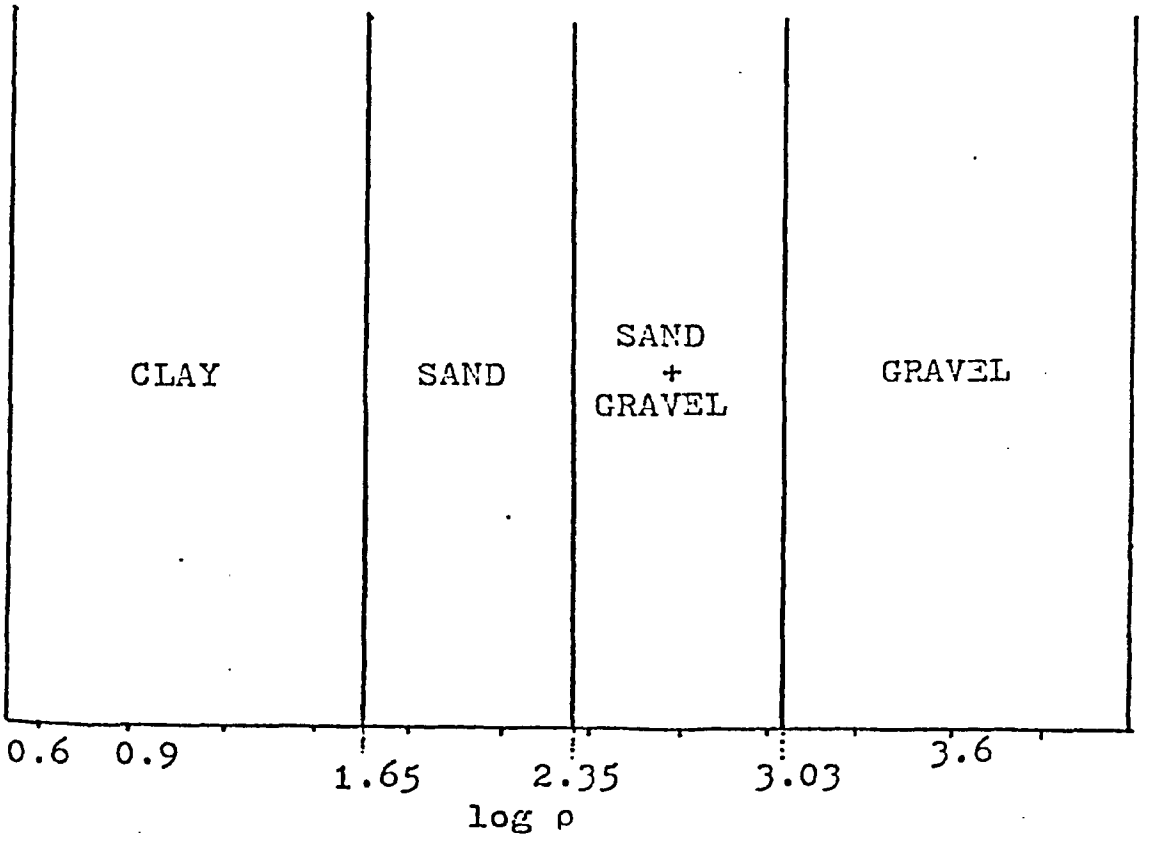

Fig. 21 .Log ρ intervals for the GRAVEL, SAND and CLAY groups.

Sediment is:	CLAY if log ρ <1.65 (or, if ρ <44.5)
	SAND if 1.65 log ρ <2.35 (or 45<ρ <224)
	SAND or GRAVEL if 2.35 <log ρ <3.0
	or if 224<ρ <1000)
	GRAVEL if log ρ >3.0 (or, if ρ >1000)

Table 10. Log ρ values for GRAVEL, SAND and CLAY

gradient. This happens because "clay minerals such as kaolinite, halloysite, montmorillonite and others have the property of sorbing certain anions and cations and retaining these in an exchangeable state. The common exchangeable ions adsorbed on clay are Ca, Mg, H, K, and NH_3 in order of decreasing abundance" (Keller and Frischnecht, 1966). These ions will make easier the passing of current in clay which consequently becomes more conductive than sand and gravel.

The high content of quartz also affects the conductivity of sand and gravel. Quartz has high resistivity. Unlike sand and gravel, clay does not have this mineral in abundance. This, in turn, increases the conductivity of clay while it decreases the conductivity of sand and gravel. Thus the resistivity of clay will be much lower than that of sand and gravel.

5.4 Integration of Electrical Resistivity and Seismic Data

The investigation of possible relationships between the electrical resistivity and seismic velocity of GRAVEL, SAND and CLAY was done by means of various plots for each group separately and for all sites combined.

The most useful plot for comparing these two variables is the log V - log ρ plot shown on Fig. 22. Although there is some overlap between the GRAVEL and SAND groups, the CLAY group can be separated. Boundary limits are shown

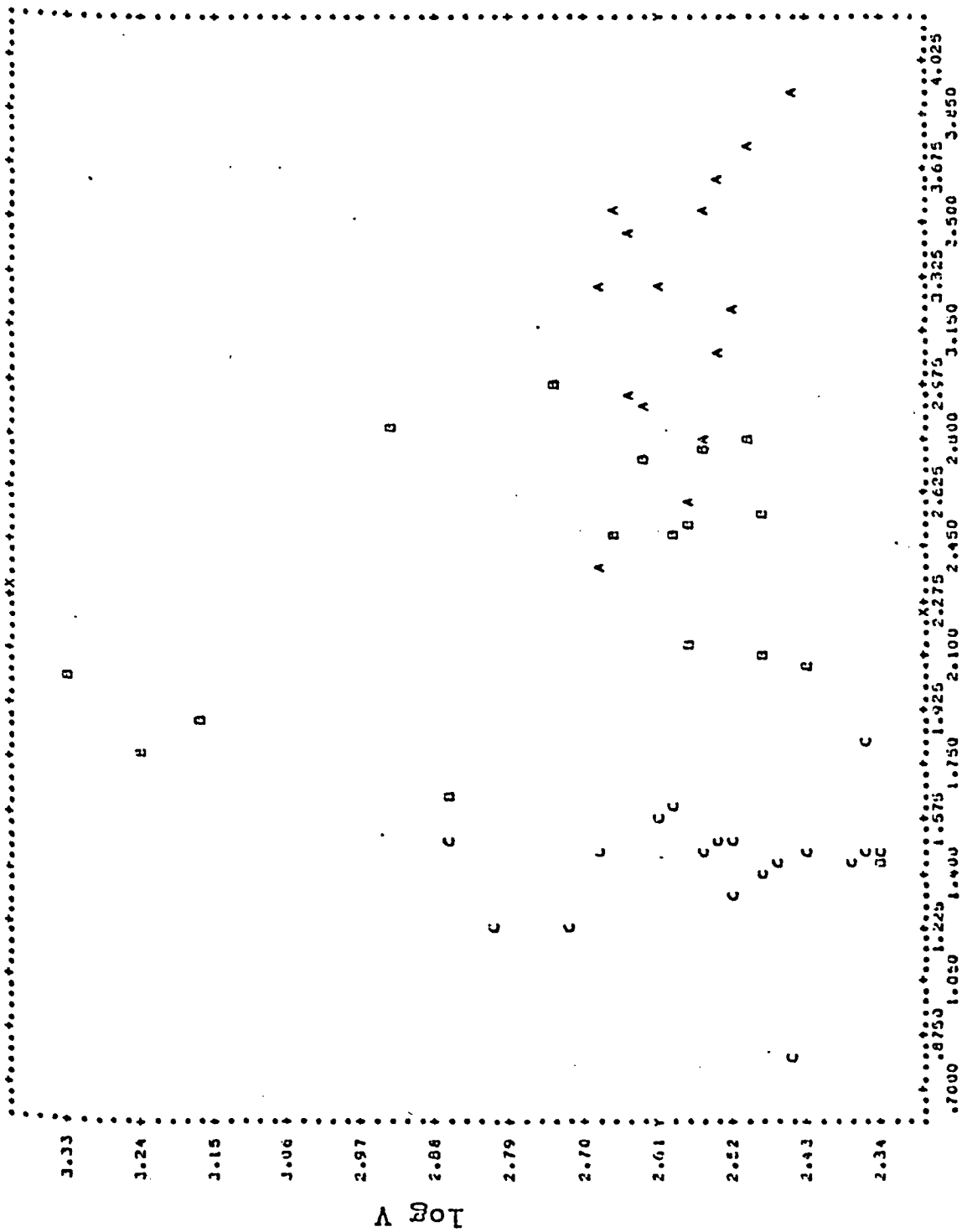

Fig. 22. log ρ - logV plot. All samples included. N=50. A, B, C as in Fig. 14.

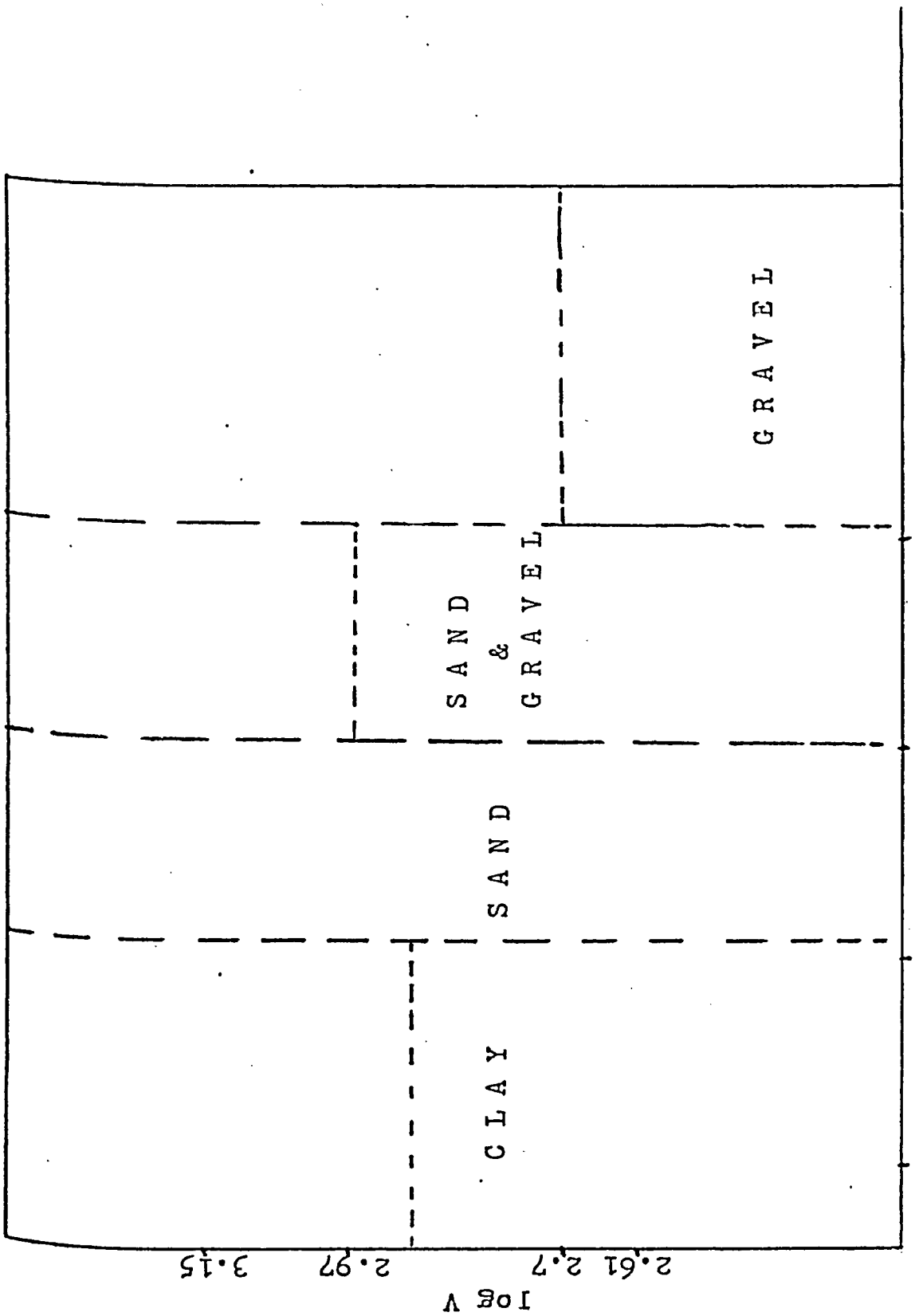

Fig. 23. Boundary limits of log V, log ρ for GRAVEL, SAND and CLAY.

on Fig. 23.

Comparing Fig. 21 and Fig. 23 it becomes apparent that the combination of both the electrical resistivity and seismic velocity methods does not improve on the information already derived from the electrical resistivity method alone.

CHAPTER VI

CONCLUSIONS

The investigation of the seismic velocities and electrical resistivities of GRAVEL, SAND and CLAY in Essex County show that for wide range of physical conditions:

1. The mean seismic velocity of GRAVEL is not significantly different from that of CLAY. The mean seismic velocity of SAND is significantly different from those of GRAVEL and CLAY at the 93.5 and 94.9 confidence level of significance respectively.

2. The large dispersion of the seismic velocities in the three sediments suggests that the seismic refraction survey will not effectively detect the gravel and/or sand underneath clay. Thus both the seismic refraction and reflection method would be ineffective in the geophysical exploration for gravel and sand deposits in Essex County.

3. The mean electrical resistivities of GRAVEL, SAND and CLAY are statistically different: GRAVEL from SAND at the 99.8% confidence level; GRAVEL from CLAY at the 99.9% confidence level; SAND from CLAY at the 99.9% confidence level.

4. The dispersion of the electrical resistivities of GRAVEL, SAND and CLAY is relatively small. The large contrast in the mean resistivity values of 2511, 318 and 29 ohm-m respectively suggest that the electrical resis-

tivity survey method would be an effective geophysical exploration tool in the search for gravel and sand deposits in Essex County.

5. Finally it is apparent that in a combined electrical and seismic survey offers no advantage in the exploration for gravel and sand deposits over running an electrical survey only.

REFERENCES

Armitage, P. 1971. Statistical methods in medical research. Blackwell Scientific Publications, 504p.

Bates, R. L. 1969. Geology of the industrial rocks and minerals. Dover Publications, 459p.

Burk, K. B. S. 1967. A review of some problems of seismic prospecting for groundwater in surficial deposits. Mining and Groundwater Geophysics, pp. 569-578.

Chapman, L. J. and Putnam, D. F. 1969. The Physiography of Southern Ontario. Univ. of Toronto Press, 386p.

Chasen, S. 1977. BMDP6D computer program. Biomedical computer programs, P-Series. Univ. of California, pp. 230-240.

Dobrin, M. B. 1976. Introduction to geophysical prospecting. McGraw-Hill, 630p.

Fu, S. and Douglas, J. BMDP3D computer program. Biomedical computer programs, P-Series. Univ. of California, pp. 170-183.

Geological Survey of Canada, 1958. Geological map of Southwestern Ontario, Map 1062A.

Goldthwait, R. P. 1973. The Wiskonsinan Stage. Geol. Soc. America, 334p.

Green, R. 1962. The hidden layer problem. Geophys. Prosp. 10, pp. 166-170.

Griffiths, D. H. and King, R. F. 1975. Applied Geophysics for Engineers and Geologists. Pergamon Press, 223p.

Hawkins, L. V. and Maggs, D. 1960. Nomograms for determining maximum errors and limiting conditions in seismic refraction method with a blind zone problem. Geophys. Prospect. 9, pp. 526-532.

Hewitt, D. F. 1963. Sand and Gravel deposits in Southern Ontario. Ont. Dept. of Mines, Ind. Min. Report, 151p.

_____. 1969. Sand and Gravel in Southern Ontario. Ont. Dept. of Mines, Ind. Min. Report, 105p.

Jakosky, J. J. 1955. Exploration Geophysics. Trija Pub. Co. 1152p.

Jacobson, R. P. 1955. Geophysical case history of a commercial sand and gravel deposit. Min. Eng. 7, pp. 158-162.

Johnson, R. B. 1959. Resistivity: a good bet in preliminary search for deposits. Rock Products, 63, No. 3, pp. 82-85.

Keller, G. V. and Frischknecht, F. C. 1970. Electric methods in geophysical prospecting. International Series in Electromagnetic Waves, 10. Pergamon Press, 519p.

Kennedy, J. B. and Neville, A. M. 1964. Basic statistical methods for Engineers and Scientists. International Textbook Company, 324p.

Knott, C. C. 1899. Reflection and refraction of elastic waves with seismological applications. Philosophical Mag. 48, pp. 64-97.

Kurtenacker, K. S. 1934. Use of resistivity method for locating and exploring deposits of stone and gravel. Rock Products, 37, No. 7, pp. 32-34.

Leverett, F. and Taylor, F. B. 1915. The Pleistocene of Indiana and Michigan and the history of the Great Lakes. U.S. Geol. Surv. Mono. 53.

Moore, W. R. 1945. An emirical method of interpretation of earth resistivity measurements. Min. Eng., Technical Publ., No. 1743.

_____. 1944. Prospecting for gravel deposits by resistivity methods. Public Roads, 24, No. 1, pp. 27-32.

_____. 1950. Geophysical methods of surface exploration applied to the location and evaluation of sand and gravel deposits. National Sand and Gravel Assoc. Circular No. 37, 18p.

Morgan, N. A. 1966. The use of continuous seismic profiler to solve hidden layer problems. Geophysics, 31, pp. 35-43.

Ontario Dept. Mines. 1975. 1976-1977. Mineral Review.

Orellana, E. and Mooney, H. M. 1966. Master tables and curves for vertical electrical sounding over layered structures. Interciencia Costanilla de Los Angeles, 15 Madrid, 160p.

Proctor and Redfern Ltd., Gartner Lee Assoc. Ltd. 1975. Mineral aggregate study and Geological inventory. Southwestern region of Ontario, 37p., 129 maps, 45 plates.

Soske, J. L. 1959. The blind zone in Engineering Geophysics. Geophysics, 24, pp. 356-365.

Taylor, F. B. 1913. The moraine systems of southwestern Ontario. Trans. Roy. Can. Inst., 10, pp. 1-23.

Telford, W. M. et al. 1976. Applied Geophysics. Cambridge Univ. Press, 860p.

Wilcox, S. W. 1944. Sand and gravel prospecting by the earth resistivity methods. Geophysics, 9, pp. 36-46.

Wilkinson, J. C. 1978. The relationship between: the Atterberg limits and the natural sorption capacity of clay soils. B.A.Sc. Thesis, Univ. of Windsor, Ont., 64p.

APPENDIX I

GRAIN SIZE ANALYSIS

Tables-Graphs

Site #	Cumulative Percent Passing Sieve									
	3/4"	1/2"	3/8"	#4	#8	#16	#30	#50	#100	#200
16	100	100	100	100	99.9	99.8	99.3	79.4	5.3	.8
17	87.6	85.6	83.3	79.0	77.9	73.9	68.6	46.7	7.0	.9
18	100	100	100	93.7	87.2	65.4	29.6	10.9	.8	.1
19	100	100	100	100	98.8	96.9	89.8	69.5	21.4	.7
20	100	100	100	100	99.3	97.0	80.8	52.4	4.9	.3
21	100	100	100	100	99.9	99.7	98.2	78.2	5.5	.2
22	100	100	100	100	87.0	24.2	6.0	4.7	.1	.0
23	100	100	100	99.0	90.0	80.2	76.7	58.2	6.3	.8
24	100	100	100	99.6	98.2	94.3	84.9	60.2	32.5	.7
25	100	100	100	98.0	90.1	64.8	44.2	20.6	4.2	.7
26	100	93.9	90.4	79.4	70.2	60.7	47.7	28.1	7.1	1.0
27	100	95.1	92.9	88.4	82.7	78.5	73.6	52.3	26.7	.8
28	100	100	100	100	99.2	96.1	91.1	71.4	19.3	1.0
29	100	100	100	99.2	97.8	96.0	78.0	52.3	10.1	.7
30	100	100	99.3	97.0	96.0	94.2	75.1	54.8	18.1	.4
31	100	100	100	100	99.2	98.7	94.3	49.6	2.6	.4
32	100	100	100	100	99.0	98.1	92.0	51.7	13.6	.5

Table 12. Grain size analyses for the samples of the SAND group.

Site #	Cumulative Percent Passing Sieve									
	3/4"	1/2"	3/8"	#4	#8	#16	#30	#50	#100	#200
1	95.0	91.8	86.7	72.2	54.0	36.3	19.5	5.2	2.7	1.0
2	92.0	74.2	60.1	50.5	40.1	20.8	8.4	3.2	1.8	.7
3	100	96.8	96.0	74.3	44.4	26.5	19.9	4.8	2.4	.8
4	85.1	73.2	65.9	57.5	49.5	41.6	29.8	7.7	3.2	.9
5	88.5	80.3	76.5	62.8	47.9	34.3	20.8	7.8	4.0	1.0
6	81.9	74.6	65.1	58.0	47.1	37.2	28.0	12.5	4.1	.7
7	85.3	79.2	75.0	65.6	45.9	42.0	38.3	13.1	1.9	.8
8	88.7	80.7	75.2	62.4	46.0	39.9	29.9	18.6	9.3	1.0
9	100	99.5	91.6	72.2	52.1	42.8	32.3	17.1	5.5	.9
10	100	93.3	89.9	75.9	56.1	36.0	13.9	2.1	1.8	.7
11	100	98.7	84.5	70.9	52.0	35.7	18.4	7.0	2.0	.9
12	88.0	71.9	66.0	50.1	36.2	32.0	29.9	26.2	2.1	.8
13	83.6	83.1	74.0	55.1	36.3	17.7	6.0	3.8	2.0	.8
14	96.0	86.1	71.9	48.0	33.8	28.1	10.0	2.7	1.0	.7
15	87.5	81.2	70.0	52.8	41.6	32.9	27.6	9.6	3.0	1.0

Table 11. Grain size analyses for the samples of the GRAVEL group.

Site #	% Clay+Silt	% Sand
33	85	15
34	78	22
35	68	32
36	66	34
37	68	32
38	68	32
39	79	21
40	84	16
41	62	38
42	61	39
43	66	34
44	61	39
45	78	22
46	75	25
47	90	10
48	92	8
49	79	21
50	63	37

Table 13. Grain size analyses for the samples of the CLAY group

Figure #	Sites plotted
24.1	1, 2, 8, 10, 12
24.2	3, 4, 5, 6, 7
24.3	9, 11, 13, 14, 15
24.4	16, 18, 19, 22, 23, 26
24.5	17, 24, 25, 28, 31
24.6	20, 21, 27, 29, 30, 32

Table 14. Grain size plots included in Appendix I.

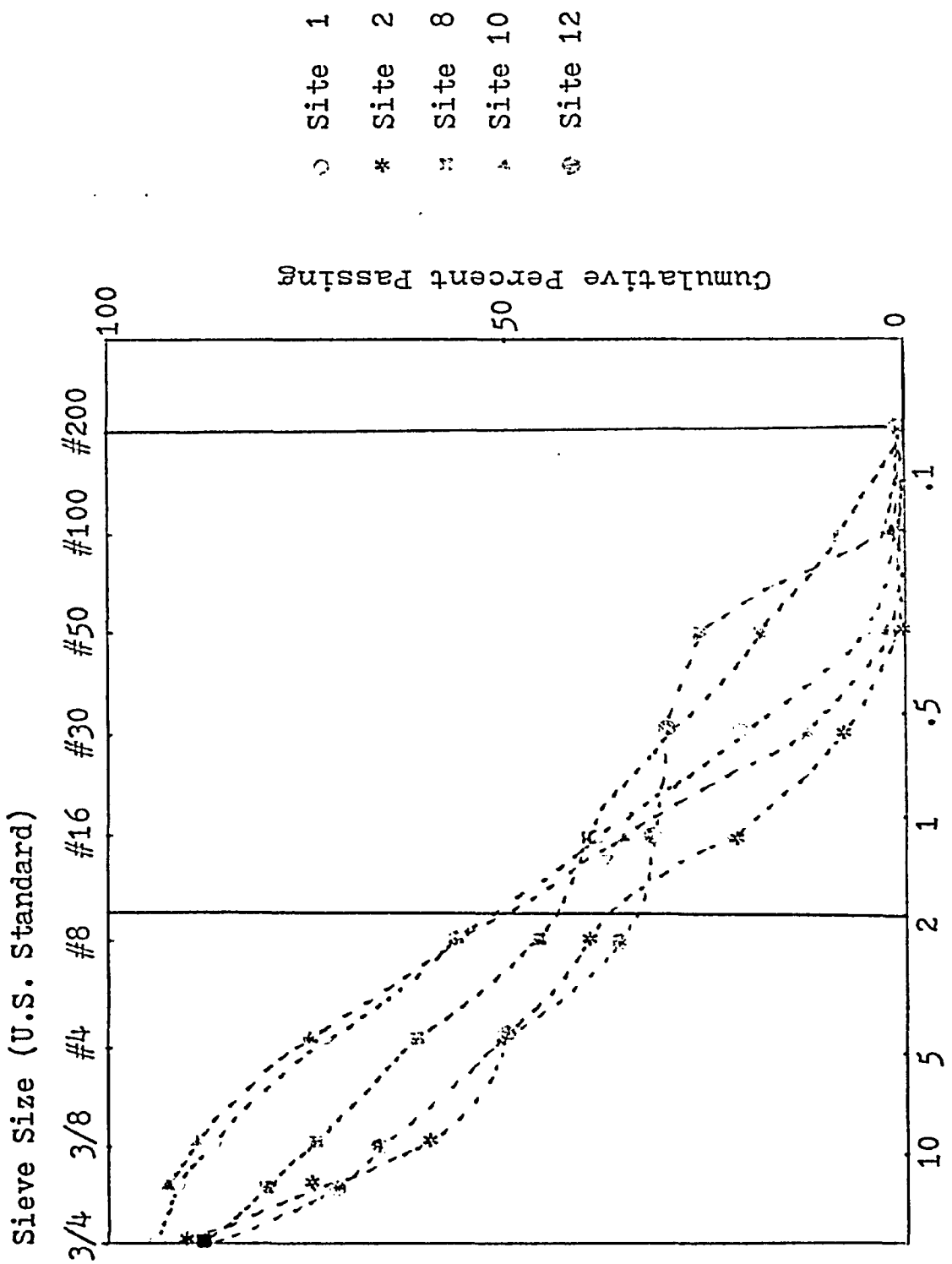

Fig. 24.1.

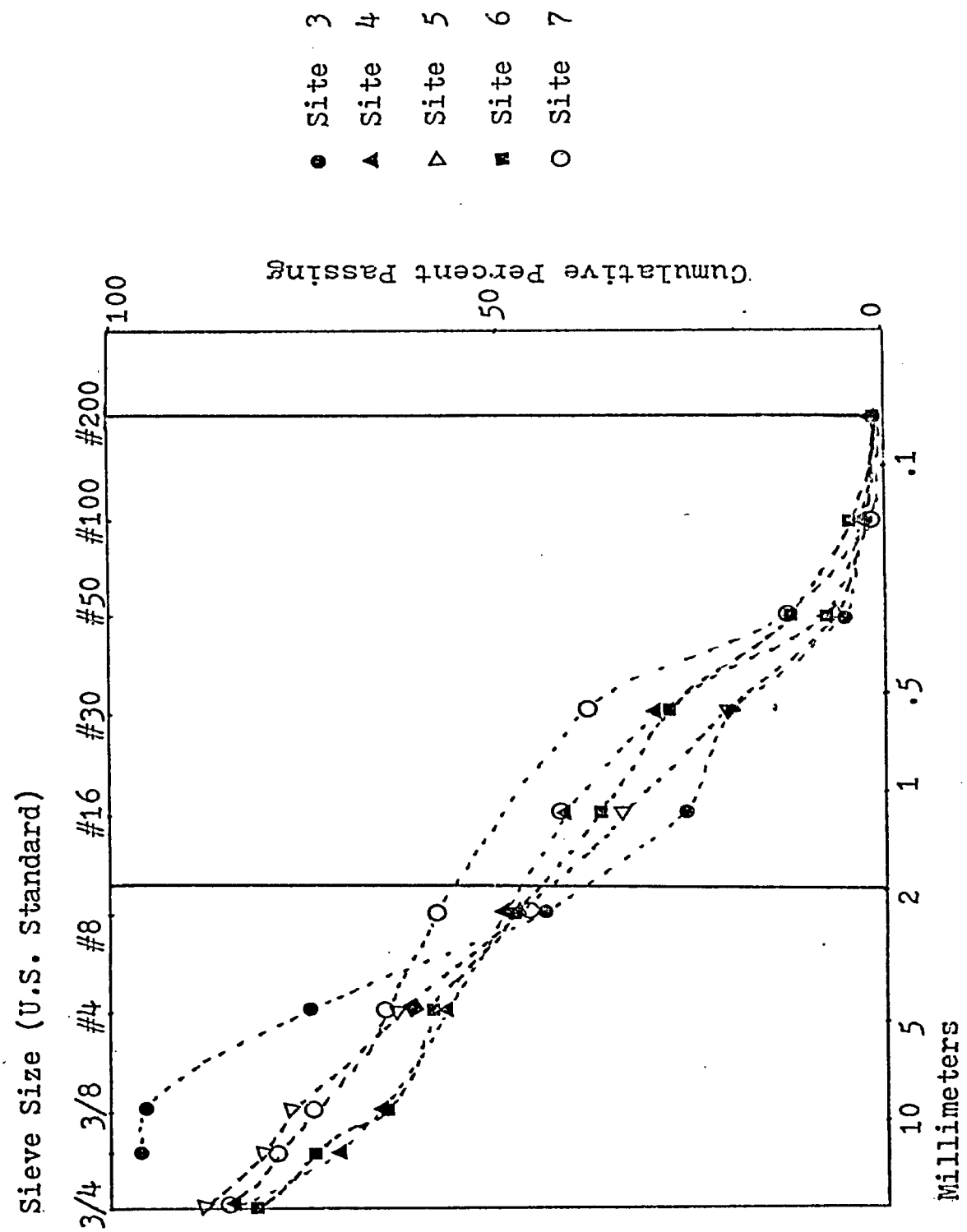

Fig. 24.2.

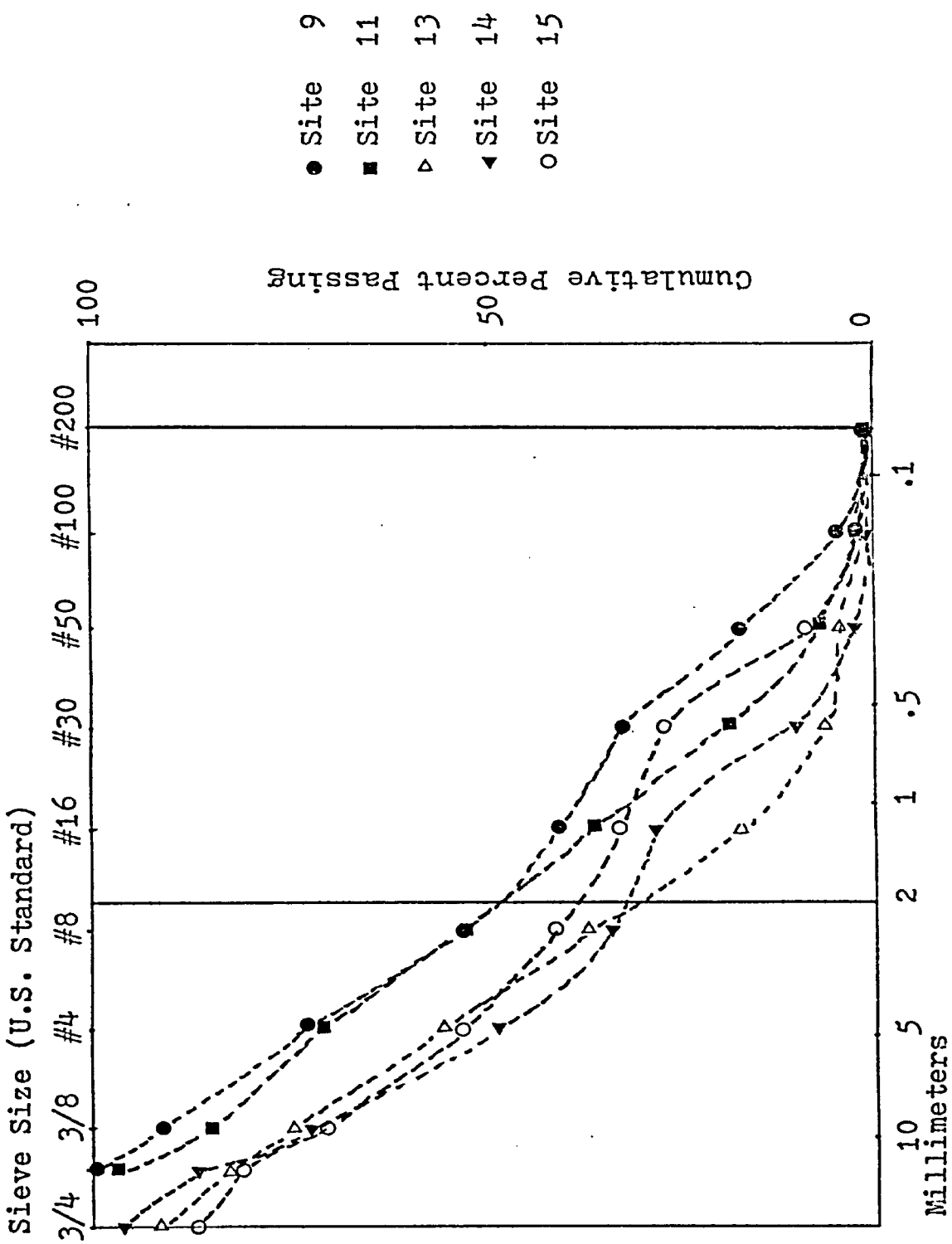

Fig. 24.3.

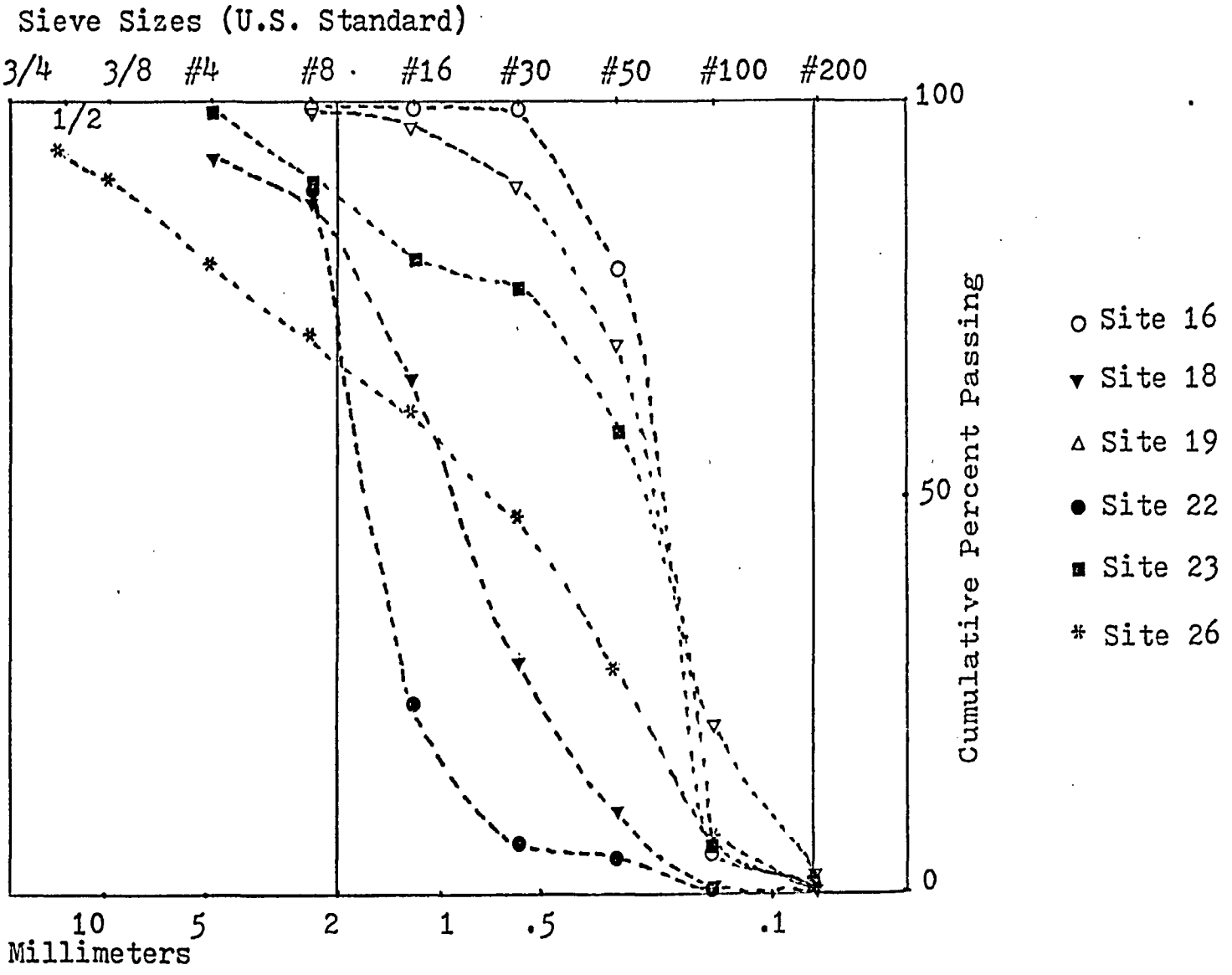

Fig. 24.4.

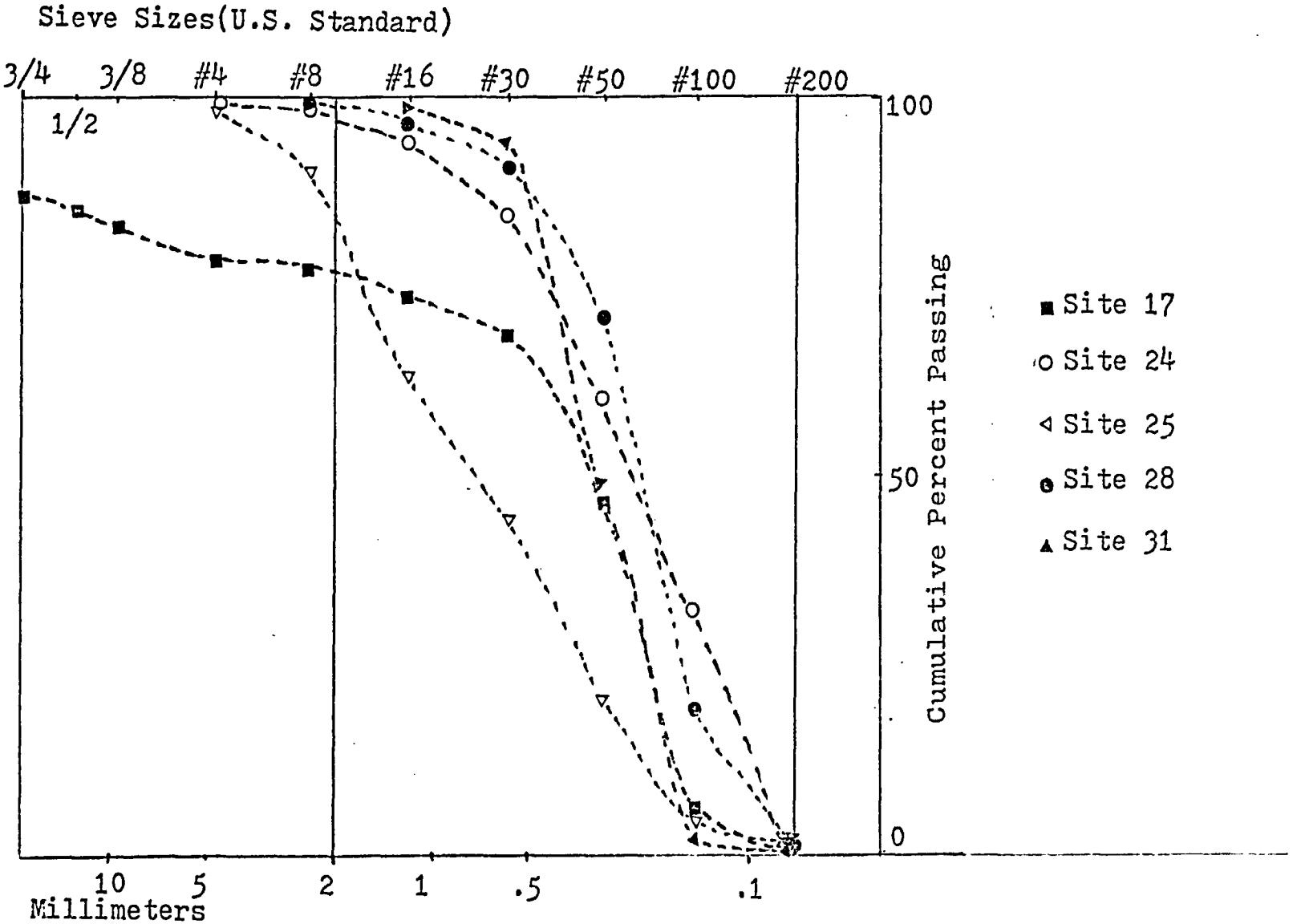

Fig. 24.5.

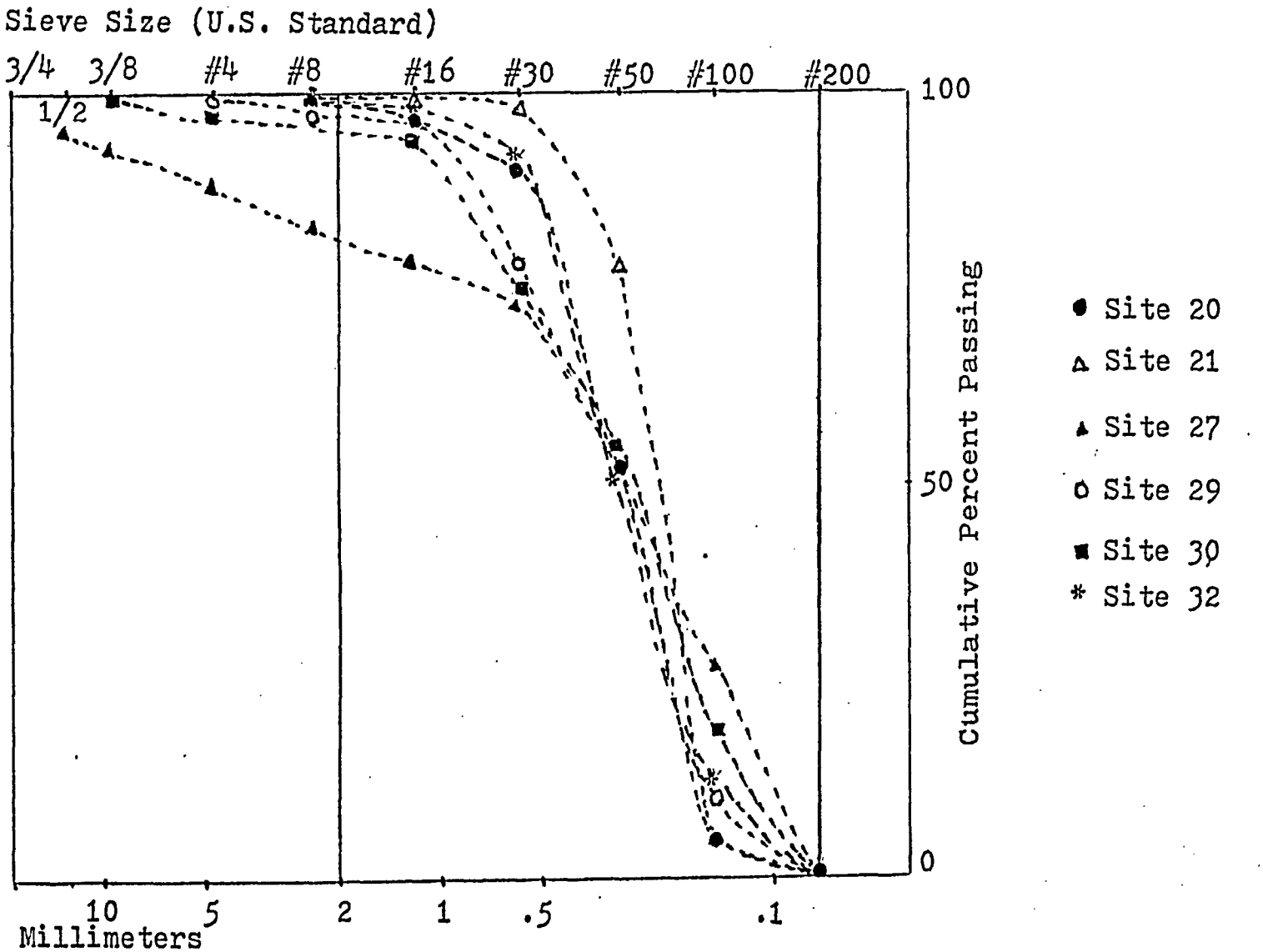

Fig. 24.6.

APPENDIX II

SEISMIC VELOCITIES

Tables-Seismic records

Site #	X, m	0.61	1.22	1.83	2.44	3.05	3.66	4.27	4.88	Velocity (m/sec)
2	T_i	8.6	10.3	12.1	14.2	16.0	17.2	19.2	20.7	343.2
		8.6	10.3	12.1	14.0	16.0	17.2	19.4	20.6	
		8.6	10.3	12.2	13.0	16.1	17.2	19.3	20.8	
			10.1	12.2	13.8	16.2	17.2	19.3	20.7	
	T_{av}	8.6	10.25	12.15	13.75	16.07	17.2	19.3	20.7	
3	T_i	3.3	5.5	7.2	9.0	10.9	12.7	14.7		312.4
		3.2	5.1	7.1	9.3	11.0	12.9	14.7		
		3.0	5.3	7.2	9.0	10.9	12.8	14.7		
		3.2	5.2	7.3	8.9	10.9	12.8	14.7		
	T_{av}	3.17	5.22	7.2	9.1	10.92	12.8	14.7		
4	T_i	1.4	3.8	5.7	8.5	10.6	11.9	14.2		281.3
		1.6	4.0	5.8	8.4	10.1	12.2	14.2		
		1.5	3.8	5.9	8.2	10.4	12.4	14.2		
		1.5	3.9		8.2	10.4	12.4	14.2		
	T_{av}	1.5	3.87	5.8	8.32	10.37	12.22	14.2		
5	T_i	9.4	9.1	10.2	12.1	13.2	15.5	17.1	17.9	435.2
		9.0	9.2	10.4	11.9	13.2	15.6	16.7	17.7	
		8.8	8.9	10.1	11.9	13.5	15.4	16.8	17.8	
		8.8	8.9	10.2	11.9	13.4	15.5	16.9	18.0	
	T_{av}	9.0	9.06	10.22	11.95	13.32	15.5	16.9	17.85	

Table 15. Arrival times and calculated seismic velocities for 26 sites in Essex County. T_i is the arrival time of a seismic wave at a distance X. 3-4 readings were taken at each station. T_{av} is the average reading. Table 15 continues up to page 113.

Site #	X,m	0.61	1.22	1.83	2.44	3.05	3.66	4.27	4.88	Velocity (m/sec)
6		7.0	7.9	9.4	10.9	13.4	15.1	16.2		
		6.8	7.8	9.4	10.7	13.3	15.0	16.1		348.1
		7.1	7.8	9.3	10.7	13.2	14.8	16.2		
		7.2		9.2	10.8	13.3	14.9	16.2		
	T_{av}	7.02	7.83	9.32	10.77	13.3	14.95	16.17		
19		5.6	6.4	7.0	7.5	8.4	9.3	10.1	10.6	
		5.6	6.4	7.0	7.5	8.5	9.2	10.0	10.6	
		5.6	6.5	7.0	7.4	8.6v	9.2	9.9	10.6	853.4
		5.6	6.3	7.1	7.8	8.6	9.3	10.0		
	T_{av}	5.6	6.4	7.025	7.55	8.525	9.25	10.0	10.6	
20		5.2	6.6	8.4	12.0	10.2	13.6	15.1		
		5.2	6.6	8.4	12.0	10.2	13.6	15.4		
		5.3	6.6	8.4	12.0	10.2	13.7	15.3		365.8
		5.3		8.5	12.1	10.2	13.7	15.2		
	T_{av}	5.25	6.6	8.425	10.2	12.025	13.65	15.25		
21		7.5	9.4	11.3	13.2	14.6	17.2	18.6		
		7.6	9.5	11.4	13.2	14.6	17.2	18.7		
		7.4	9.6	11.4	13.2	14.5	17.2	18.6		320.6
		7.4	9.4	11.3		14.7		18.7		
	T_{av}	7.5	9.475	11.35	13.2	14.60	17.2	18.65		

Site #	X,m	0.61	1.22	1.83	2.44	3.05	3.66	4.27	4.88	Velocity (m/sec)
23	T_i	6.7 6.7 6.7	7.6 7.6 7.6	8.8 8.7 8.7 8.8	10.0 10.0 10.0	11.1 11.1 11.1	12.3 12.3 12.3	13.4 13.3 13.3 13.4	14.4 14.4 14.4	548.6
	T_{av}	6.7	7.6	8.75	10.0	11.1	12.3	13.35	14.4	
24	T_i	7.8 7.6 8.3 8.2	9.6 9.9 9.7 9.8 10.0	11.5 11.5 11.7 11.8	14.1 14.3 14.1 14.1	16.1 15.9 15.8 16.1 16.0	18.3 17.7 17.7 18.3 18.5	20.2 20.1 20.3 20.2		381.0
	T_{av}	7.975	9.8	11.625	14.15	15.98	18.1	20.2		
25	T_i	8.0 7.9 8.1 8.0	9.1 9.3 9.2 9.2	10.8 11.3 11.5 11.0	12.7 12.6 12.6 12.5	14.6 14.6 14.5 14.5	15.9 15.8 15.9 16.2	17.3 17.5 17.4 17.4		369.4
	T_{av}	8.0	9.2	11.15	12.6	14.55	15.95	17.4		
26	T_i	7.8 7.6 7.6 7.7	9.7 9.7 9.8 9.9	12.5 12.4 12.4 12.6	14.6 14.5 14.5 14.4	16.7 16.6 16.4 16.6	18.9 18.6 18.4 18.5	20.9 21.0 21.1 21.0		270.7
	T_{av}	7.675	9.775	12.475	14.5	16.575	18.6	21.0		

Site #	X, m	0.61	1.22	1.83	2.44	3.05	3.66	4.27	4.88	Velocity (m/sec)
27	T_i	3.4 3.4 3.4 3.4	5.3 5.3 5.3 5.2	7.3 7.3 7.3 7.3	9.5 9.3 9.3 9.4	11.7 11.5 11.4 11.5	13.9 13.5 13.5 13.7	15.7 14.6 14.5		304.8
	T_{av}	3.4	5.275	7.3	9.375	11.725	13.85	14.93		
32	T_i	4.3 4.3 4.3	5.7 5.7 5.7	6.8 6.7 6.7 6.8	8.0 8.0 8.0	9.4 9.4 9.4	10.6 10.6 10.4 11.0	12.2 12.1 12.2 12.1		461.8
	T_{av}	4.3	5.7	6.75	8.0	9.4	10.65	12.15		
34	T_i	11.4 11.4 11.6 11.4	12.6 12.8 12.9 12.9	13.3 13.2 13.0	14.3 14.0 13.9 14.1	15.5 15.5 15.4 15.4	16.8 16.6 16.7	17.4 17.5 17.6 17.5	18.7 18.3 18.1 18.1	641.6
	T_{av}	11.35	12.8	13.16	14.07	15.45	16.66	17.5	18.3	
35	T_i	7.3 7.0 6.2 6.4	9.4 8.7 9.1 9.0	12.6 12.7 12.7 12.6	15.2 15.1 14.9 14.9	17.1 17.8 17.5 17.6	19.5 20.7 19.7 19.9	23.4 23.0 22.8 23.0		234.4
	T_{av}	6.72	9.05	12.65	15.02	17.5	19.95	23.05		

Site	X,m	0.61	1.22	1.83	2.44	3.05	3.66	4.27	4.88	Velocity (m/sec)
36	T_i	4.0	6.4	9.0	11.6	13.2	15.3	18.5		268.2
		3.8	6.5	9.0	11.1	13.3	15.4	18.5		
		3.9	6.7	9.0	11.2	12.6	15.2	18.3		
		3.5	6.5	9.0	11.3	12.9	15.3	18.4		
	T_{av}	3.8	6.27	9.0	11.3	12.97	15.3	18.42		
37	T_i	3.3	5.3	6.4	9.4	10.7	13.2	15.3		329.9
		3.3	5.2	6.5	9.1	10.7	13.4	15.1		
		3.5	5.2	6.5	9.0	10.6	13.3	15.2		
		3.2	5.1	6.3	9.2	10.6	13.2	15.2		
	T_{av}	3.325	5.2	6.42	9.17	10.65	13.25	15.2		
38	T_i	3.5	6.4	8.5	11.9	14.9	17.3	20.0		218.8
		3.3	6.2	8.7	11.7	14.7	17.5	19.7		
		3.5	6.3	8.8	11.8	14.8	17.5	19.7		
			6.3	8.8	11.8	14.8	17.5	19.9		
	T_{av}	3.45	6.3	8.7	11.8	14.8	17.45	19.83		
39	T_i	9.7	11.2	13.2	15.4	17.1	19.4	20.3	26.7	328.0
		9.5	11.4	13.3	15.8	17.2	19.3	20.4	22.6	
		9.6	11.1	13.5	15.5	17.3	19.0	20.3	22.6	
		9.3	10.8	13.2	15.2	17.2	19.1	20.1	22.5	
	T_{av}	9.52	11.12	13.3	15.47	17.2	19.2	20.27	22.6	

Site #	X, m	0.61	1.22	1.83	2.44	3.05	3.66	4.27	Velocity (m/sec)
40	T_i	5.9	8.6	11.2	13.4	16.1	18.8	21.2	228.9
		5.6	8.3	11.5	13.8	16.5	19.1	21.2	
		5.4	8.7	10.9	13.7	16.5	19.1	21.3	
		5.7	7.9	11.4	13.8	16.3	18.9	21.1	
	T_{av}	5.65	8.37	11.25	13.67	16.35	18.97	21.2	
41	T_i	6.7	8.6	10.0	11.8	13.4	14.9	16.5	391.4
		6.7	7.4	10.2	11.8	13.5	14.9	16.1	
		6.8	8.5	10.0	11.6	13.2	14.9	16.2	
		6.7	8.5	10.1	11.7	13.3	14.9	16.4	
	T_{av}	6.72	8.5	10.07	11.72	13.35	14.9	16.3	
42	T_i	3.1	4.8	6.9	9.6	11.4	12.8	15.8	304.8
		3.1	4.8	6.9	9.3	11.1	13.0	14.9	
		3.1	4.8	6.8	9.0	10.9	13.0	14.8	
		3.1	4.8	7.0	9.2	11.3	12.9	14.7	
								14.9	
	T_{av}	3.1	4.8	6.9	9.27	11.17	15.92	15.22	
43	T_i	9.3	11.4	13.4	15.6	16.5	18.5	20.3	484.3
		9.3	11.2	13.1	15.0	16.4	18.3	20.2	
		9.2	11.2	12.9	14.8	16.4	18.4	20.4	
		9.2	11.3	12.9	15.0	16.6	18.5	20.3	
				12.9					
	T_{av}	9,25	11.27	13.04	15.1	16.47	18.42	20.3	

Site #	X,m	0.61	1.22	1.83	2.44	3.05	3.66	4.27	4.88	Velocity (m/sec)
49		4.8	6.2	8.5	10.3	12.0	13.6	15.6	17.4	
		4.8	6.4	8.4	10.1	11.9	13.6	15.7	17.2	
	T_i	4.8	6.6	8.6	10.2	12.1	13.6	15.8	17.3	341.4
				8.4	10.4	12.0		15.7	17.3	
	T_{av}	4.8	6.45	8.47	10.25	12.0	13.6	15.7	17.3	
50		9.6	11.5	13.3	15.7	18.2	20.0	22.3		
		9.6	11.9	13.6	15.6	18.0	20.2	22.1		
	T_i	9.6	11.6	13.5	15.8	17.8	20.4	22.2		290.2
		9.6	11.8	13.6	15.7	17.8	19.8	22.2		
	T_{av}	9.6	11.7	13.5	15.7	17.95	20.1	22.2		

Figure #	Seismic record of site
25. 1	1
25. 2	7
25. 3	8
25. 4	9
25. 5	10
25. 6	11
25. 7	12
25. 8	13
25. 9	14
25.10	15
25.11	16
25.12	17
25.13	18
25.14	22
25.15	28
25.16	29
25.17	30
25.18	31
25.19	33
25.20	44
25.21	45
25.22	46
25.23	47
25.24	48

Table 16. Seismic records included in Appendix II.

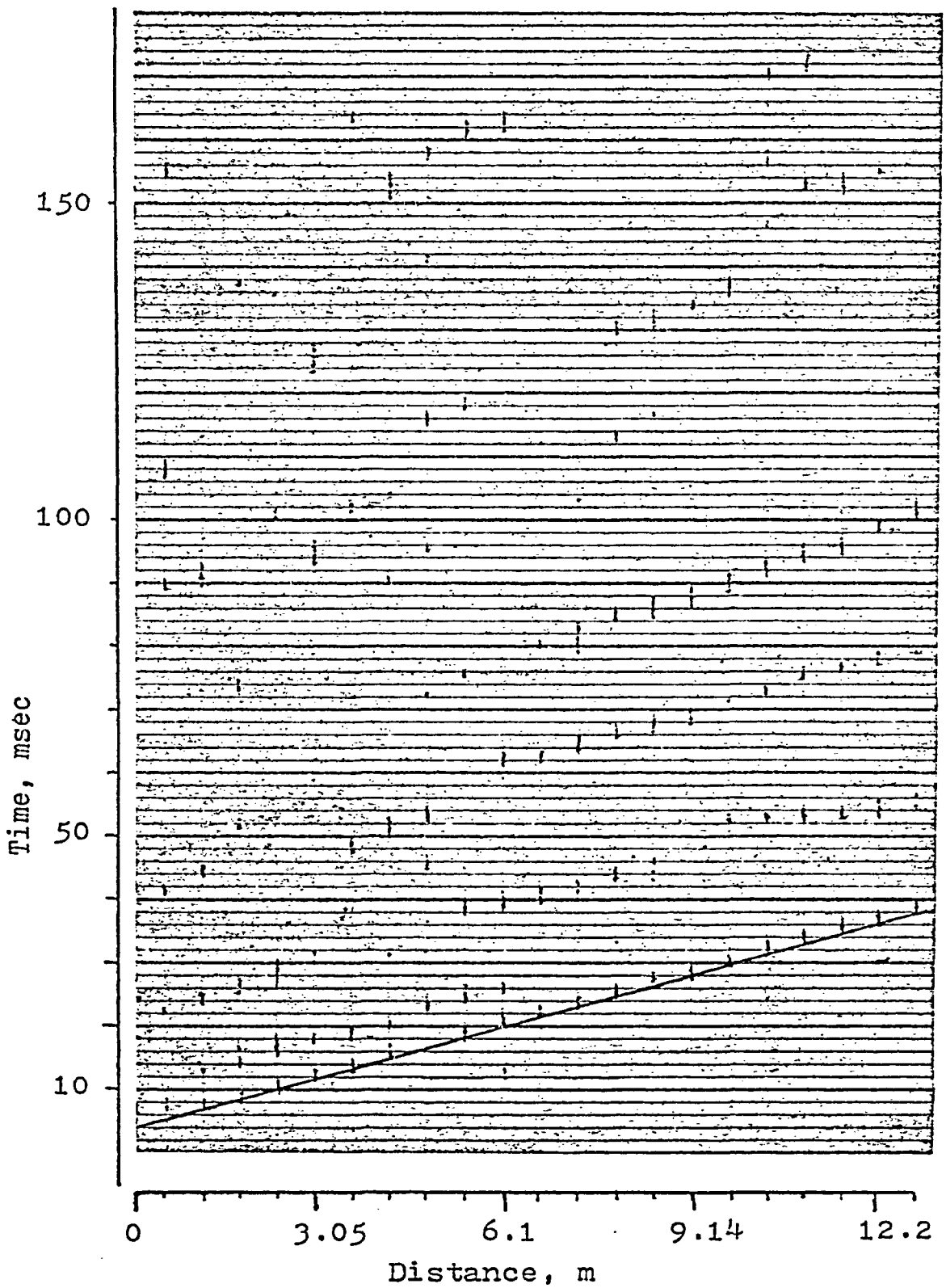

Fig. 25.1.

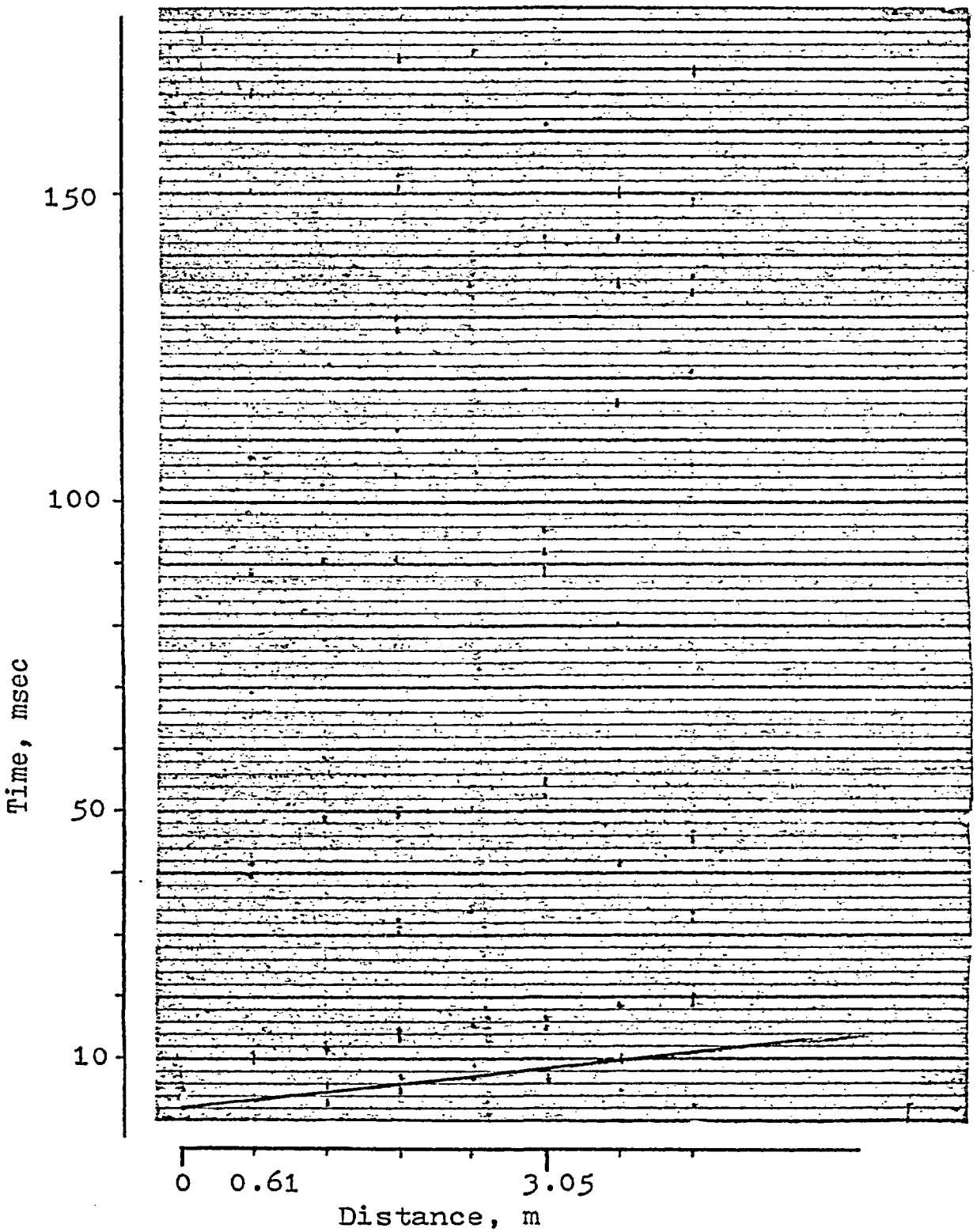

Fig.25.2.

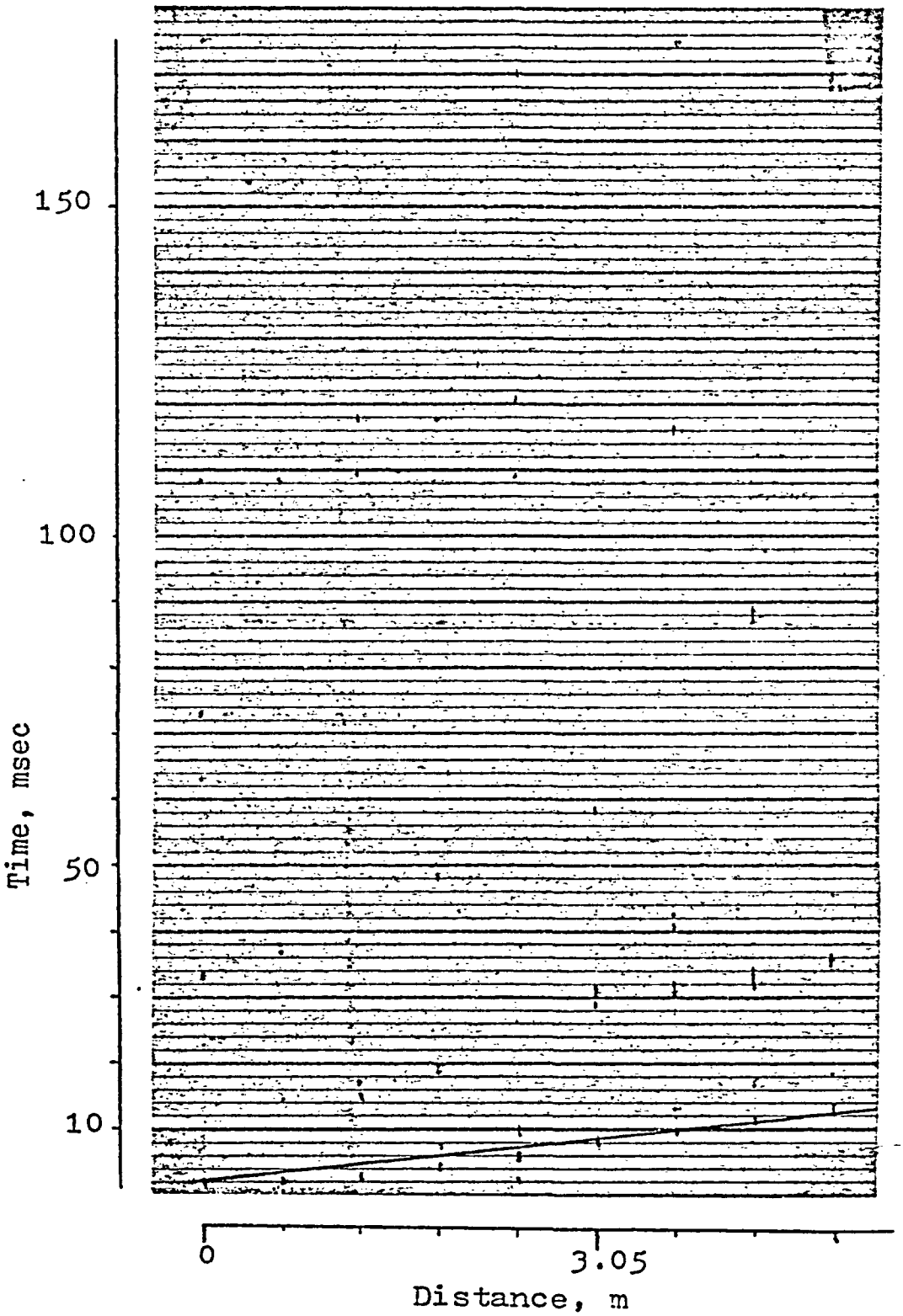

Fig. 25.3.

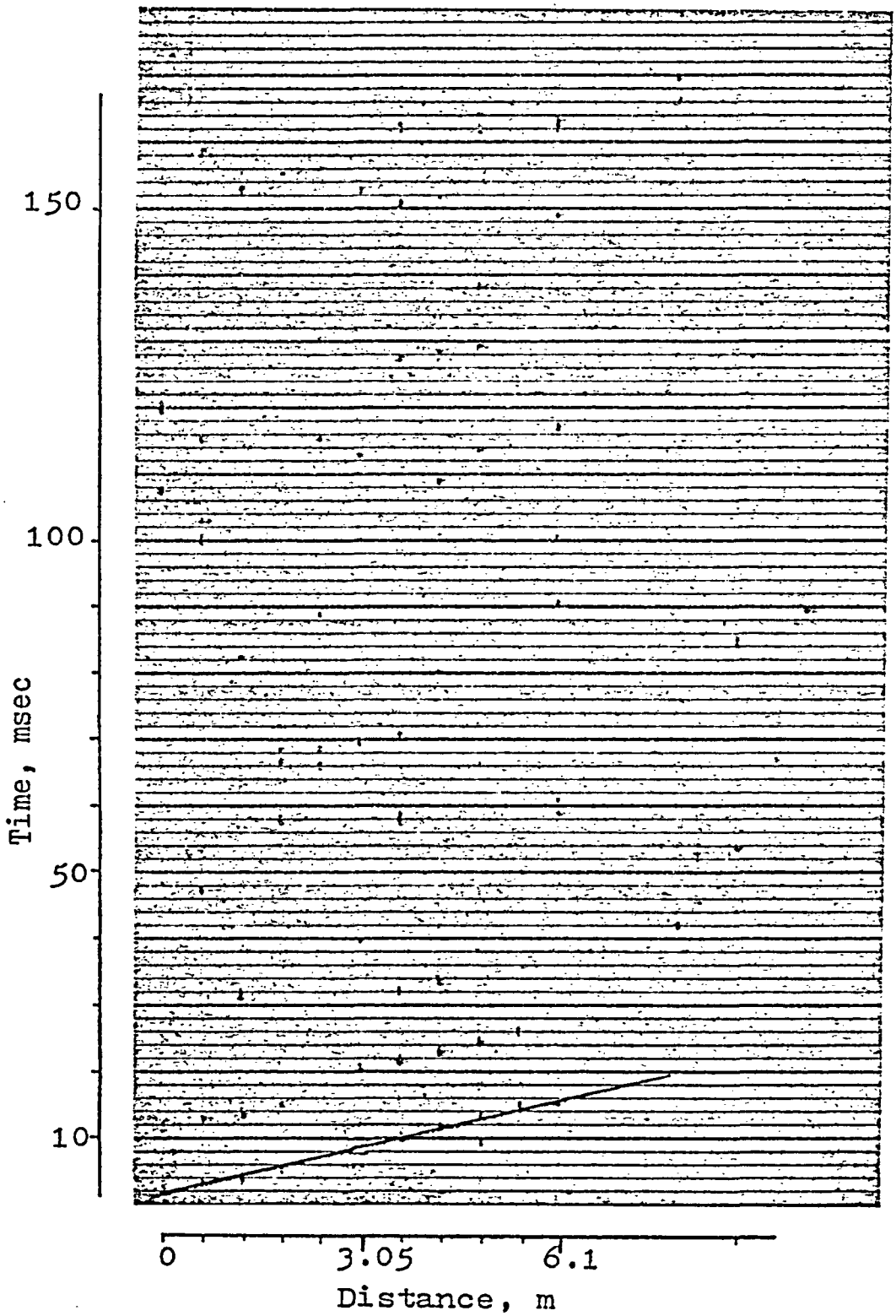

Fig. 25.4.

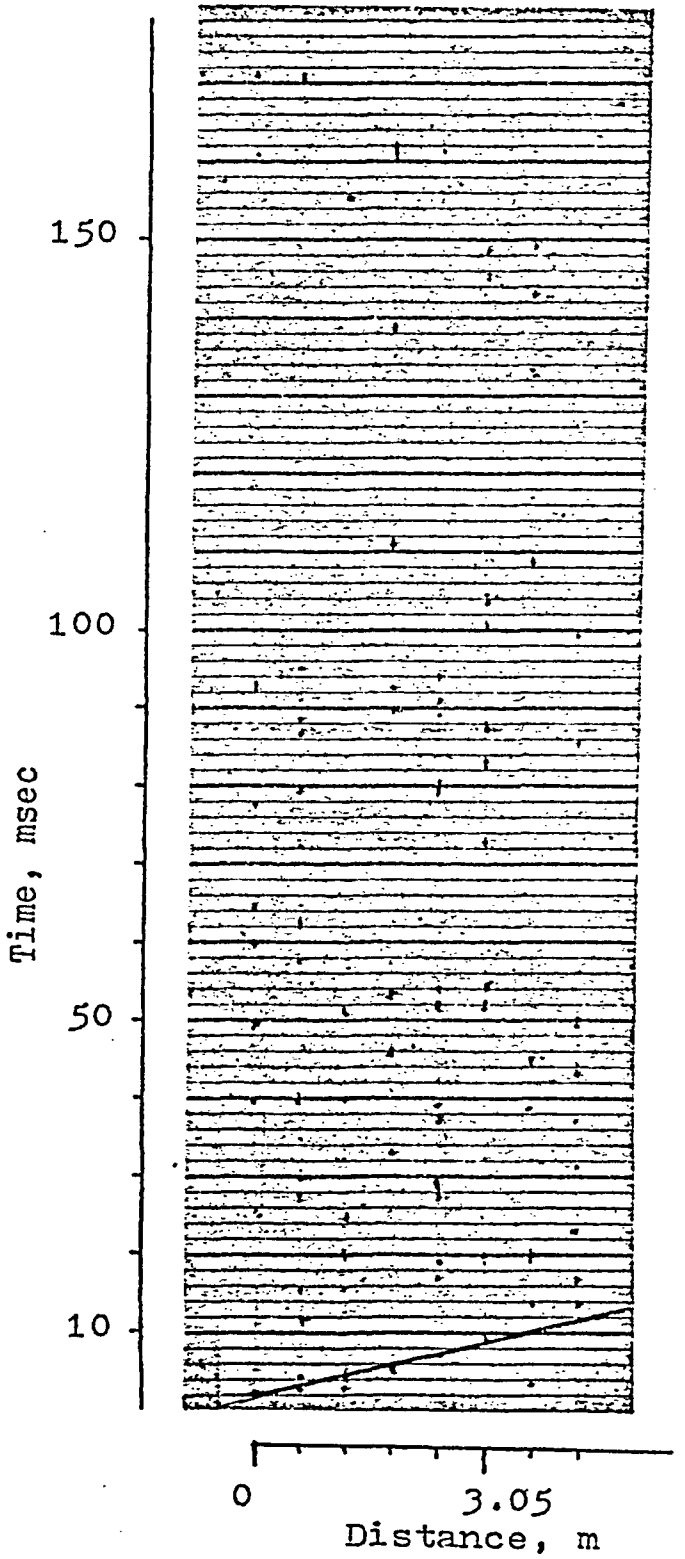

Fig. 25.5

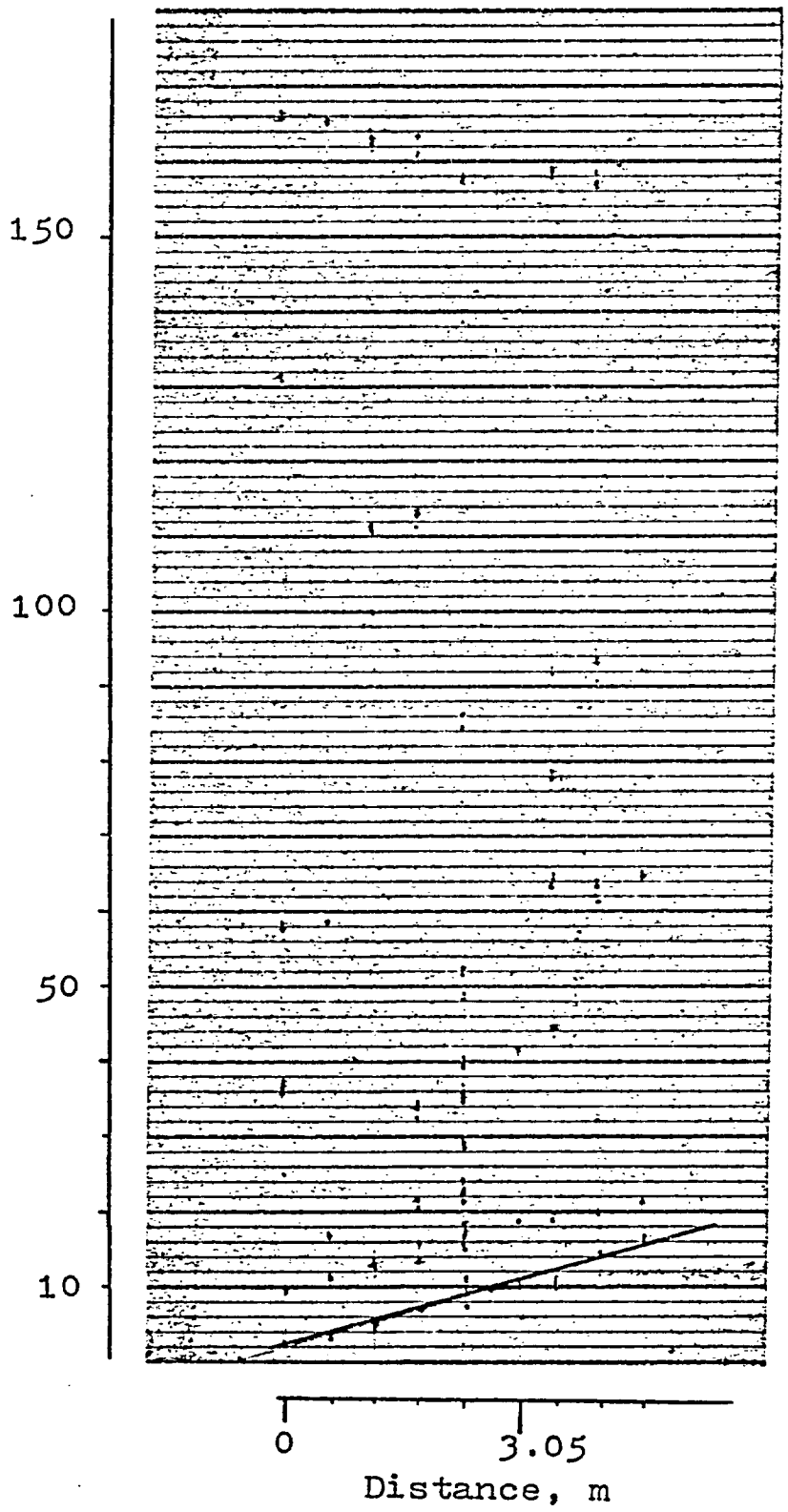

Fig. 25.6.

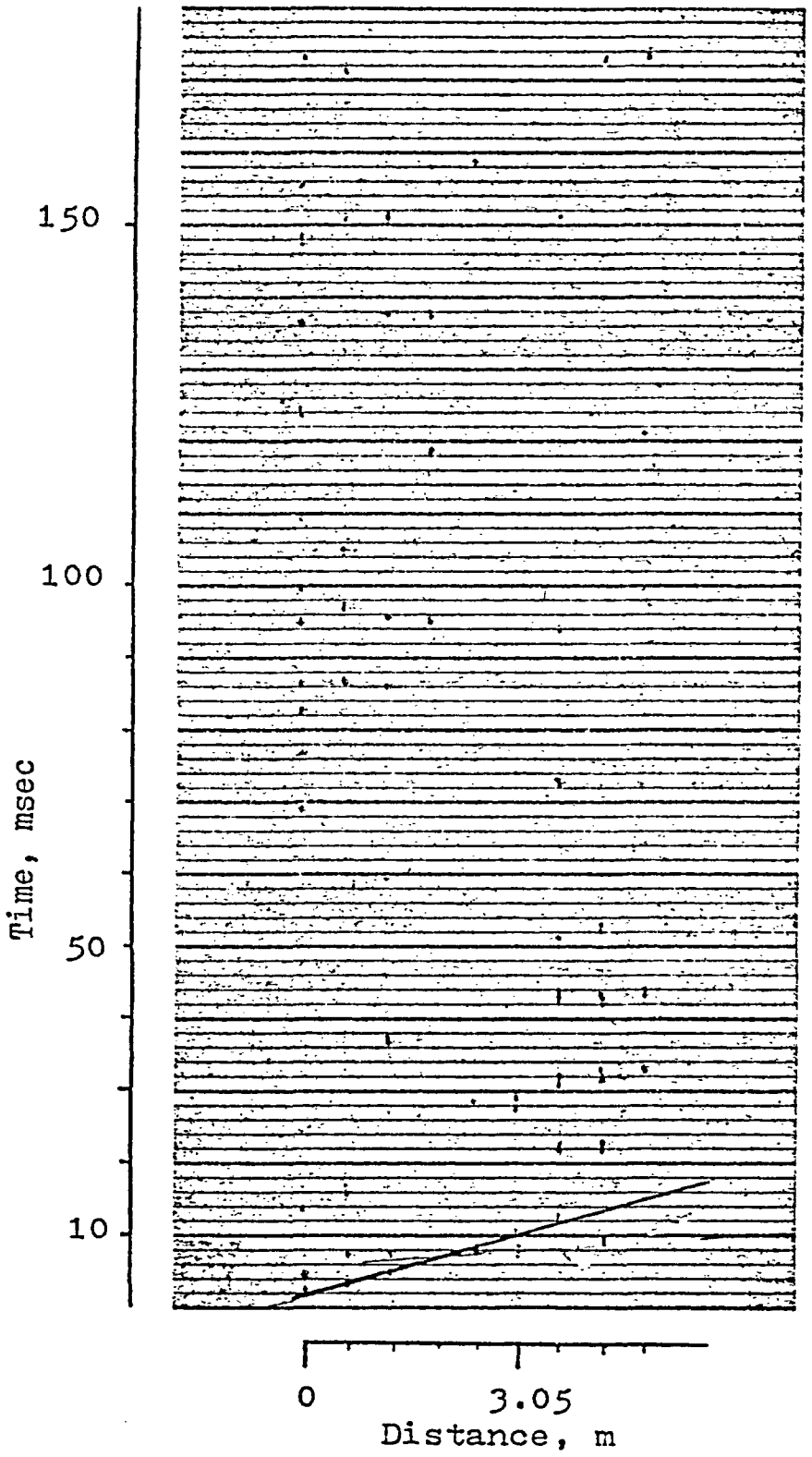

Fig. 25.7

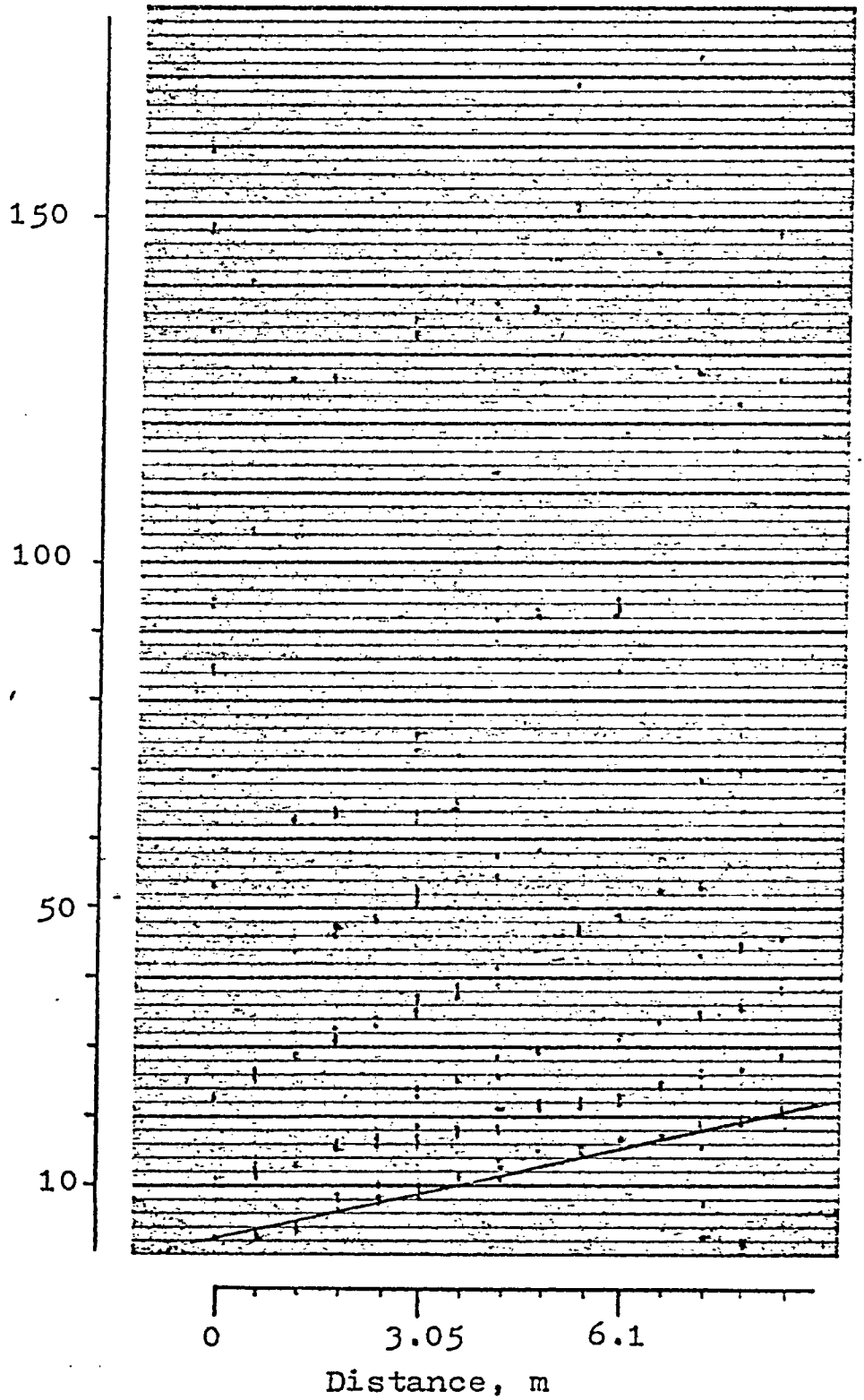

Fig. 25.8.

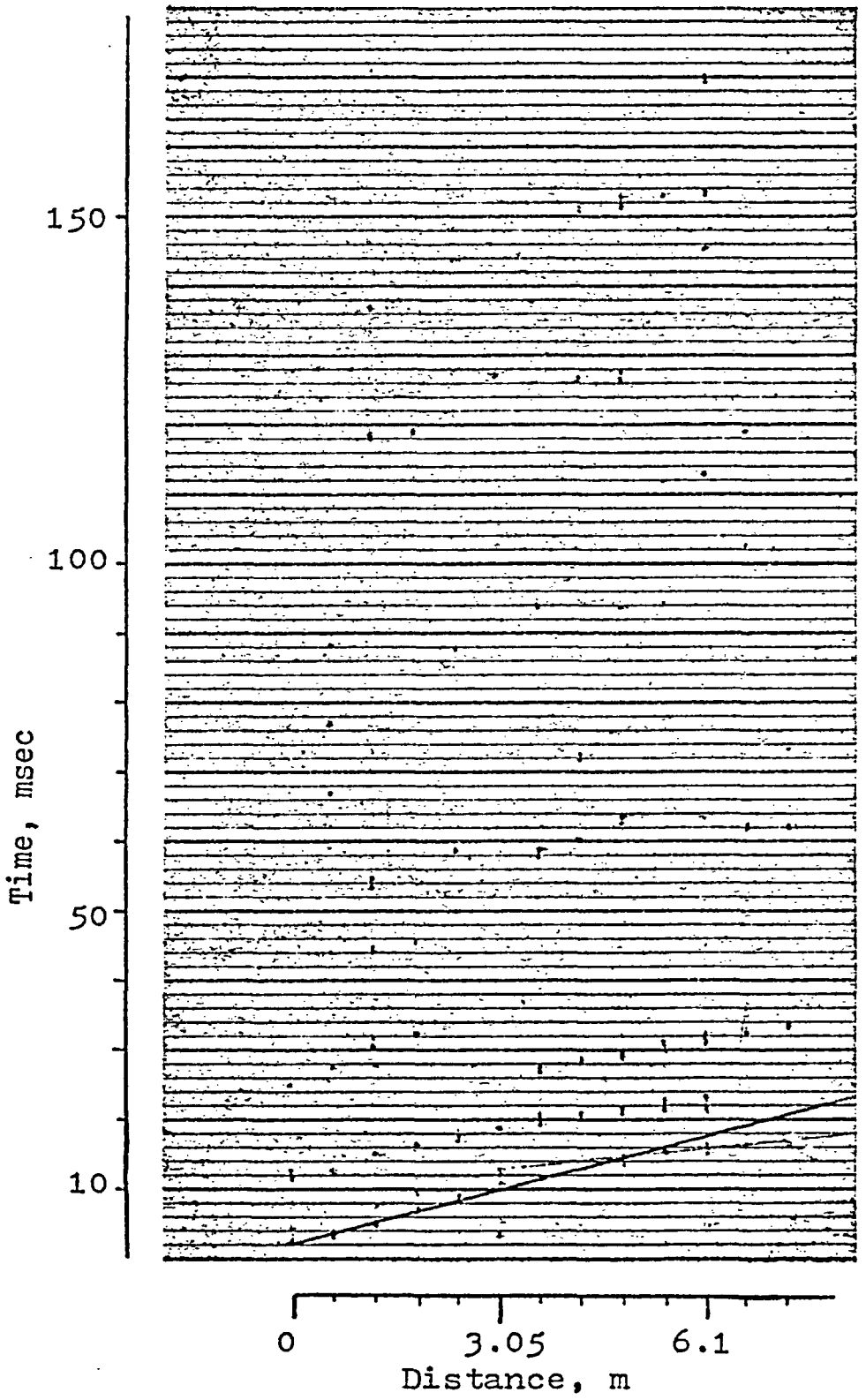

Fig. 25.9.

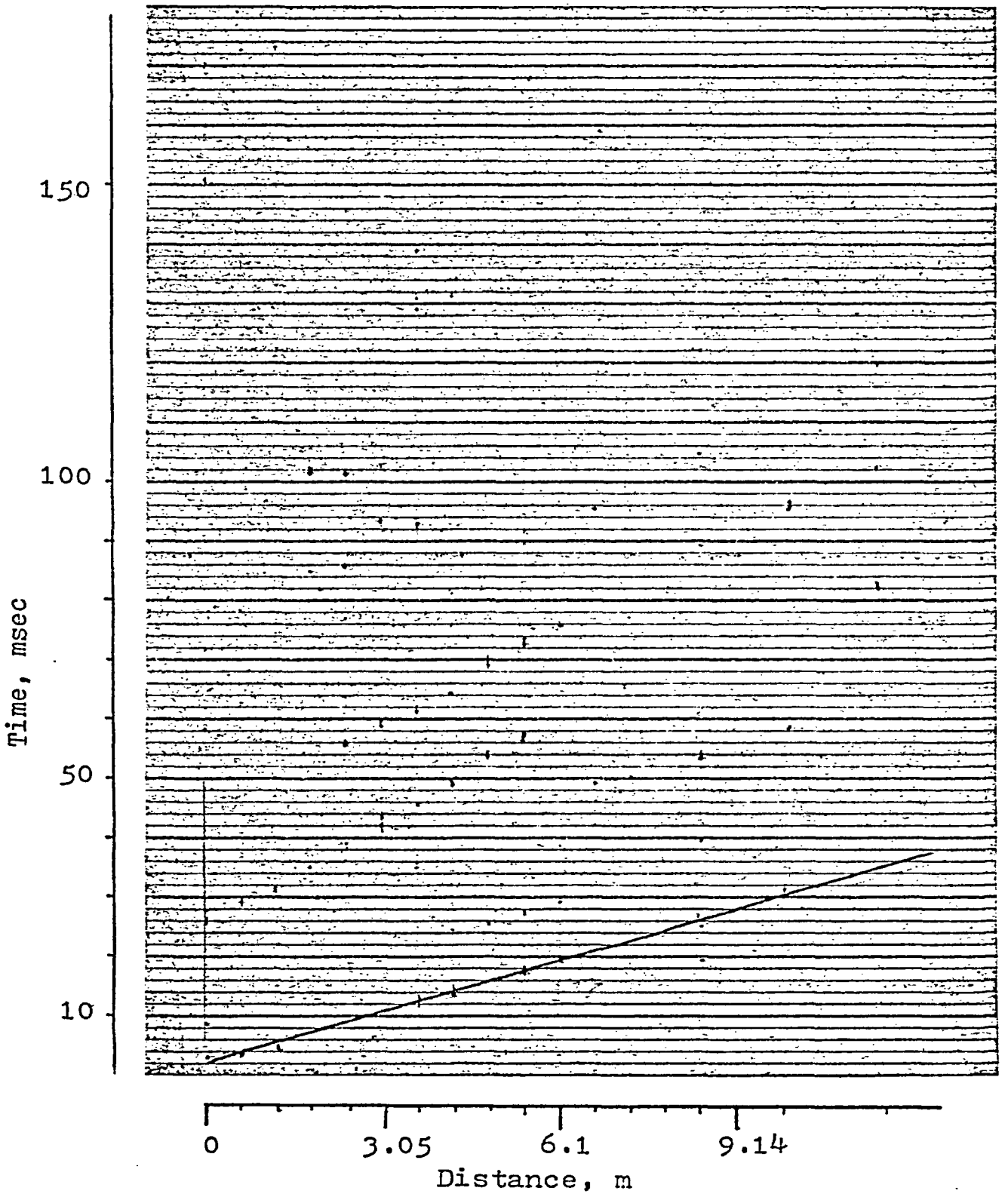

Fig. 25. 10.

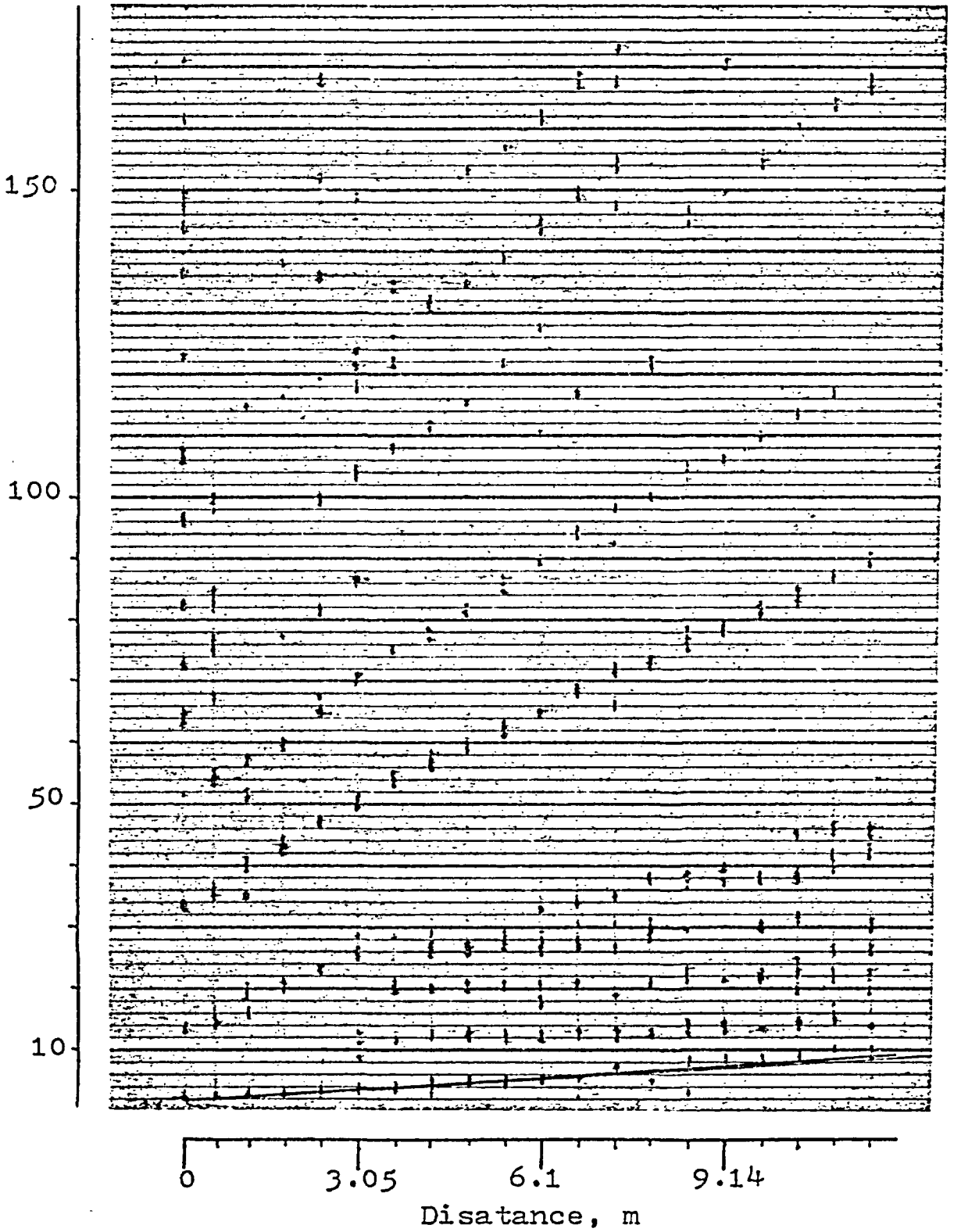

Fig. 25. 11.

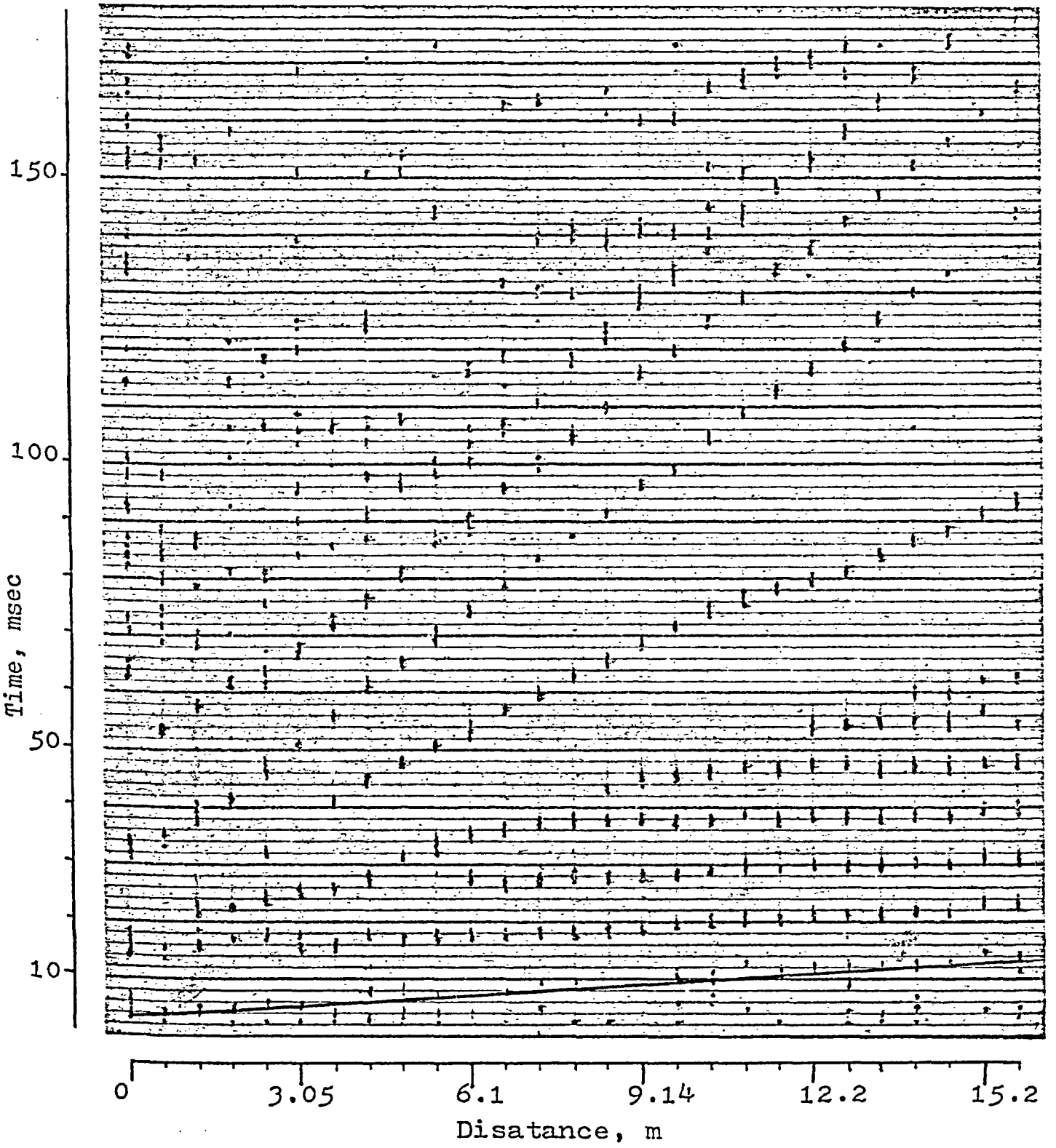

Fig. 25.12.

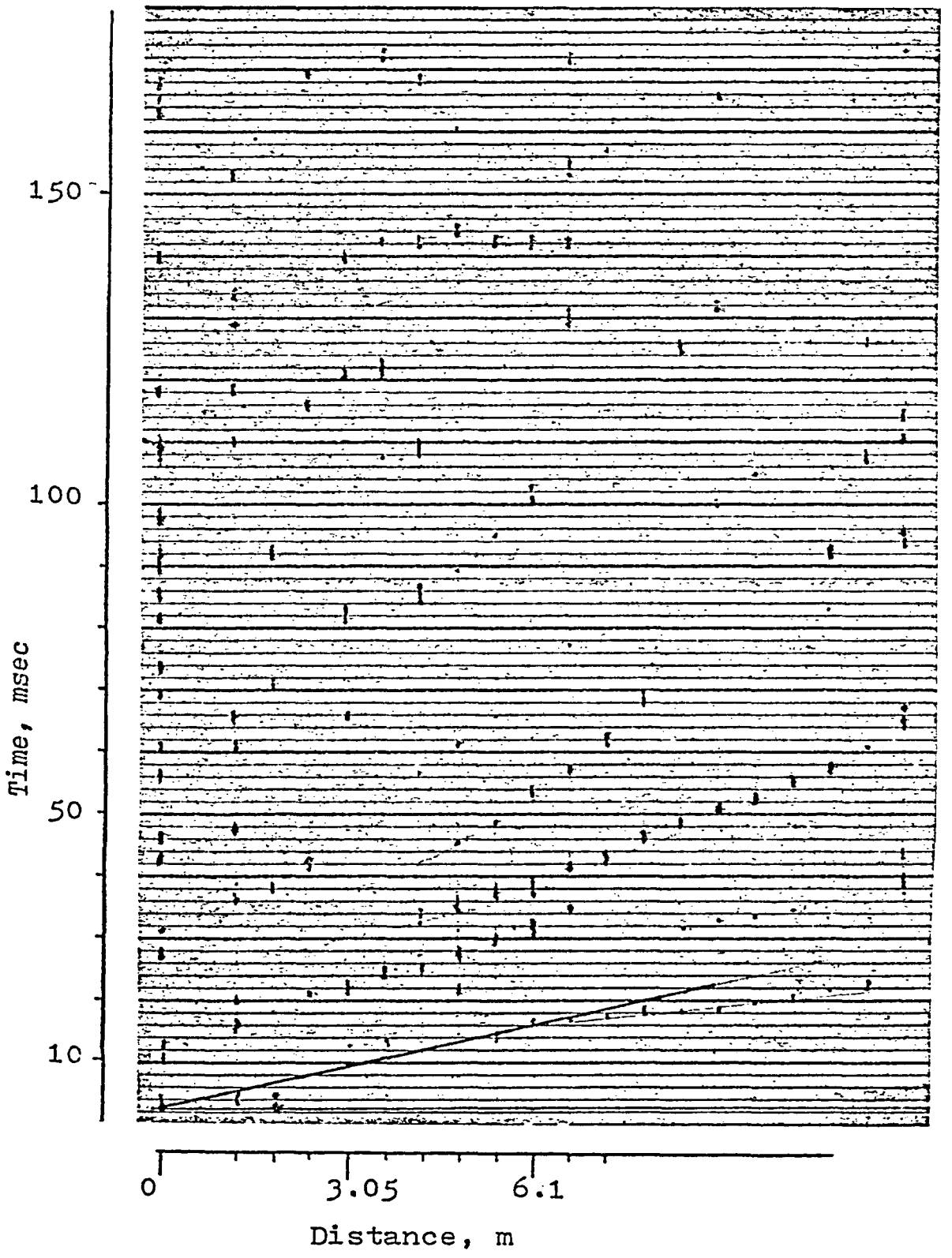

Fig. 25.13.

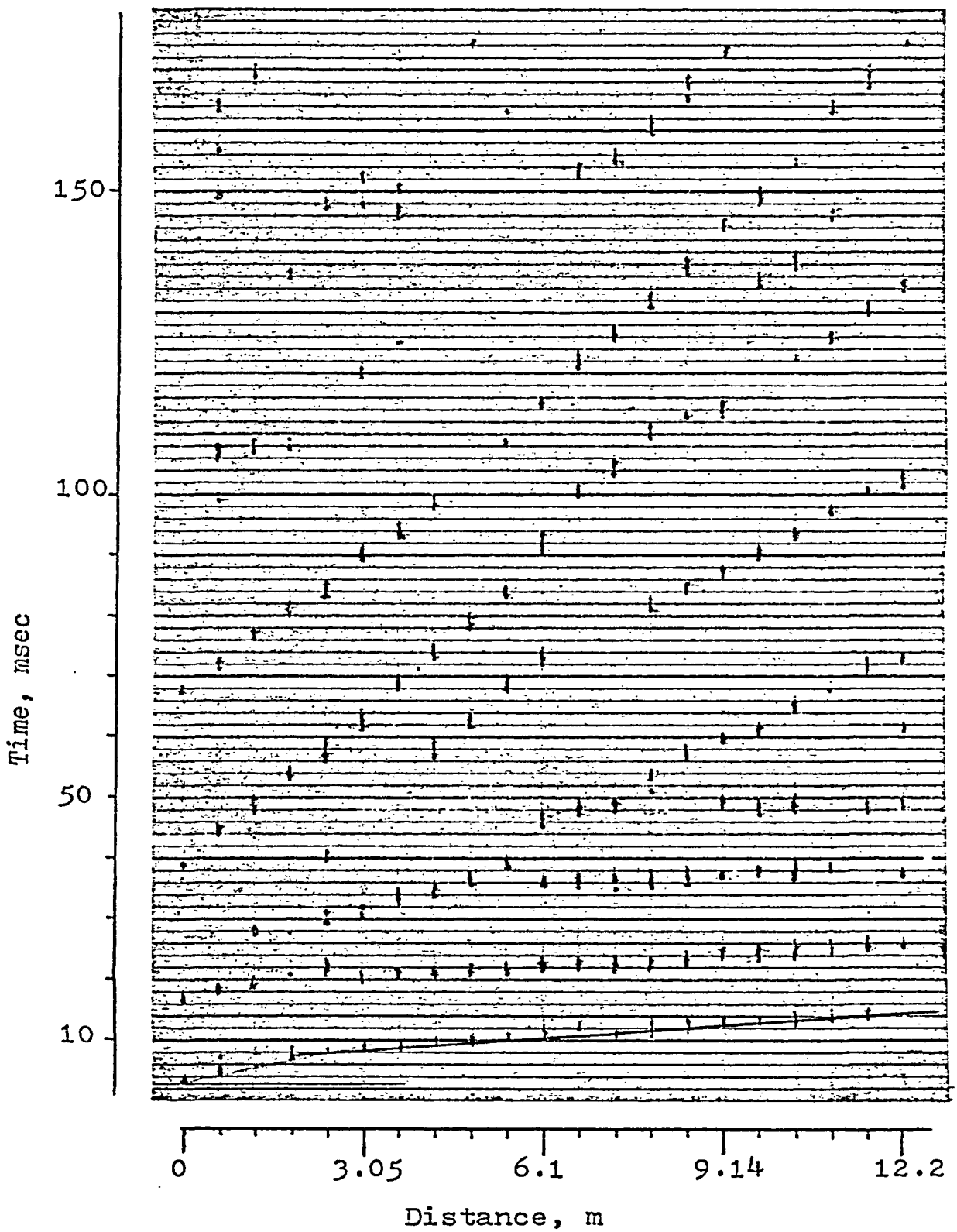

Fig. 25.14.

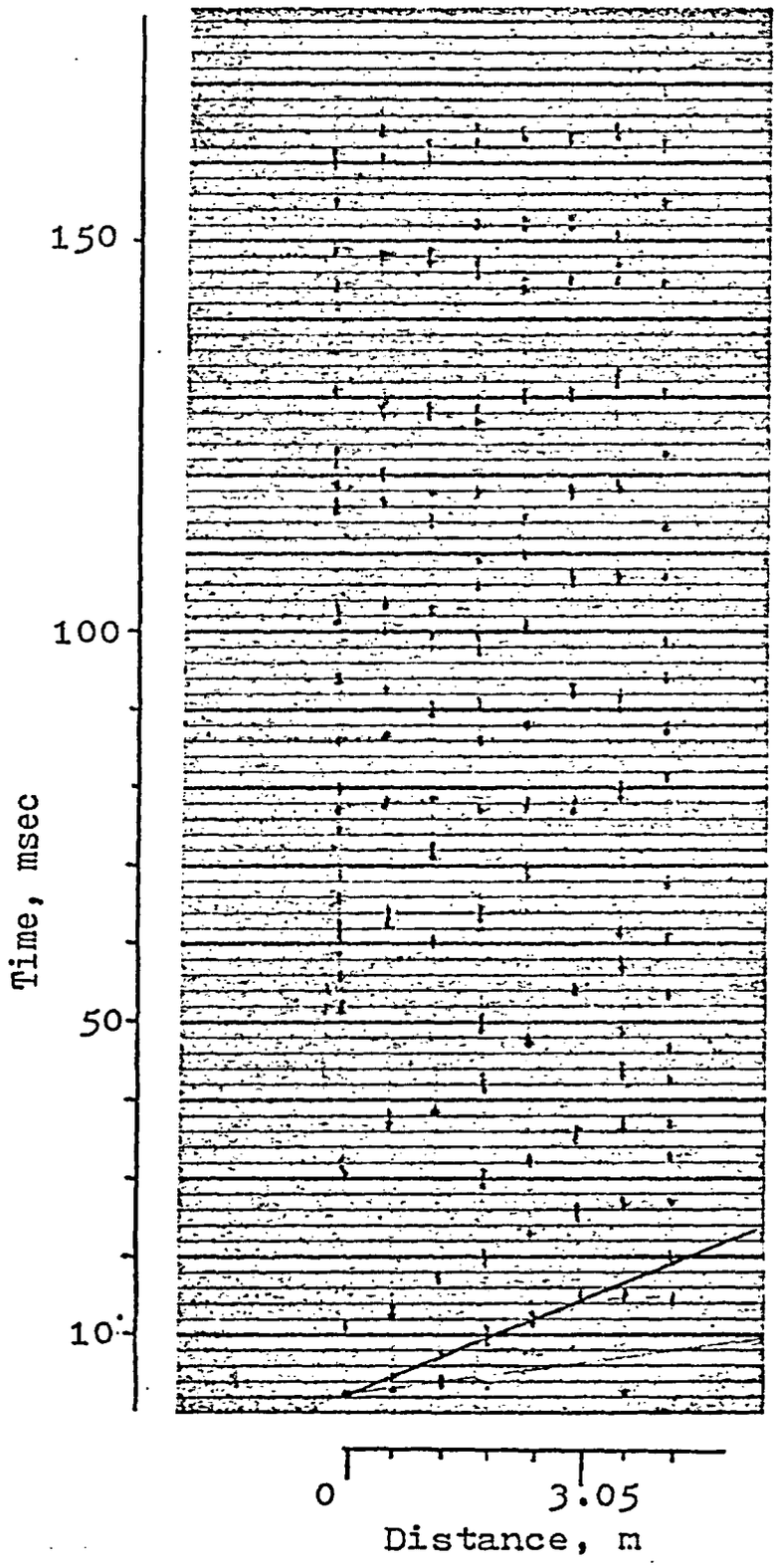

Fig. 25.15.

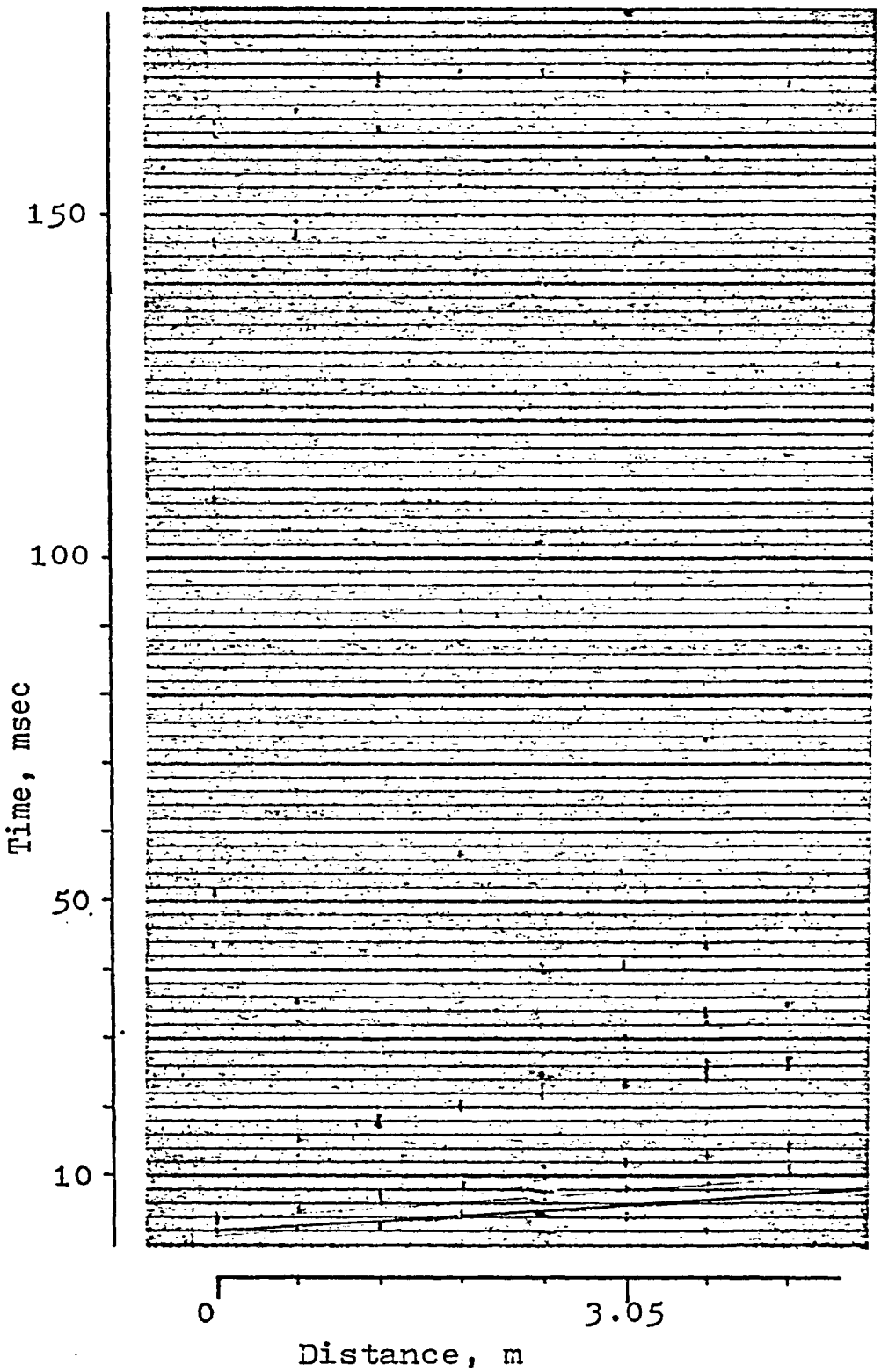

Fig. 25.16.

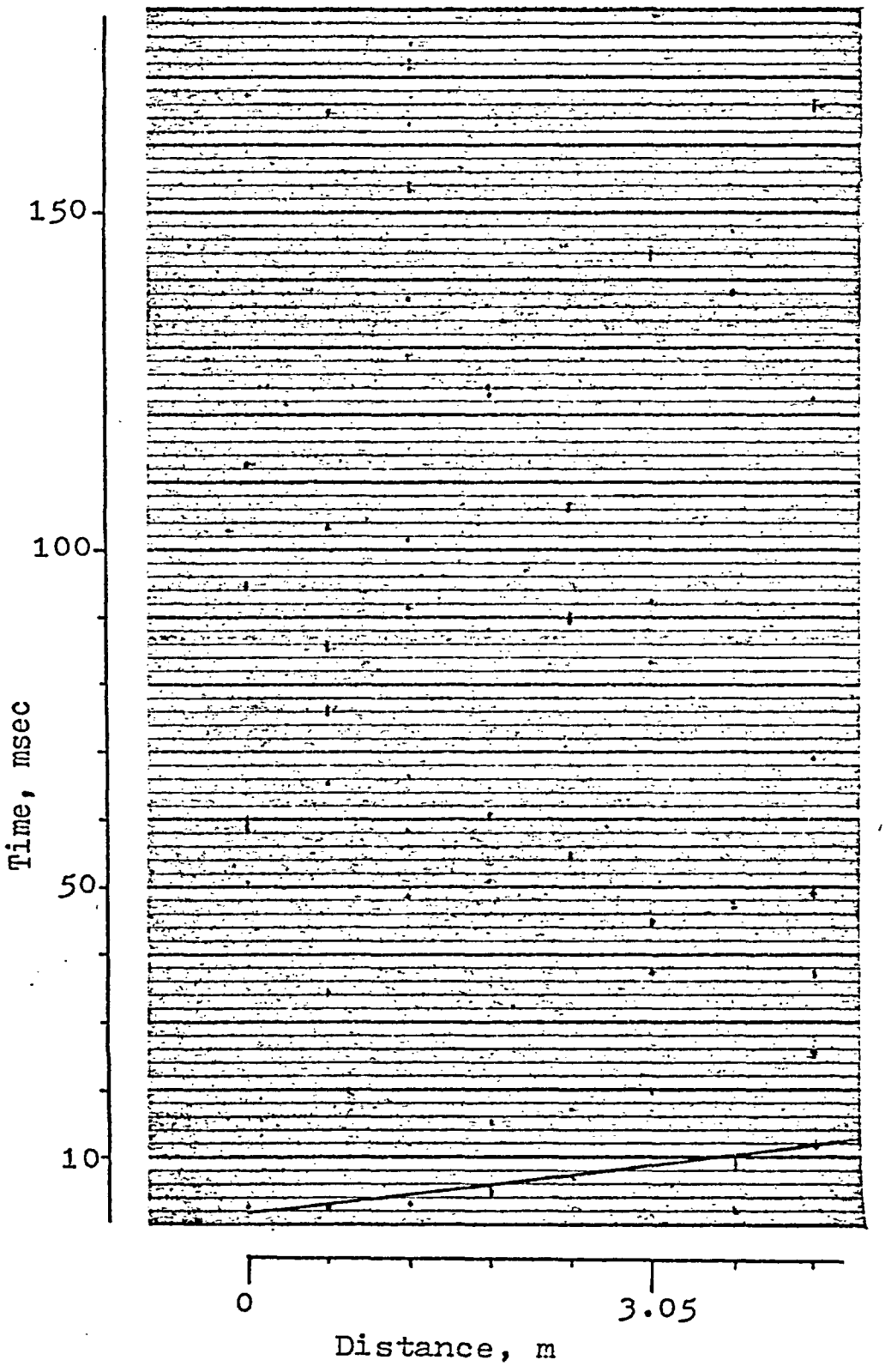

Fig. 25.17.

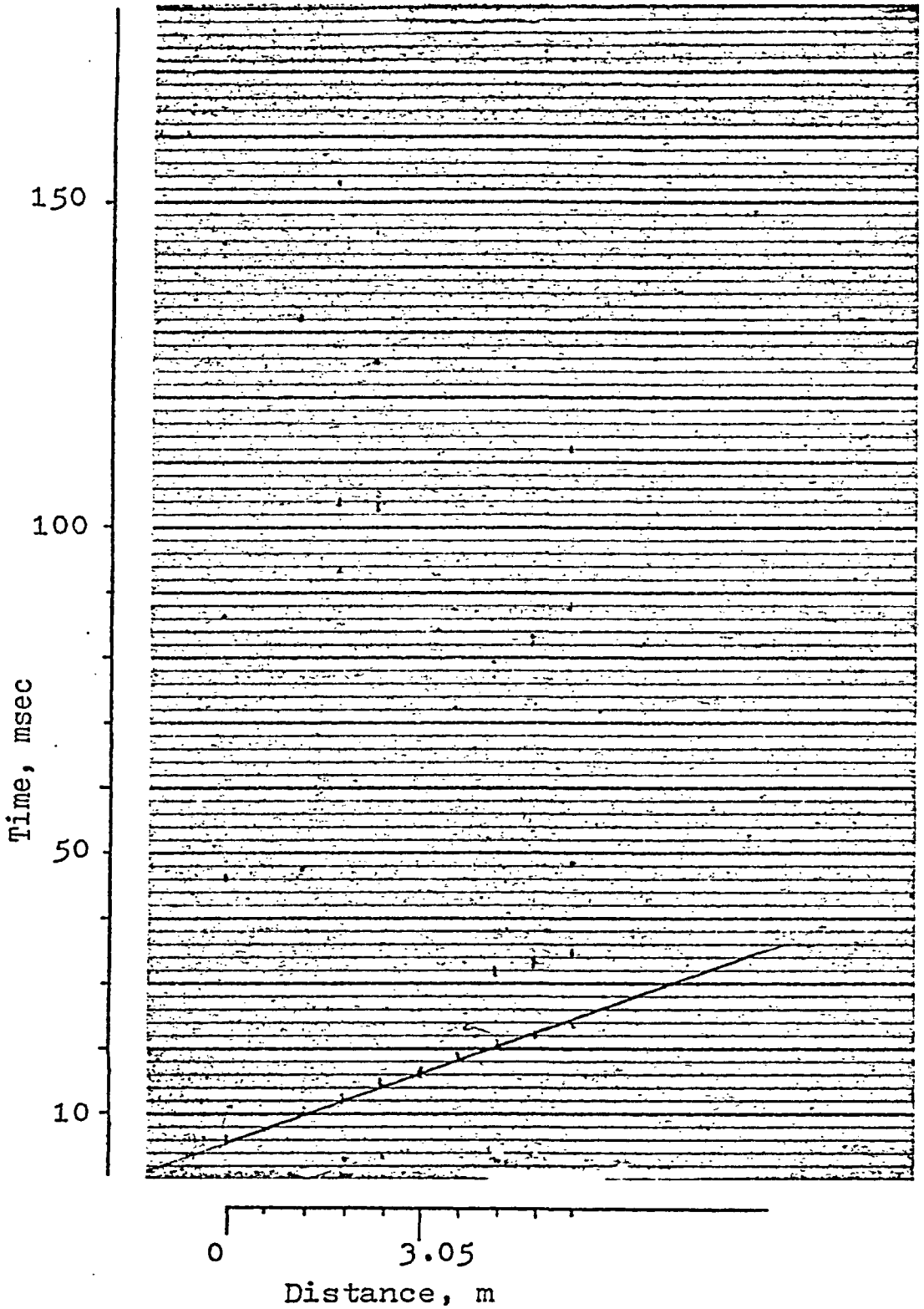

Fig. 25.18.

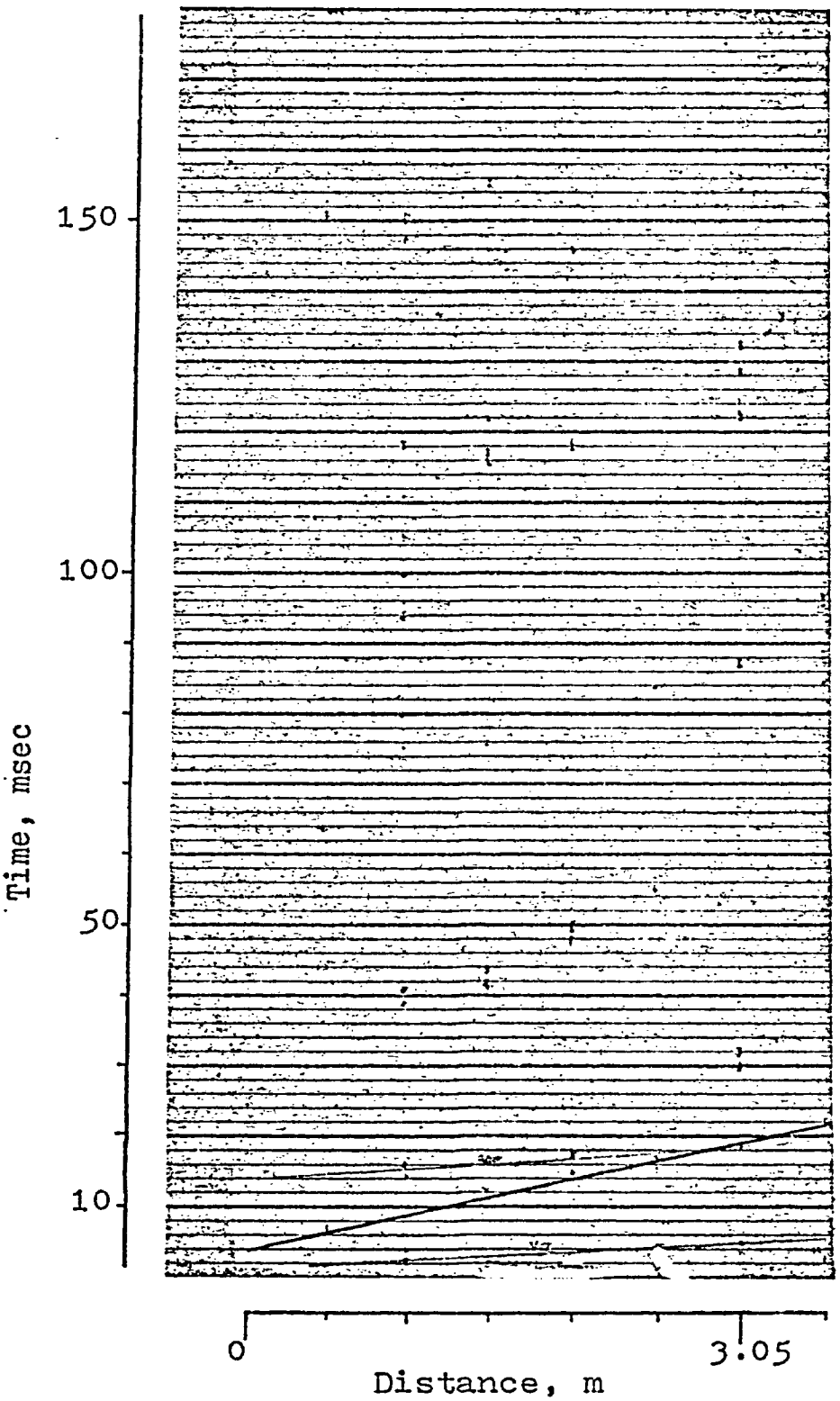

Fig. 25.19.

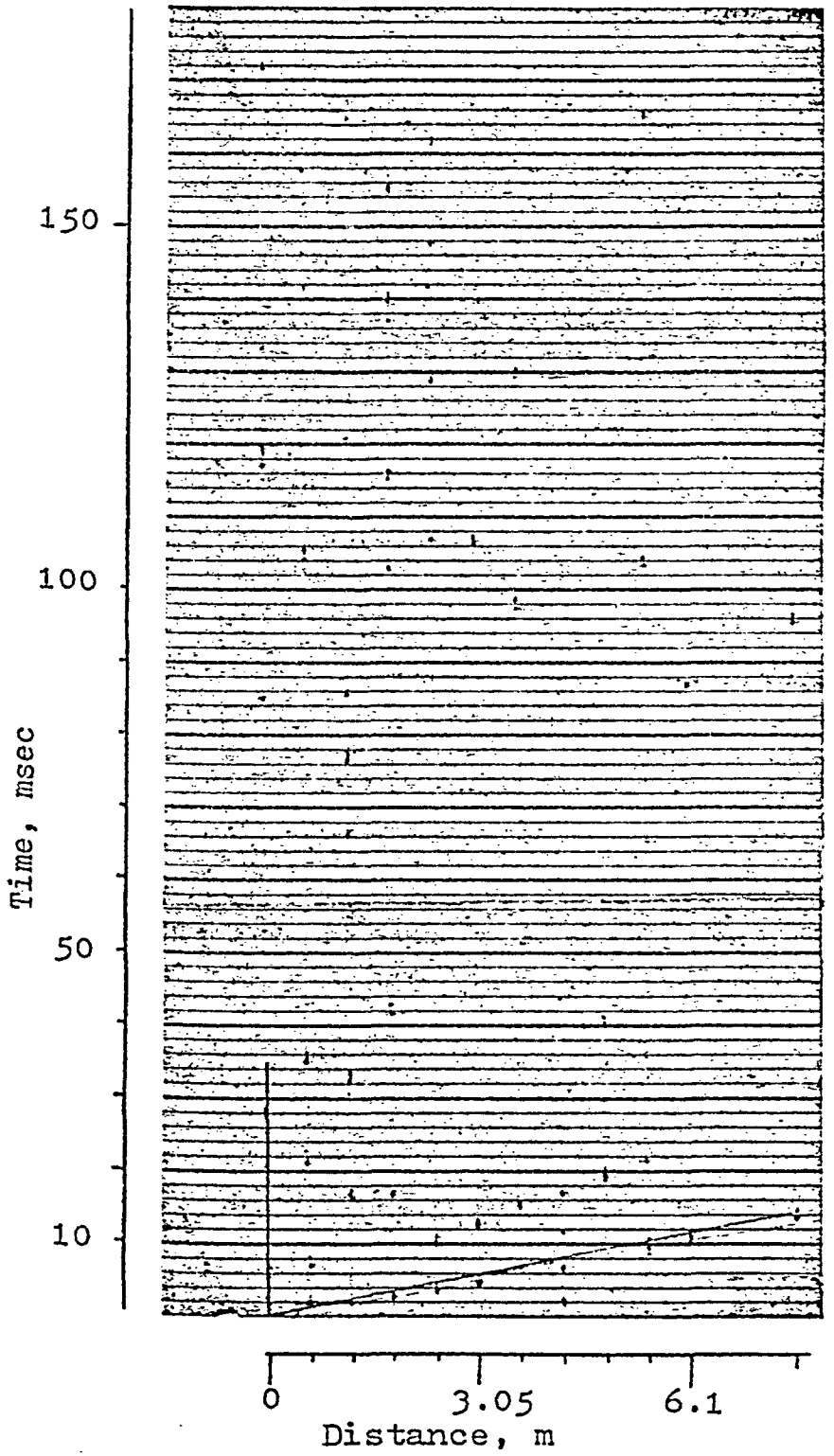

Fig. 25.20

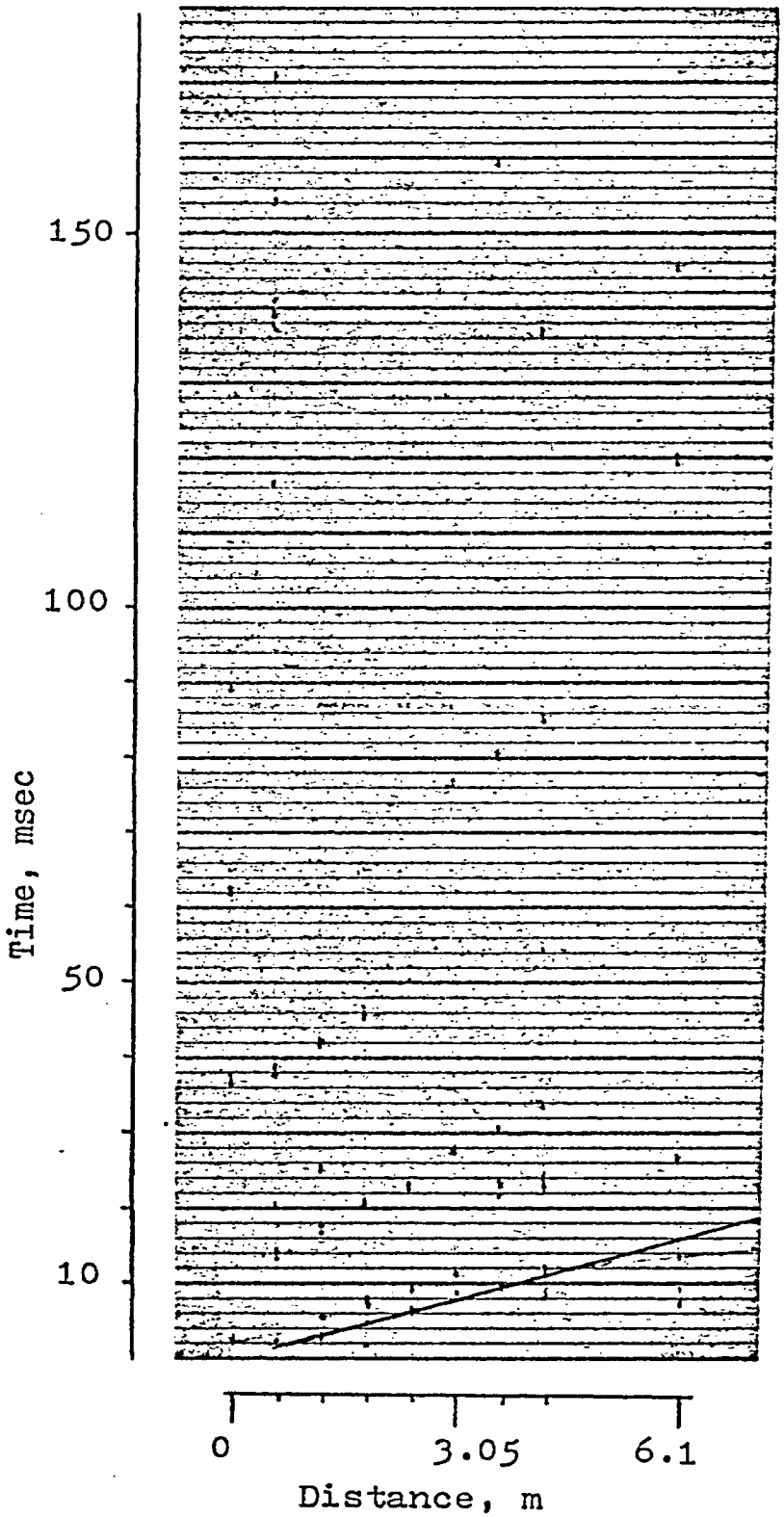

Fig. 25.21.

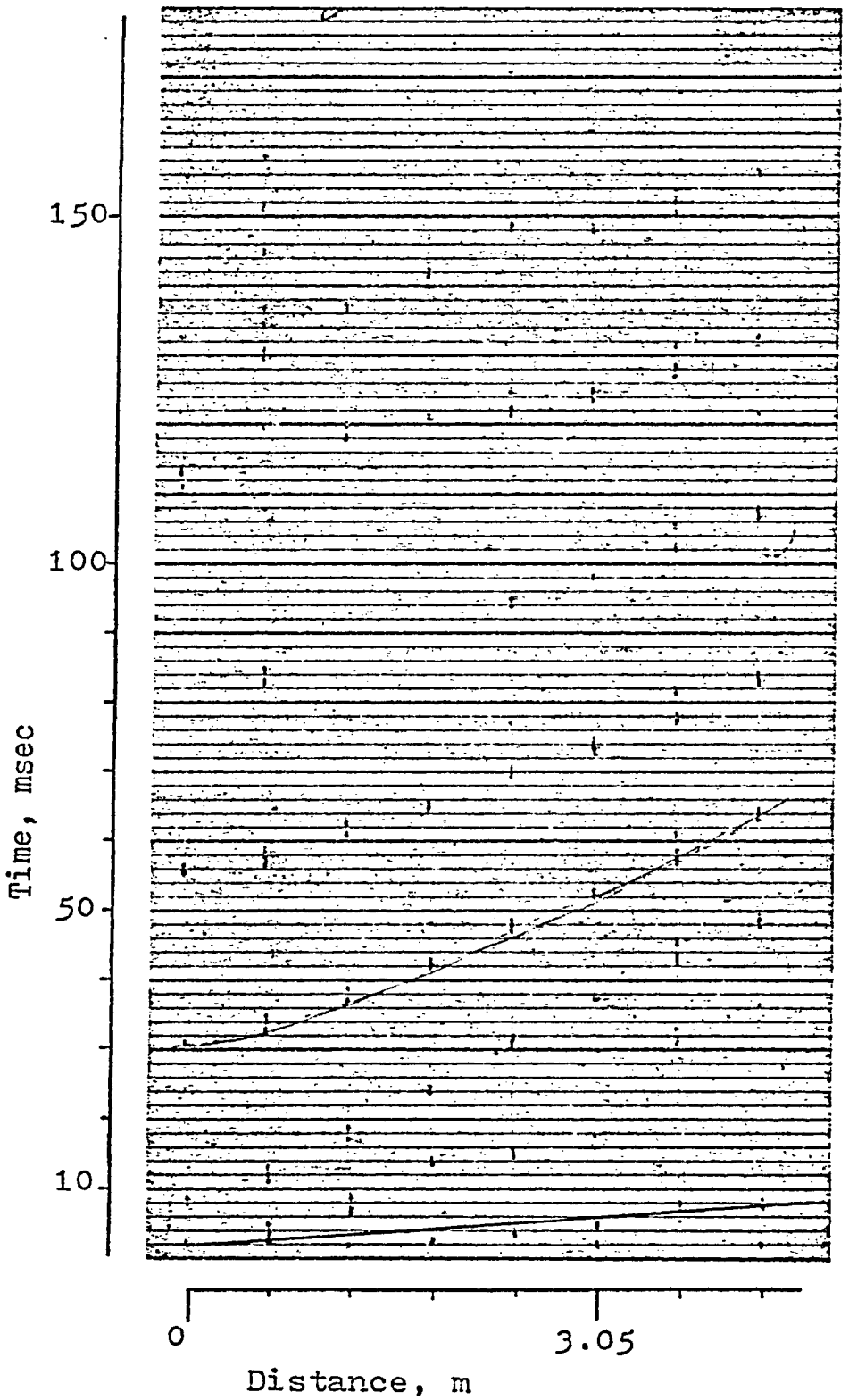

Fig. 25.22.

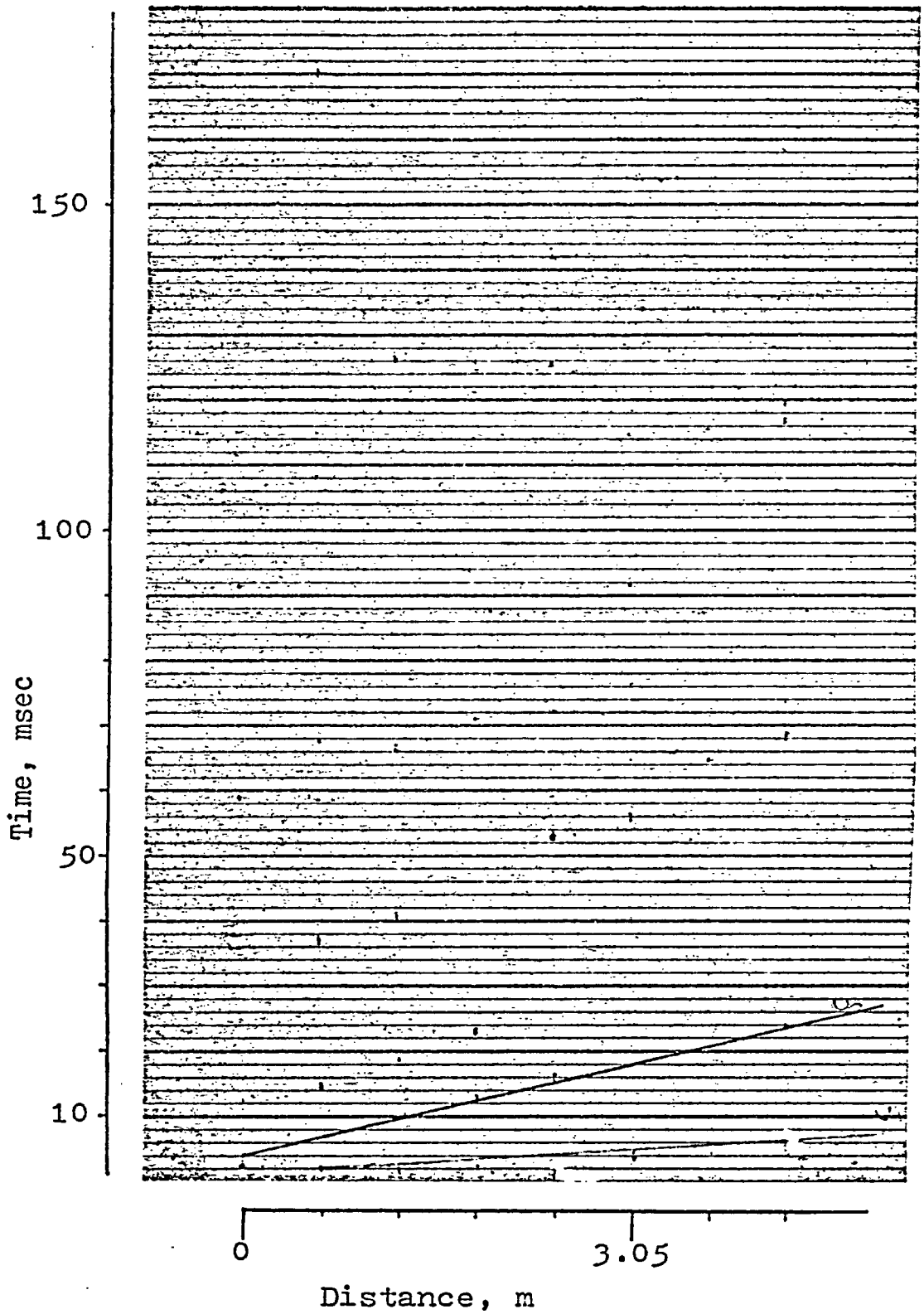

Fig. 25.23.

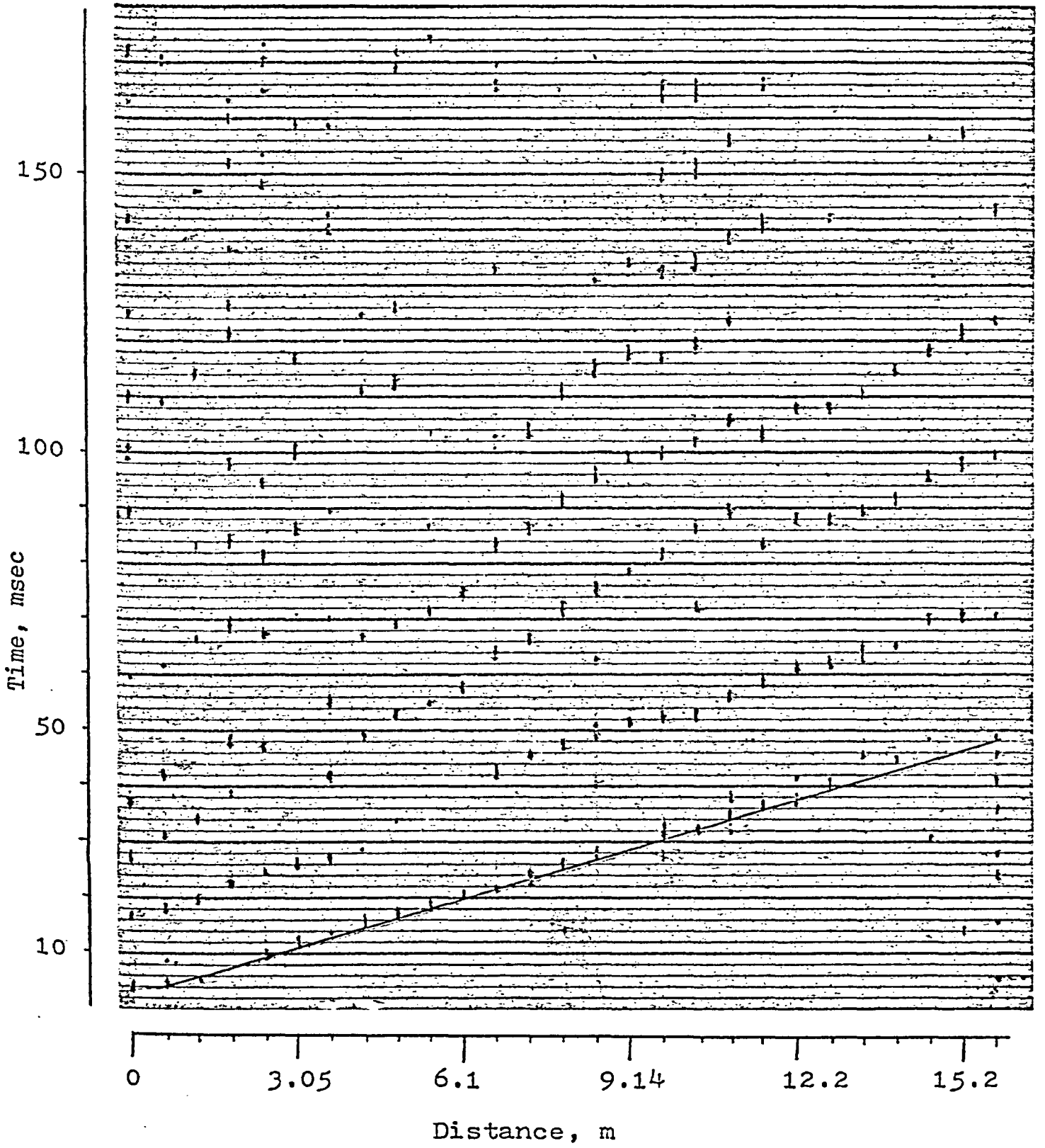

Fig. 25.24.

APPENDIX III
APPARENT RESISTIVITY RESULTS
Tables-Graphs

A. GRAVEL.

Site #	α	1.524	.914	.762	.609	.457	.304	.152
1	I	100	100	100	100	100	100	100
	V	4600	5900	6700	6950	7400	9100	9800
	ρ_α	440.5	339.0	320.8	266.2	212.6	174.3	93.8
2	I	30	30	30	20	24	20	20
	V	3950	6200	7350	6300	9600	10800	18500
	ρ_α	1260.8	1187.4	1173.0	1206.5	1149.1	1034.1	885.7
3	I	20	20	20	20	20	20	22
	V	4600	7400	7860	11455	14480	20200	35440
	ρ_α	2202.4	2152.8	2090.6	2193.8	2079.8	1934.3	1542.5
4	I	12	8	20	30	30	30	20
	V	2750	2550	7500	12570	18590	31170	26130
	ρ_α	2194.4	1831.3	1795.4	1604.9	1780.1	1989.8	1251.1
5	I	30	20	20	20	24	26	26
	V	10500	11200	13055	15815	20900	26500	37945
	ρ_α	3351.5	3217.4	3125.2	3028.7	2501.6	1951.9	1397.5
6	I	14	14	10	10	10	10	10
	V	6650	11100	9420	11140	14485	20600	32090
	ρ_α	4548.4	4555.2	4510.1	4266.9	4161.1	3945.1	3072.8
7	I	20	26	20	30	26	30	36
	V	6200	11700	10650	19100	19075	28475	47990
	ρ_α	2968.6	2585.4	2549.5	2438.6	2107.5	1817.8	1276.5

Table 17. Calculated apparent resistivity (ρ_α, ohm-m) for 50 sites in Essex County. I and V are the measured current (mA) and voltage (mV) for the corresponding electrode separation (m).

This table continues up to page 121.

Site #	α	1.524	.914	.762	.609	.457	.304	.152
8	I	100	100	90	80	100	80	38
	V	2590	4100	4400	4850	8400	9500	8600
	ρ_α	248.0	235.5	234.1	232.2	241.3	227.4	216.7
9	I	100	80	80	100	100	100	100
	V	4800	4800	4900	6500	7160	7950	8050
	ρ_α	459.6	344.7	293.2	249.0	205.7	152.2	77.1
10	I	100	100	100	100	100	100	70
	V	4800	5900	6300	6600	7100	8100	7000
	ρ_α	459.6	373.4	301.6	252.8	213.1	155.1	95.8
11	I	40	30	40	32	32	50	50
	V	5400	6000	8700	7400	8800	15500	23790
	ρ_α	1292.7	1149.1	1041.3	885.7	790.0	593.7	455.6
12	I	20	16	16	18	18	20	20
	V	1670	4550	6955	11150	17360	32300	59500
	ρ_α	799.5	1633.8	2081.2	23726	2770.5	3092.9	2848.7

Site 13, 14, 15 are on page 121.

B. SAND. (Sites 18 and 22 are on page 121).

Site #	α	1.524	.914	.762	.609	.457	.304	.152
16	I	100	100	100	100	100	100	100
	V	2050	4650	5500	7250	9150	12500	16450
	ρ_α	196.3	267.1	263.3	277.7	262.8	239.4	157.5
17	I	60	60	60	60	60	40	40
	V	990	2350	3700	5300	8200	8300	12800
	ρ_α	158.0	225.0	295.2	338.3	392.6	397.4	306.4
19	I	100	60	60	50	40	40	40
	V	10350	8770	9350	9600	10000	13800	26100
	ρ_α	991.0	839.8	746.1	735.4	718.2	660.7	624.8
20	I	100	100	100	100	100	90	60
	V	5050	6400	7100	7850	9000	9810	9700
	ρ_α	426.9	367.7	339.9	300.7	258.5	208.7	154.8
21	I	100	100	100	100	100	90	50
	V	4900	6200	6800	7400	8820	9600	8300
	ρ_α	399.4	356.2	325.5	283.2	253.4	204.3	158.9
23	I	100	100	100	100	100	100	100
	V	4000	4410	4640	5000	5600	6320	7600
	ρ_α	383.0	253.4	222.1	191.5	160.9	121.0	145.5
24	I	20	24	30	24	30	30	40
	V	1600	4250	6200	5500	7472	8262	13362
	ρ_α	766.1	1017.4	989.5	877.8	715.5	527.4	319.9
25	I	70	80	100	100	70	50	48
	V	1400	3350	5400	7150	7200	7150	9550
	ρ_α	191.5	240.6	258.5	273.9	295.5	273.9	190.5

Site #	α	1.524	.914	.762	.609	.457	.304	.152
26	I	100	100	100	100	100	90	50
	V	1300	2550	3300	4200	5950	8400	7850
	ρ_α	124.5	146.5	158.0	160.9	170.9	178.7	150.3
27	I	80	90	90	70	50	40	40
	V	3000	7200	9250	9000	8400	9000	14600
	ρ_α	359.1	459.6	492.1	492.4	483.5	430.9	347.8
28	I	100	100	100	100	100	100	100
	V	370	710	910	1350	2050	3200	7000
	ρ_α	35.4	40.8	43.6	51.7	58.9	61.3	67.0
29	I	100	100	100	100	100	90	60
	V	930	1650	2050	2900	4000	6300	11300
	ρ_α	89.1	94.8	98.1	111.1	114.9	134.0	180.3
30	I	100	100	100	100	100	100	100
	V	3600	4600	4950	5400	6000	6400	7150
	ρ_α	344.7	264.3	237.0	206.8	172.4	122.6	68.5
31	I	24	30	30	30	30	30	30
	V	2500	7200	9300	12500	17000	24000	33900
	ρ_α	997.4	1378.9	1484.2	1595.9	1627.8	1532.1	1082.0
32	I	100	100	100	100	100	100	100
	V	3075	4800	5600	6650	8300	11200	15600
	ρ_α	294.4	275.8	268.1	254.7	238.4	214.5	143.4

C. CLAY.

Site #	α	1.524	.914	.762	.609	.457	.304	.152
33	I	100	100	100	100	100	100	100
	V	65	110	120	145	180	250	360
	ρ_α	6.2	6.3	5.7	5.5	5.2	4.8	3.4
34	I	90	90	90	90	80	80	70
	V	165	270	320	375	460	650	950
	ρ_α	17.5	17.2	17.0	16.0	14.7	13.8	10.1
35	I	100	100	100	100	100	100	100
	V	280	450	535	675	795	1050	1700
	ρ_α	26.8	25.8	25.6	25.8	22.8	20.1	16.3
36	I	100	100	100	100	100	100	100
	V	295	460	490	615	740	985	1800
	ρ_α	28.3	26.4	23.5	23.6	21.2	18.9	17.2
37	I	100	100	100	100	100	100	100
	V	320	490	540	640	740	1500	1900
	ρ_α	30.6	28.1	25.8	24.5	21.2	17.2	18.2
38	I	100	100	100	100	100	100	100
	V	260	390	410	510	560	750	1150
	ρ_α	24.9	22.4	19.6	19.5	16.1	14.4	11.0
39	I	100	100	100	100	100	100	100
	V	220	360	425	470	600	735	1050
	ρ_α	21.1	20.1	20.3	18.0	17.2	14.1	10.1
40	I	100	100	100	100	100	100	100
	V	275	350	380	440	570	750	1200
	ρ_α	26.3	20.1	18.2	16.9	16.4	14.4	11.5
41	I	100	100	100	100	100	100	100
	V	435	690	820	955	1200	1650	2400
	ρ_α	41.6	39.6	39.3	36.6	34.5	31.6	22.4
42	I	100	100	100	100	100	100	100
	V	220	330	490	815	1950	4200	13580
	ρ_α	21.1	18.9	23.4	31.2	56.0	80.4	130.0

Site #	α	.152	.3048	.457	.609	.762	.914	1.219	1.524	1.828	2.133	2.438	2.743
13	I	40	50	50	40	30	30	40	40	40	40	50	40
	V	26,340	24,410	20,625	14,870	8,900	8,000	8,450	7,250	6,050	5,210	4,750	2,450
	ρ_α	2068.7	3067.4	3887.7	4671.5	4660.0	5026.5	5309.3	5694.3	5702.0	5222.9	4775.2	3848.4
	α	.152	.3048	.457	.609	.762	.914	1.524	2.133	3.048	4.572	6.096	7.62
14	I	60	50	50	40	40	50	50	50	40	40	40	40
	V	30,650	18,550	16,130	12,110	10,240	11,130	7,975	6,575	3,550	2,550	1,910	1,575
	ρ_α	1604.8	2331.1	3040.4	3804.5	4021.2	4195.9	5010.8	5783.7	5576.3	6008.3	6000.4	6185.0
	α	.152	.3048	.457	.609	.762	.914	1.524	2.133	2.743	3.352	3.962	
15	I	90	90	90	90	90	90	90	80	80	80	80	
	V	6,800	5,100	4,250	3,500	3,140	2.940	2,820	2.380	2.385	2.320	2,200	
	ρ_α	237.4	356.0	445.1	488.7	548.0	615.7	984.4	1308.5	1685.8	2004.3	2246.2	
	α	.152	.3048	.457	.609	.762	.914	1.524	3.048	6.096	9.144	12.192	
18	I	50	50	50	50	40	50	50	50	70	80	78	
	V	17,000	8,600	4,300	2,600	1,400	1,200	450	200	130	100	80	
	ρ_α	1068.1	1080.7	810.5	653.4	549.8	452.4	282.7	251.3	233.4	235.6	257.8	
	α	.152	.3048	.457	.609	.762	.914	1.524	3.048	4.572	6.096	7.62	9.144
22	I	30	45	50	50	100	100	100	80	80	80	80	80
	V	10,500	9,450	8,250	6,820	8,800	7,200	4,400	510	350	175	135	110
	ρ_α	1099.5	1319.5	1036.7	1714.1	1382.3	1357.2	1382.3	400.5	412.3	274.8	265.1	259.2

Figure #	Sites plotted
26.1.	1, 9, 26, 28, 30, 47, 49
26.2.	2, 3, 4, 5, 6, 12, 24, 32
26.3.	7, 11, 19, 21, 23, 27, 31
26.4.	8, 25, 29, 33, 36, 38, 50
26.5.	10, 20, 35, 39, 43,
26.6.	13, 14, 15, 18, 22
26.7.	16. 17. 44, 48
26.8.	34, 37, 40, 41, 42, 45, 46

Table 18. Apparent resistivity plots included in Appendix III.

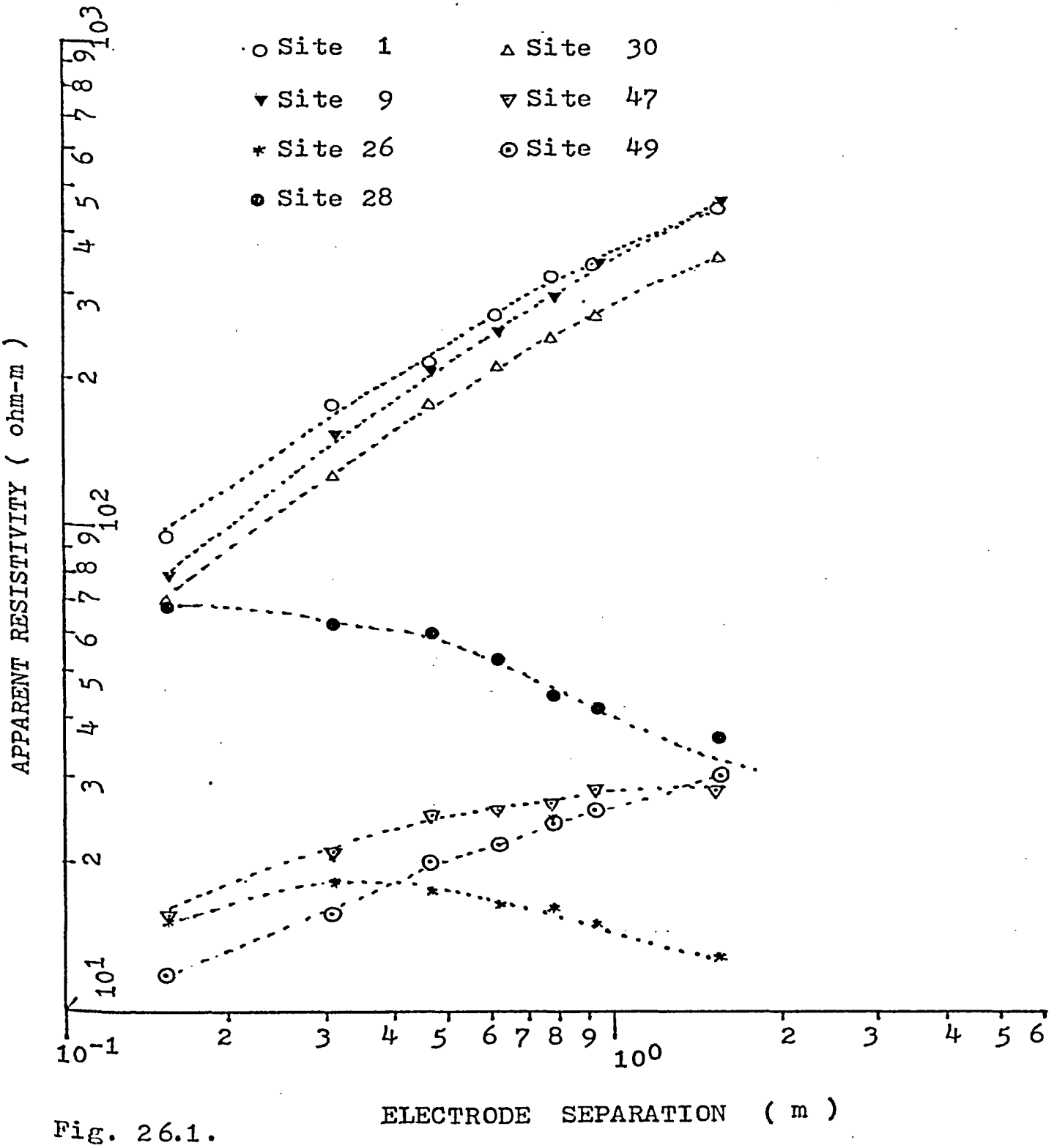

Fig. 26.1.

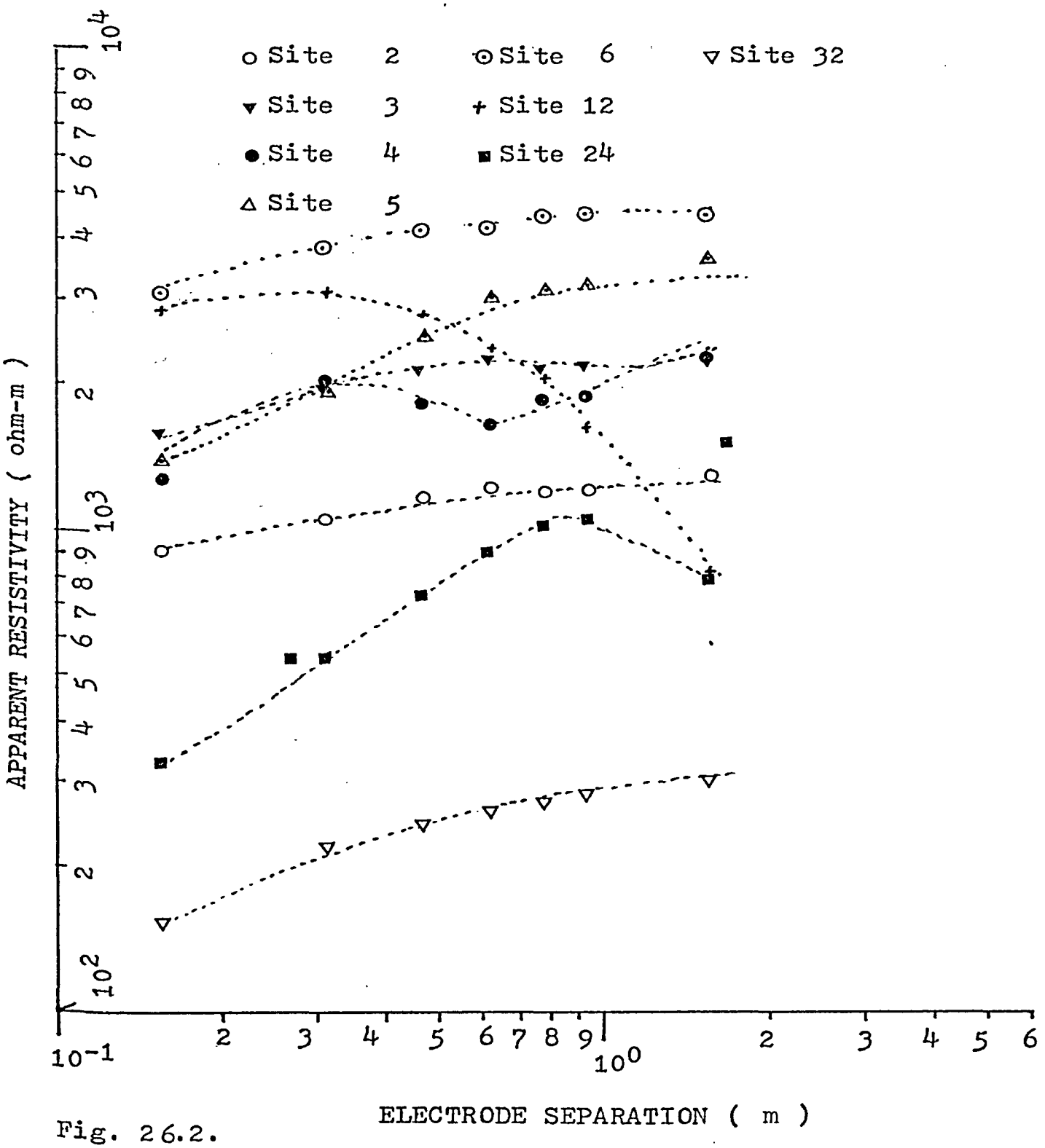

Fig. 26.2.

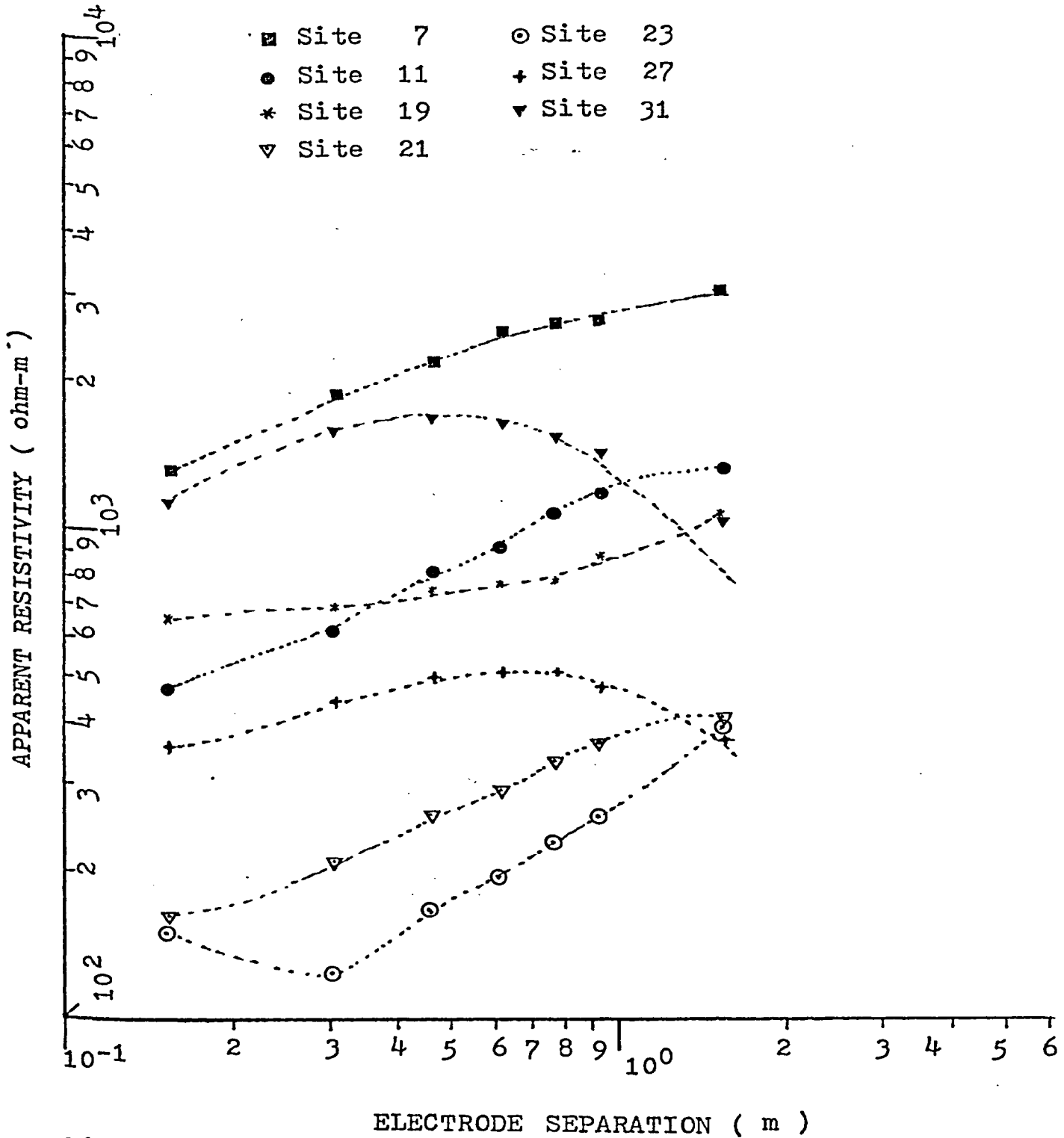

Fig. 26.3.

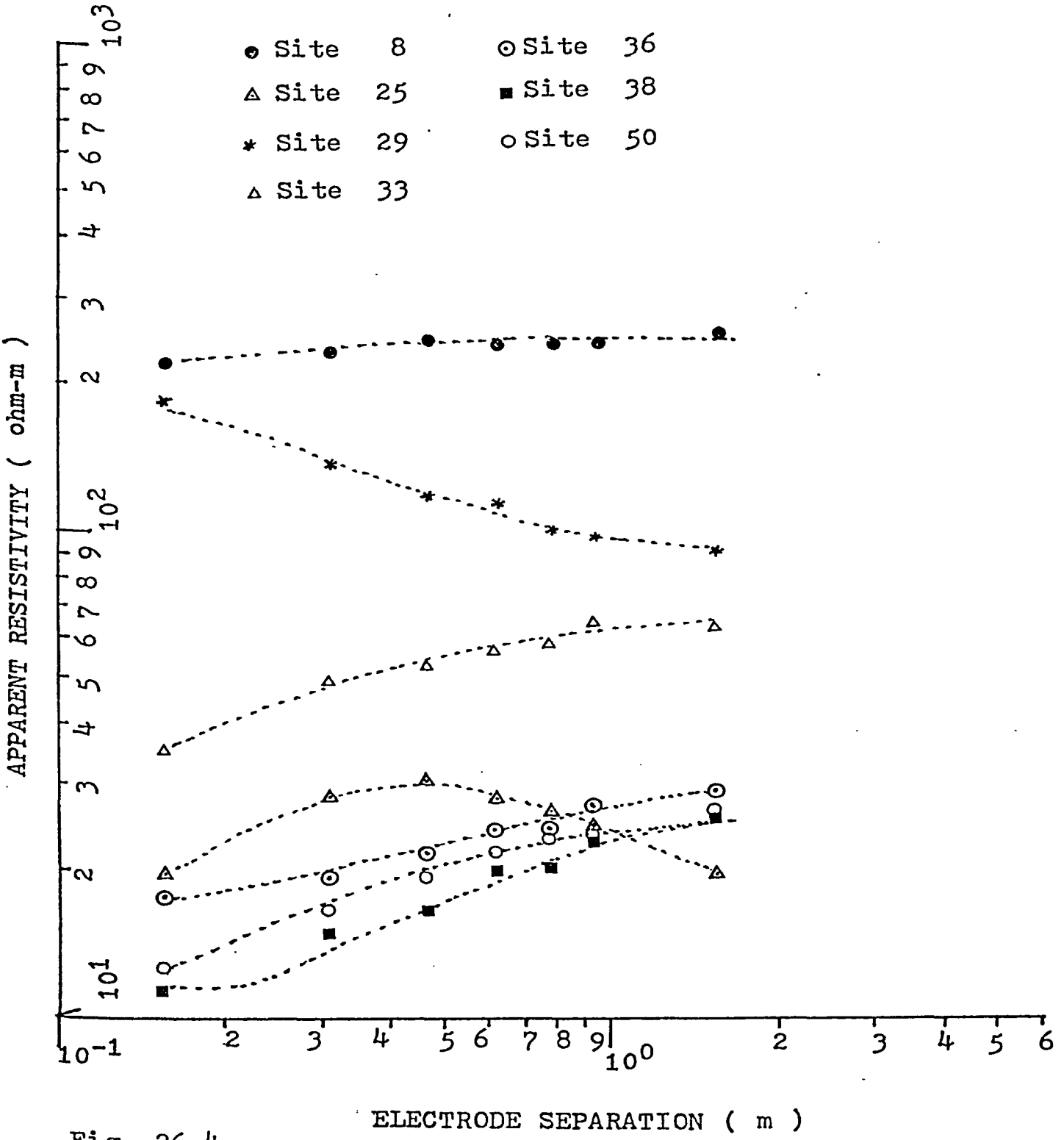

Fig. 26.4.

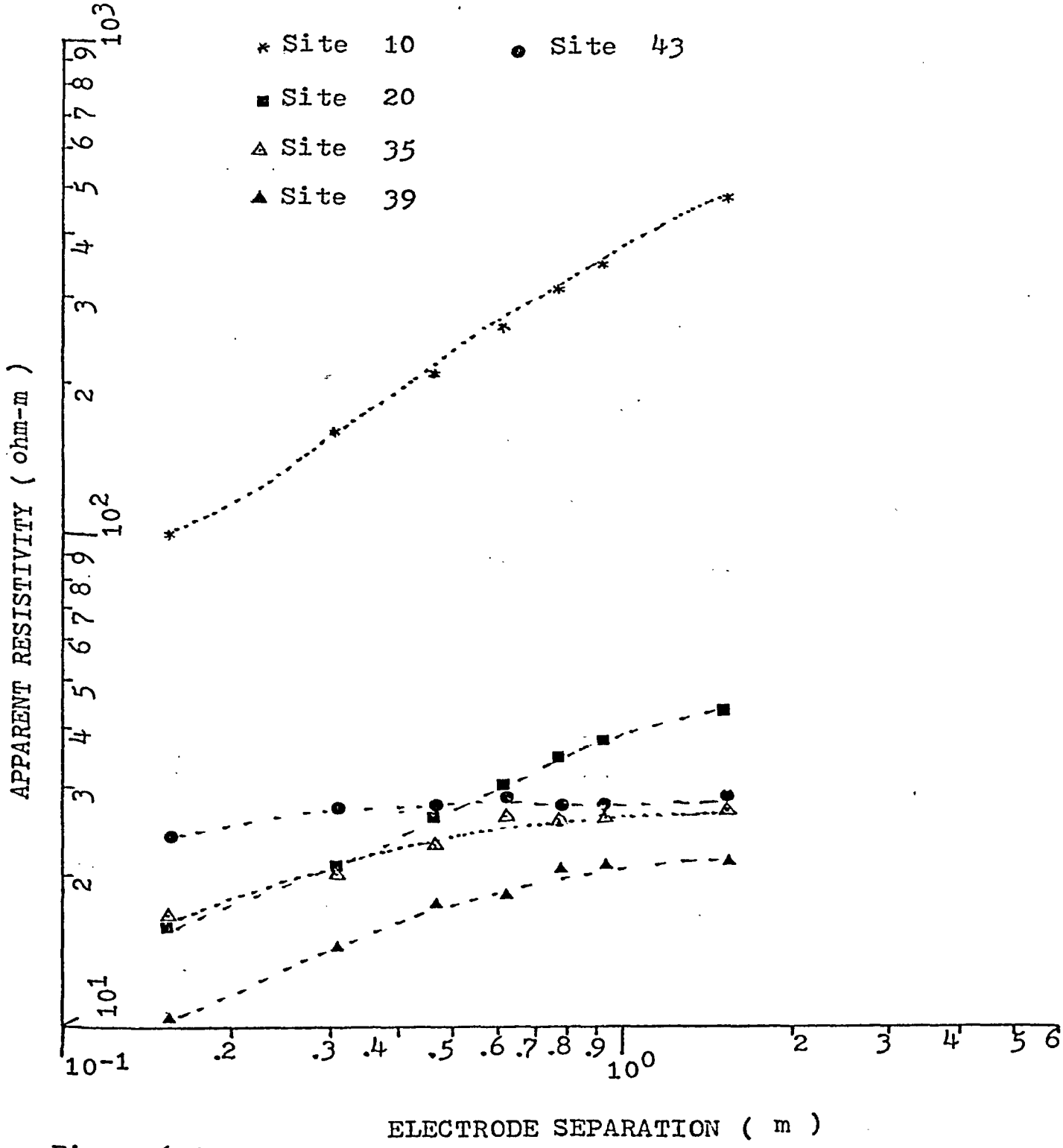

Fig. 26.5.

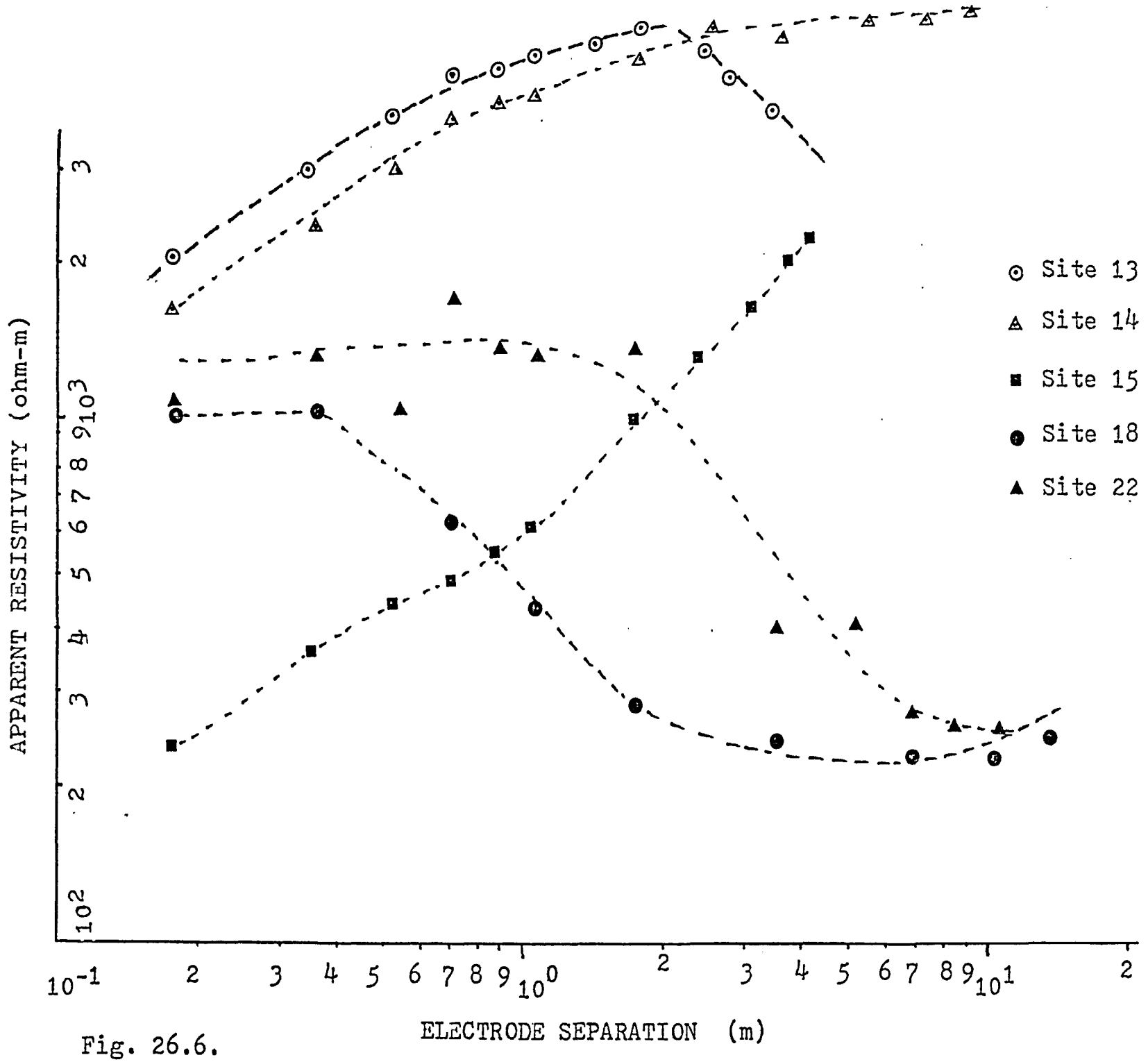

Fig. 26.6.

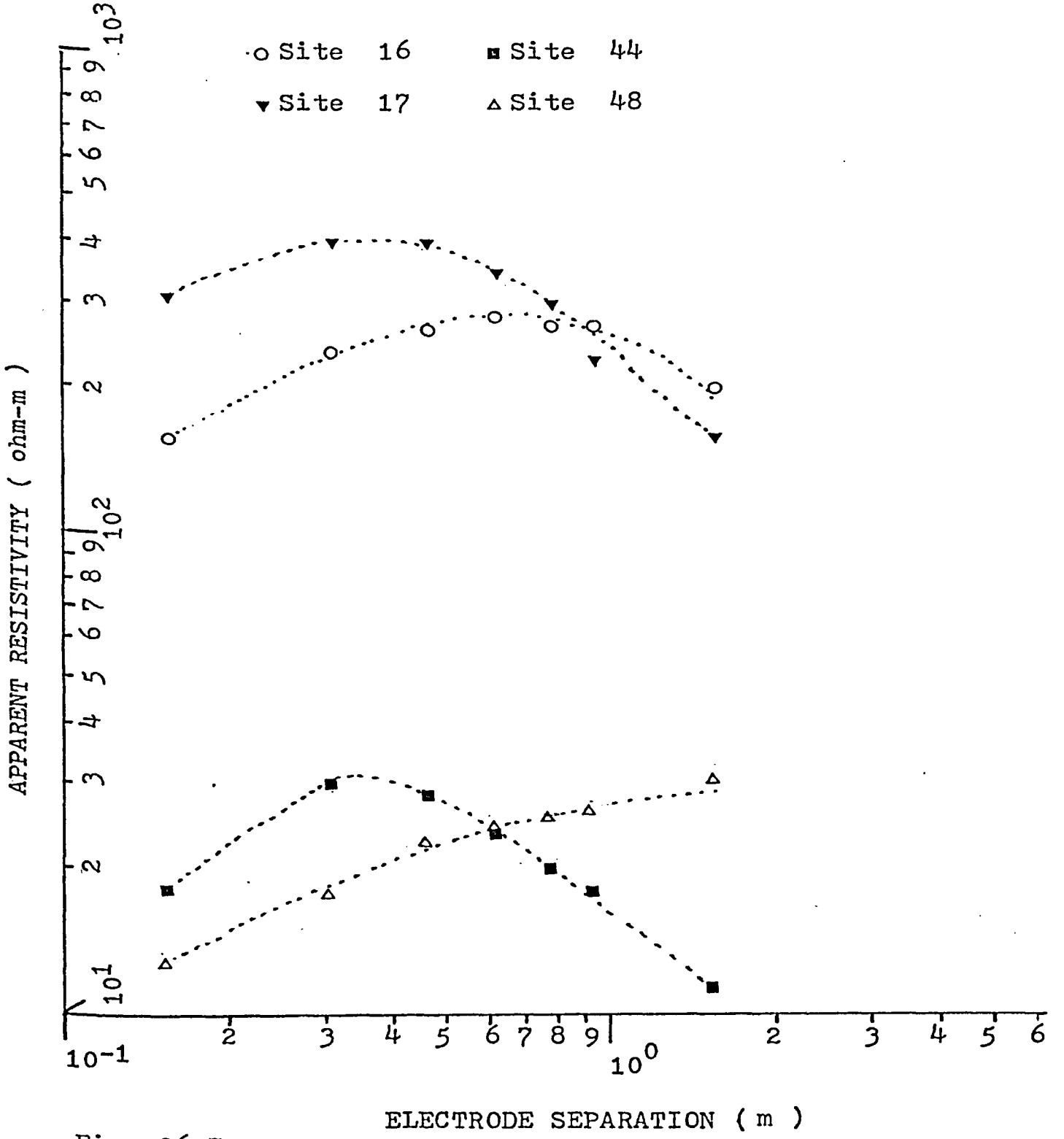

Fig. 26.7.

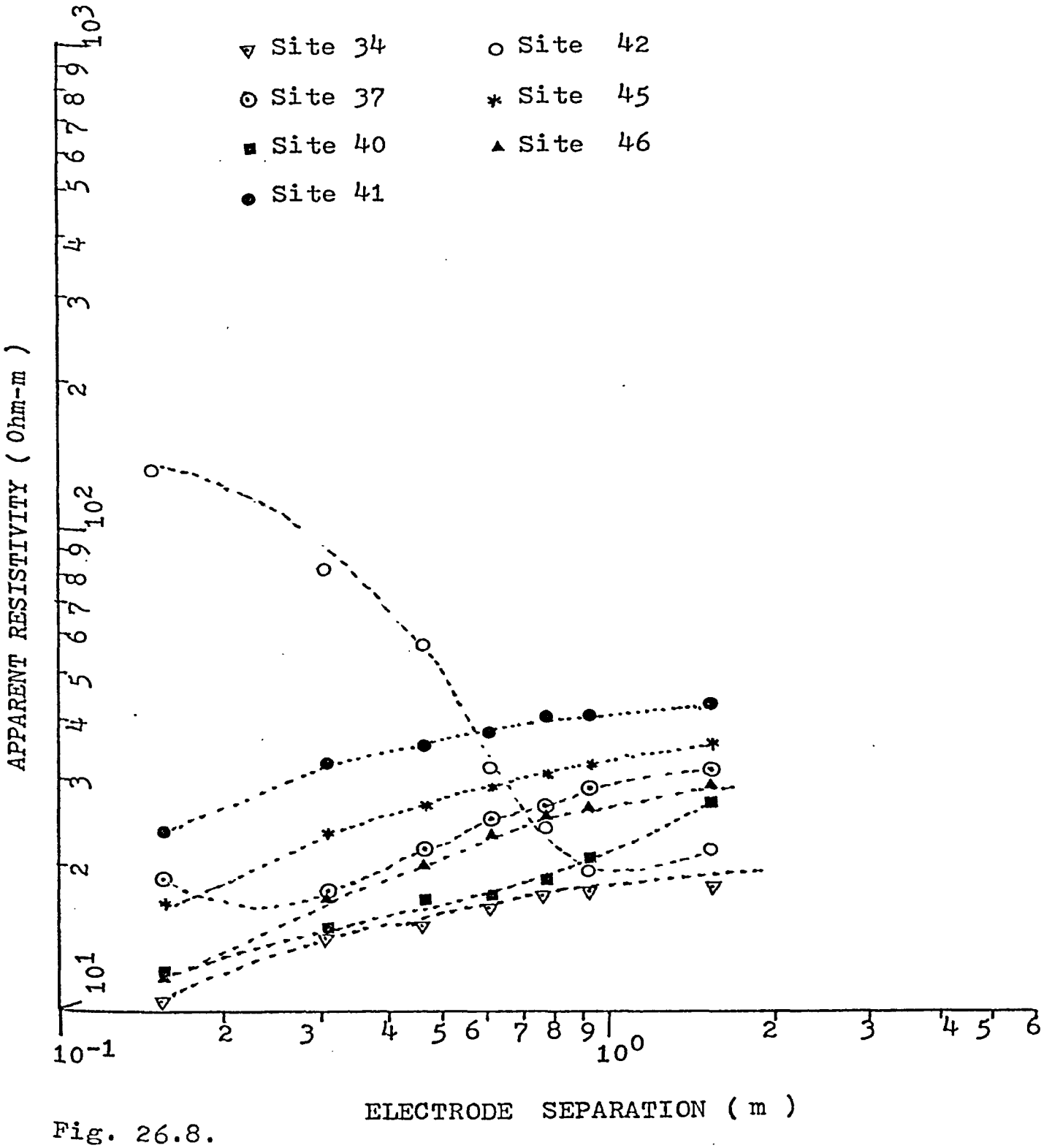

Fig. 26.8.

APPENDIX IV

DERIVATION OF THE EQUATION (4.3.2)

Derivation of equation (4.3.2).

Fig. 27 shows a point source of current of I amperes flowing into the ground. Let the resistivity of the ground be ρ. A potential electrode is placed at distance α. It is now required to determine the potential at P due to the current I.

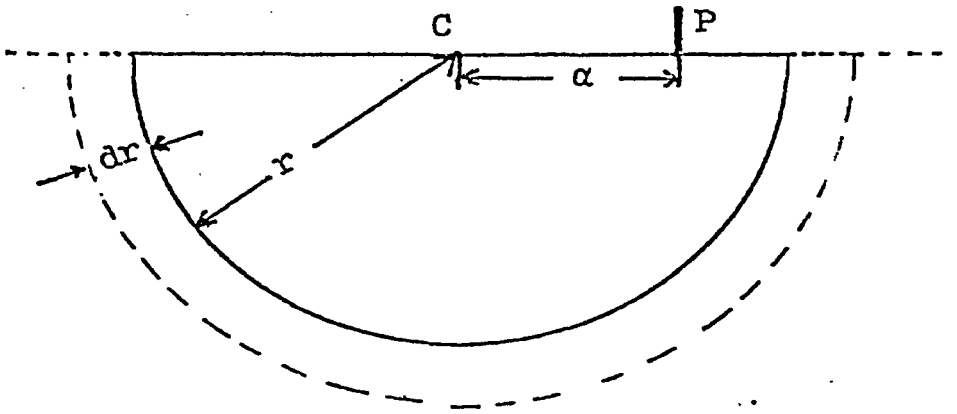

Fig. 27. Current lines from a point source of current I.

Since the medium is isotropic the current flow outward from C must be the same in all directions into the earth. No current flows upwards because the resistivity of the air is infinite. Thus the current lines are uniformly spaced radial lines, and the equipotential surfaces are concentric hemispheres with their centres at C. Considering two of these equipotential surfaces, one of radius r and one of infinitesimally greater radius dr, then all the current I must flow outward through the half-shell bounded by these two equipotential surfaces. This half-shell isvery thin. Therefore we may apply Ohm's law

for linear conductors, assuming the flow of currnt to be linear. Thus the potential drop dV from the inner surface to the outer one of this half-shell is:

$$dV = I(\rho \cdot dr/2\pi r^2) \qquad (IV.1)$$

where dr is the length and 2 r^2 the mean cross-sectional area of this linear conductor. The potential at P can now be calculated by integrating eqn. (IV.1) from α to infinity:

$$V = \int_{\alpha}^{\infty} dV = \frac{I\rho}{2\pi} \int_{\alpha}^{\infty} \frac{dr}{r^2} = \frac{I\rho}{2\pi\alpha}$$

APPENDIX V

INTEGRATED ANALYSIS

Graphs

INTEGRATED ANALYSES

Figure 26.

A, B and C designate the GRAVEL, SAND and CLAY groups.

Figure #	Variables plotted X vs Y		Group(s) examined
28.1.	log ρ	log V	A
28.2.	% Gravel	log V	A
28.3.	% Sand	log V	A
28.4.	% Gravel	log ρ	A
28.5.	% Sand	log ρ	A
28.6.	Resistivity	Velocity	A
28.7.	% Gravel	Velocity	A
28.8.	% Sand	Velocity	A
28.9.	% Gravel	Resistivity	A
28.10.	% Sand	Resistivity	A
28.11.	log ρ	log V	B
28.12.	% Gravel	log V	B
28.13.	% Sand	log V	B
28.14.	% Gravel	log ρ	B
28.15.	% Sand	log ρ	B
28.16.	Resistivity	Velocity	B
28.17.	% Gravel	Velocity	B
28.18.	% Sand	Velocity	B
28.19.	% Gravel	Resistivity	B
28.20.	% Sand	Resistivity	B
28.21.	% Gravel	Resistivity	A+B
28.22.	Resistivity	Velocity	A+B
28.23.	% Clay	Resistivity	C
28.24.	log ρ	log V	C
28.25.	% Sand	log V	C
28.26.	% Sand	log ρ	C
28.27.	% Clay	log V	C
28.28.	% Clay	log ρ	C
28.29.	Resistivity	Velocity	C
28.30.	% Sand	Velocity	C
28.31.	% Clay	Velocity	C
28.32.	% Sand	Resistivity	C

Table 19 . Plots included in Appendix V. X and Y designate the two Cartesian axes.

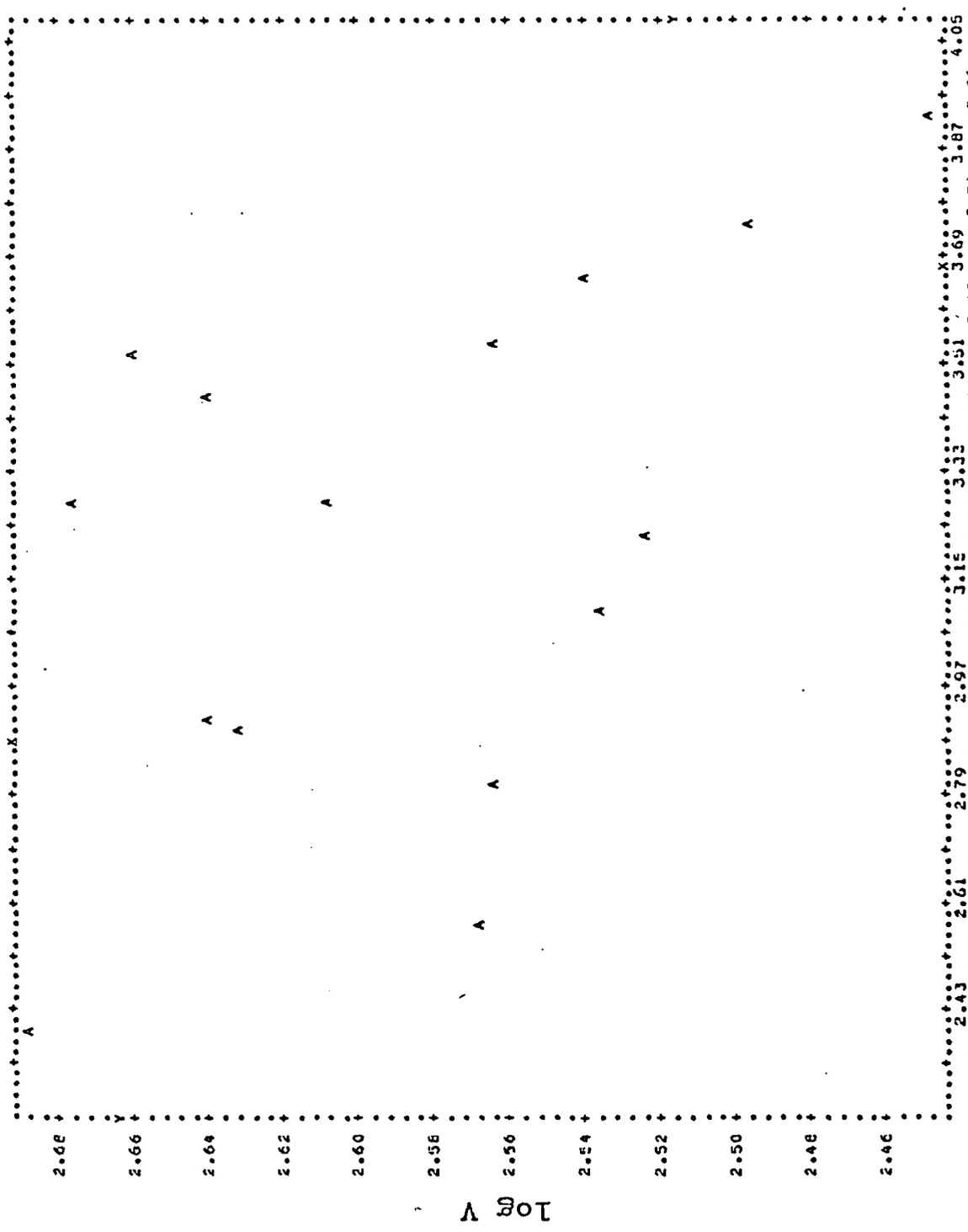

Fig. 28.1.

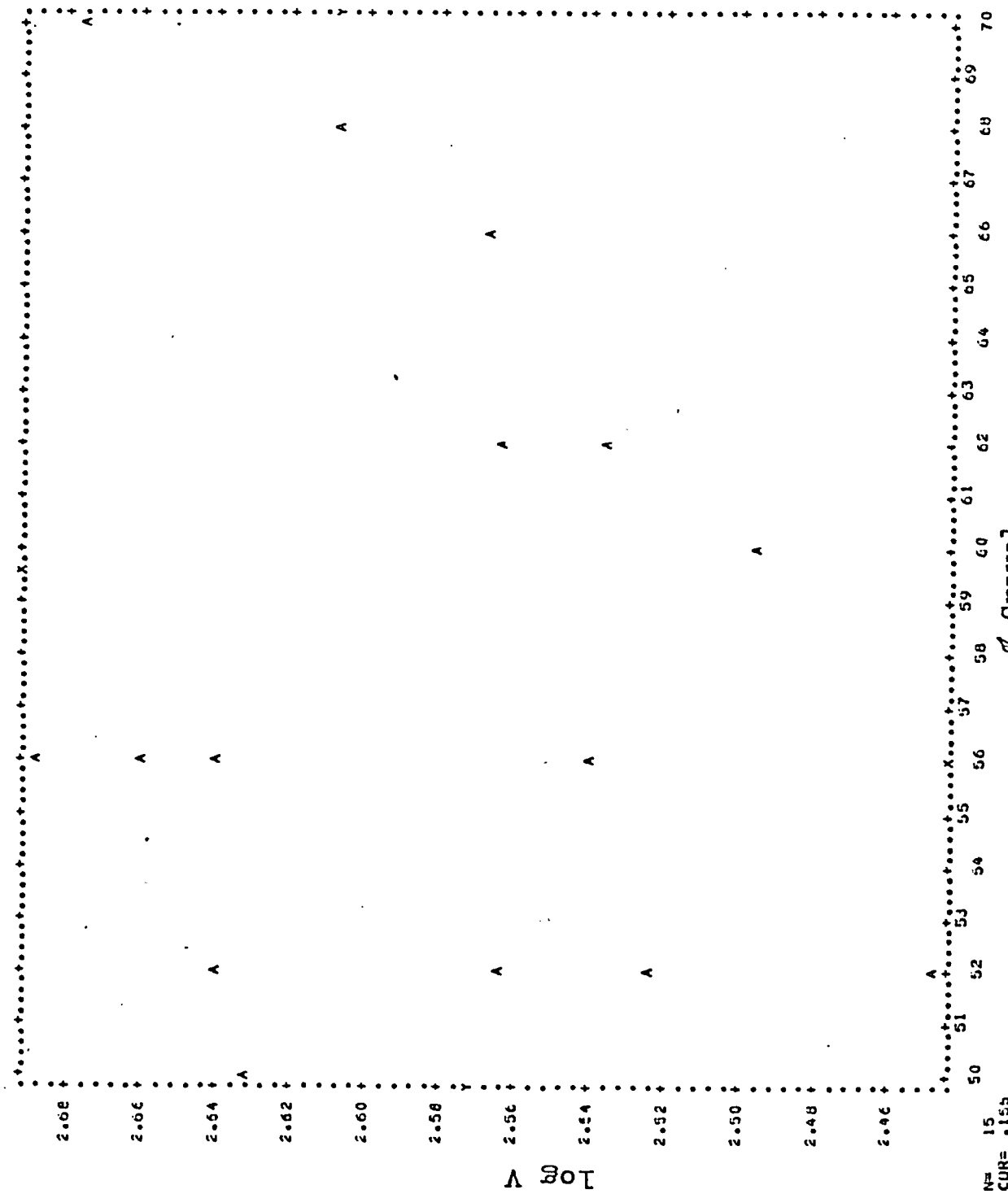

Fig. 28.2

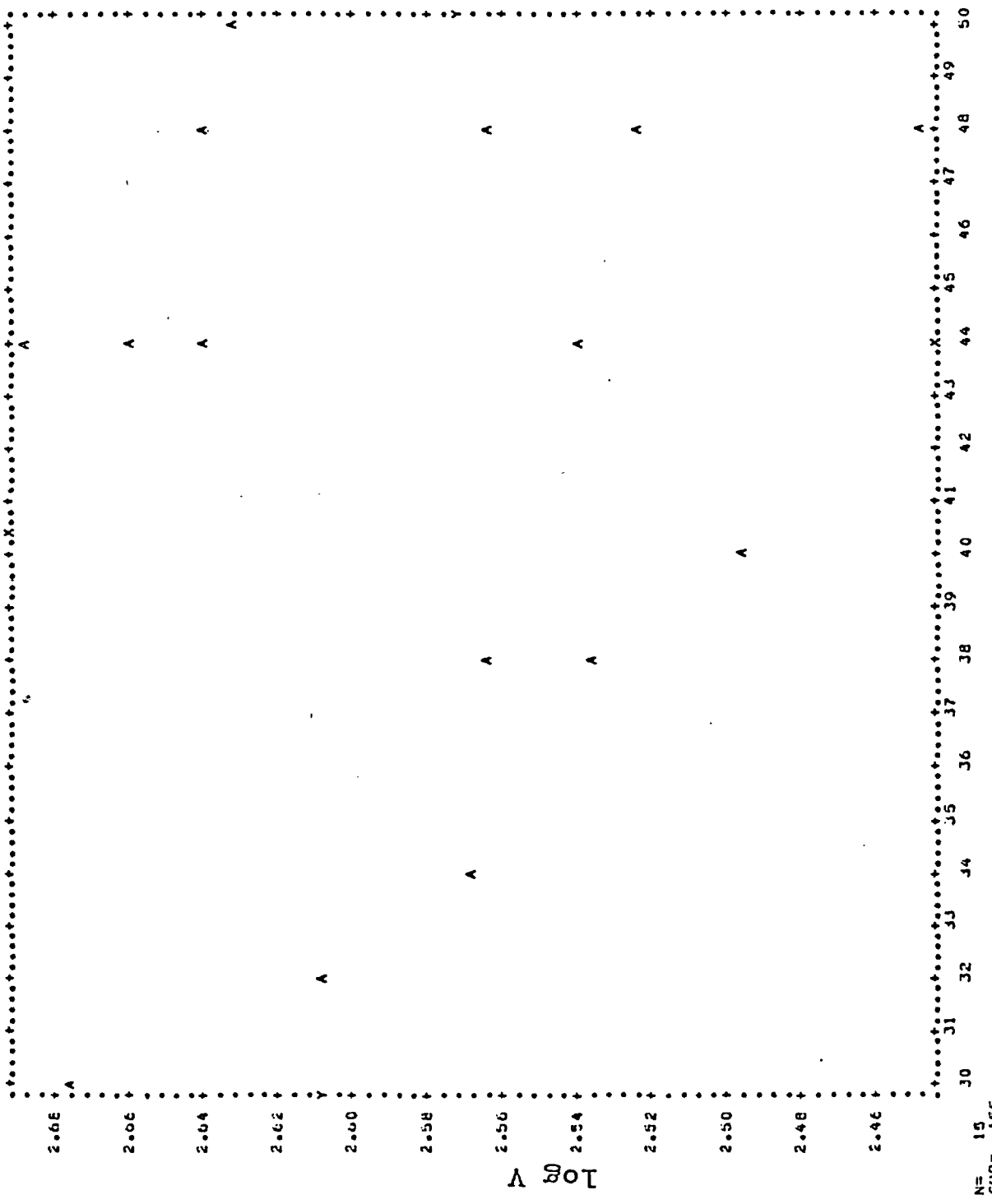

Fig. 28.3.

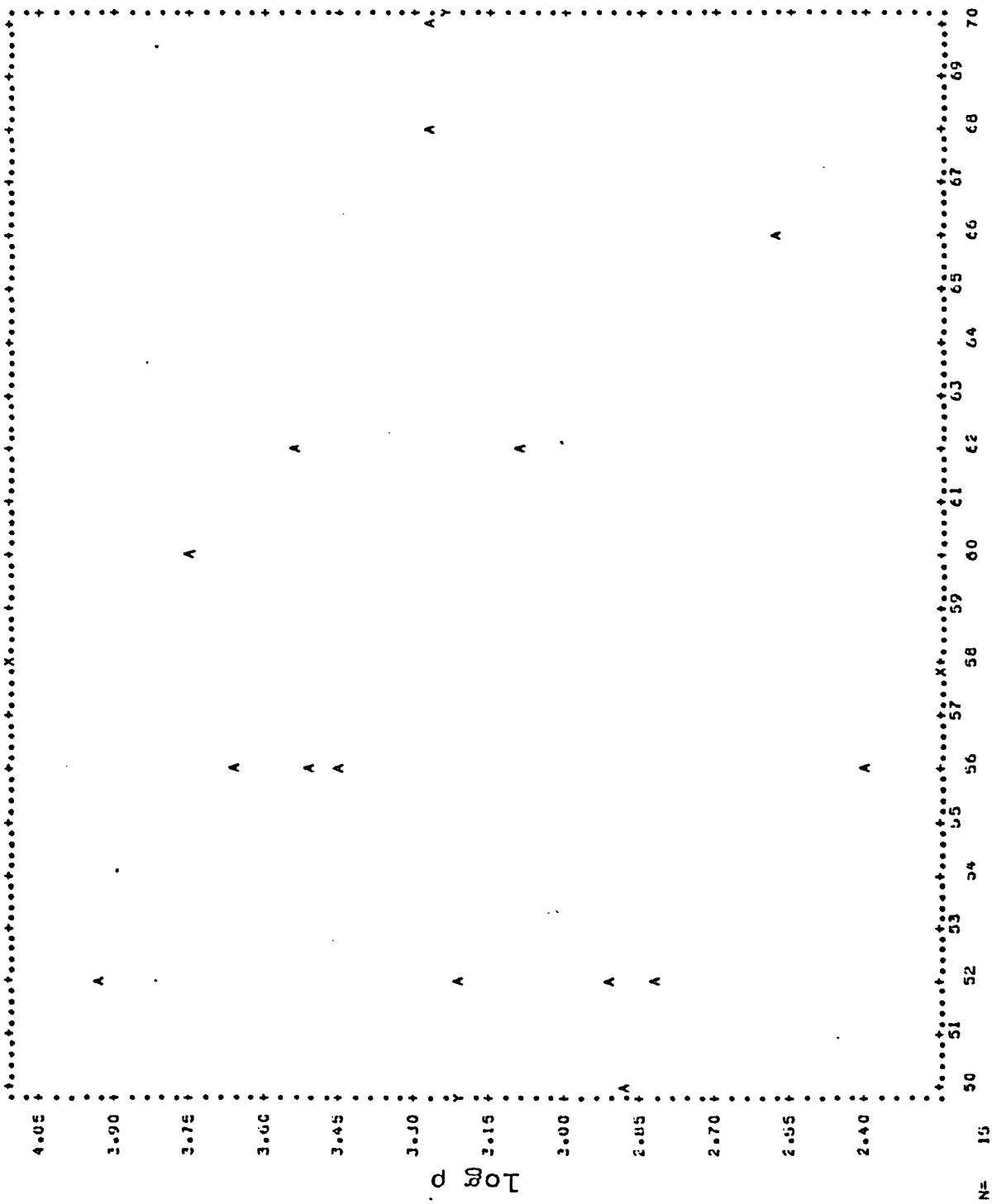

Fig. 28.4.

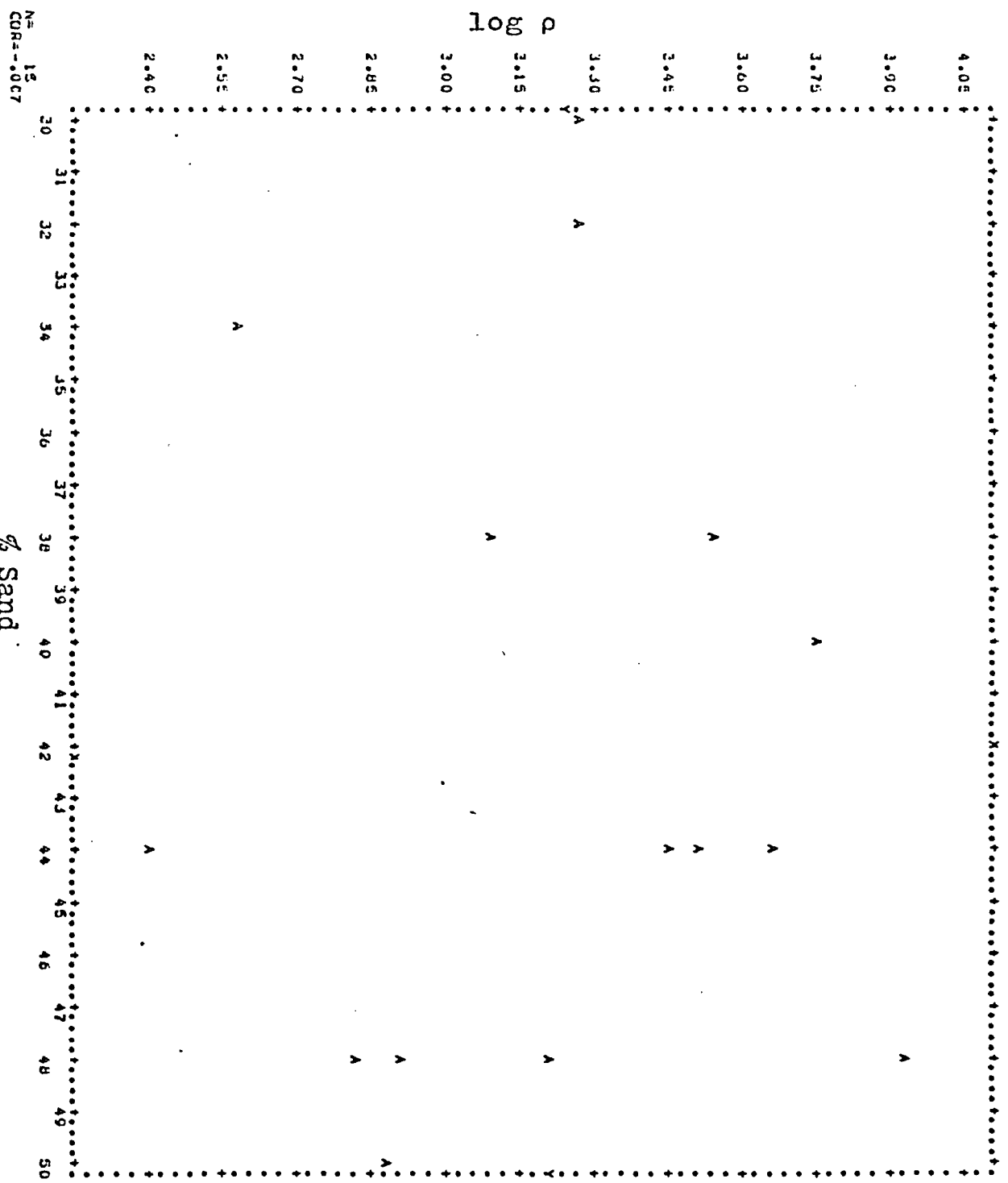

Fig. 28.5.

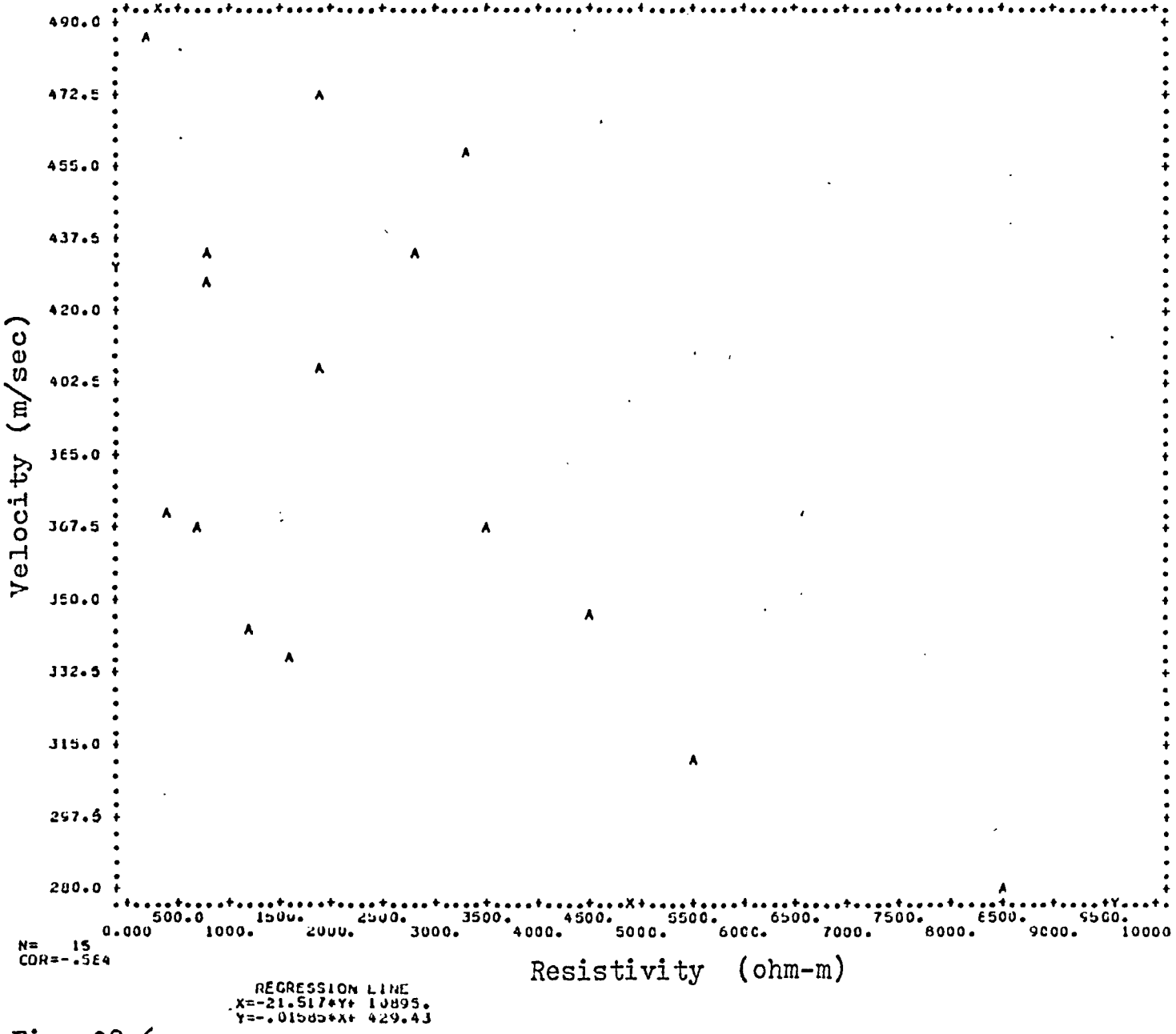

Fig. 28.6.

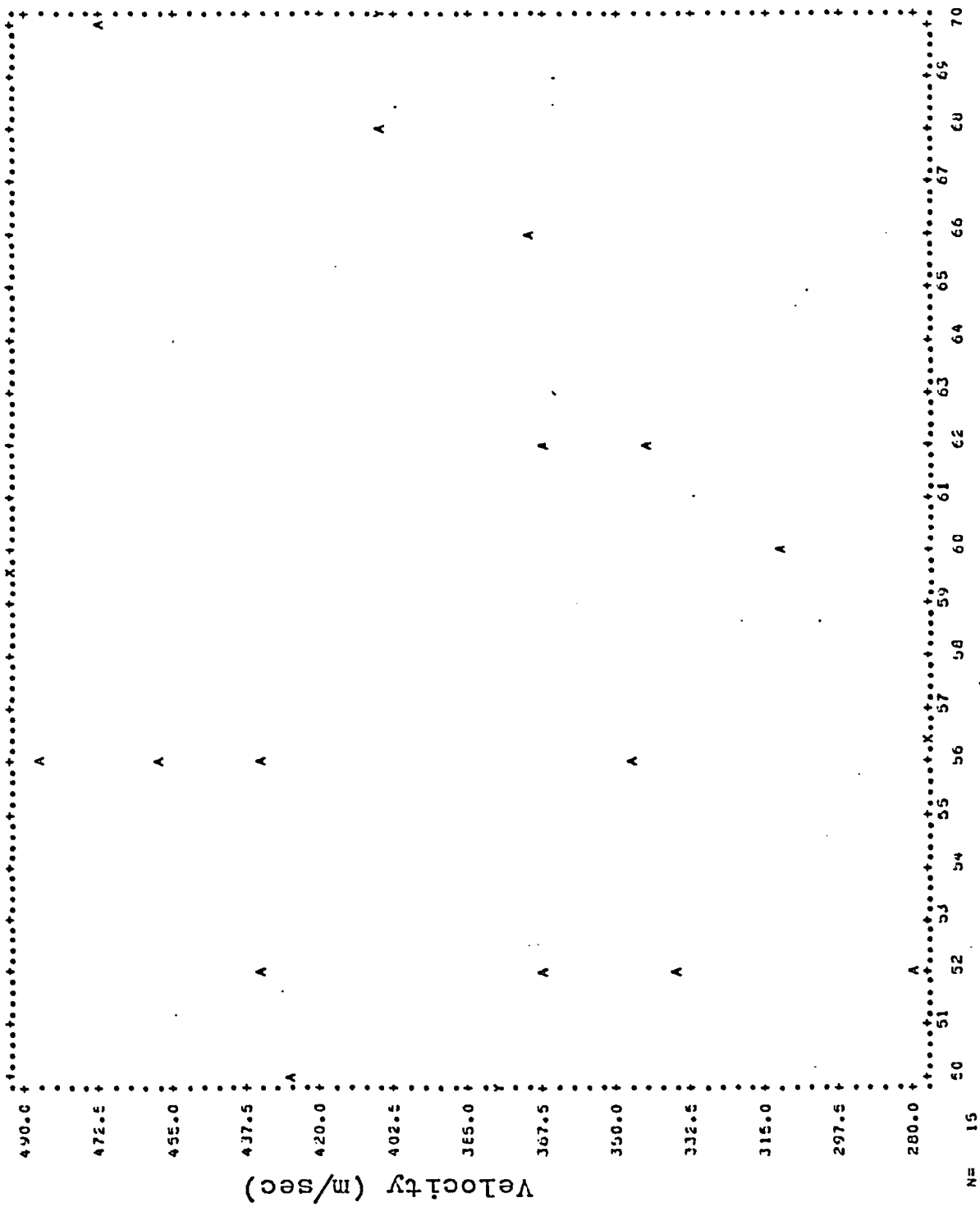

Fig. 28.7.

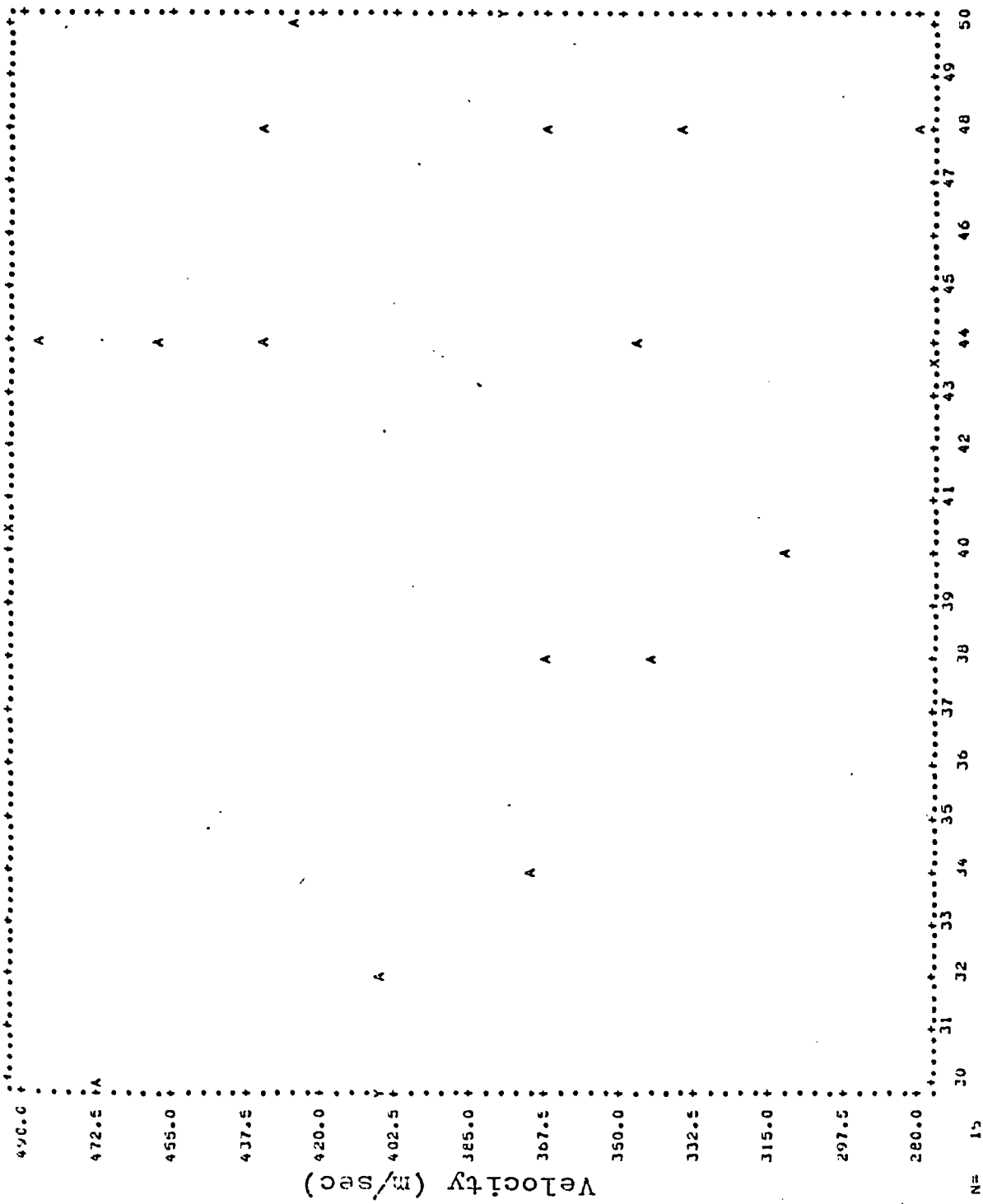

Fig. 28.8.

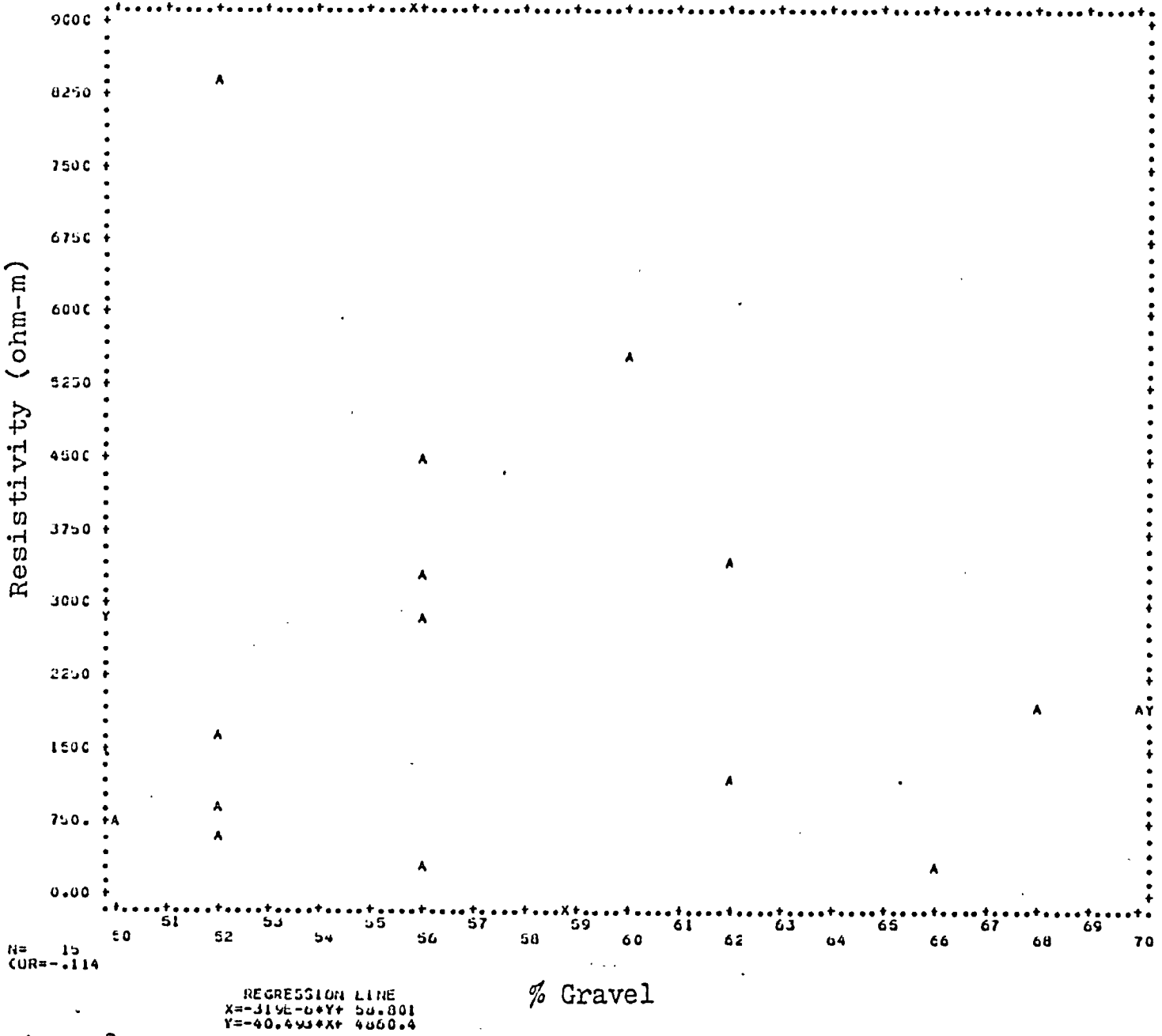

Fig. 28.9.

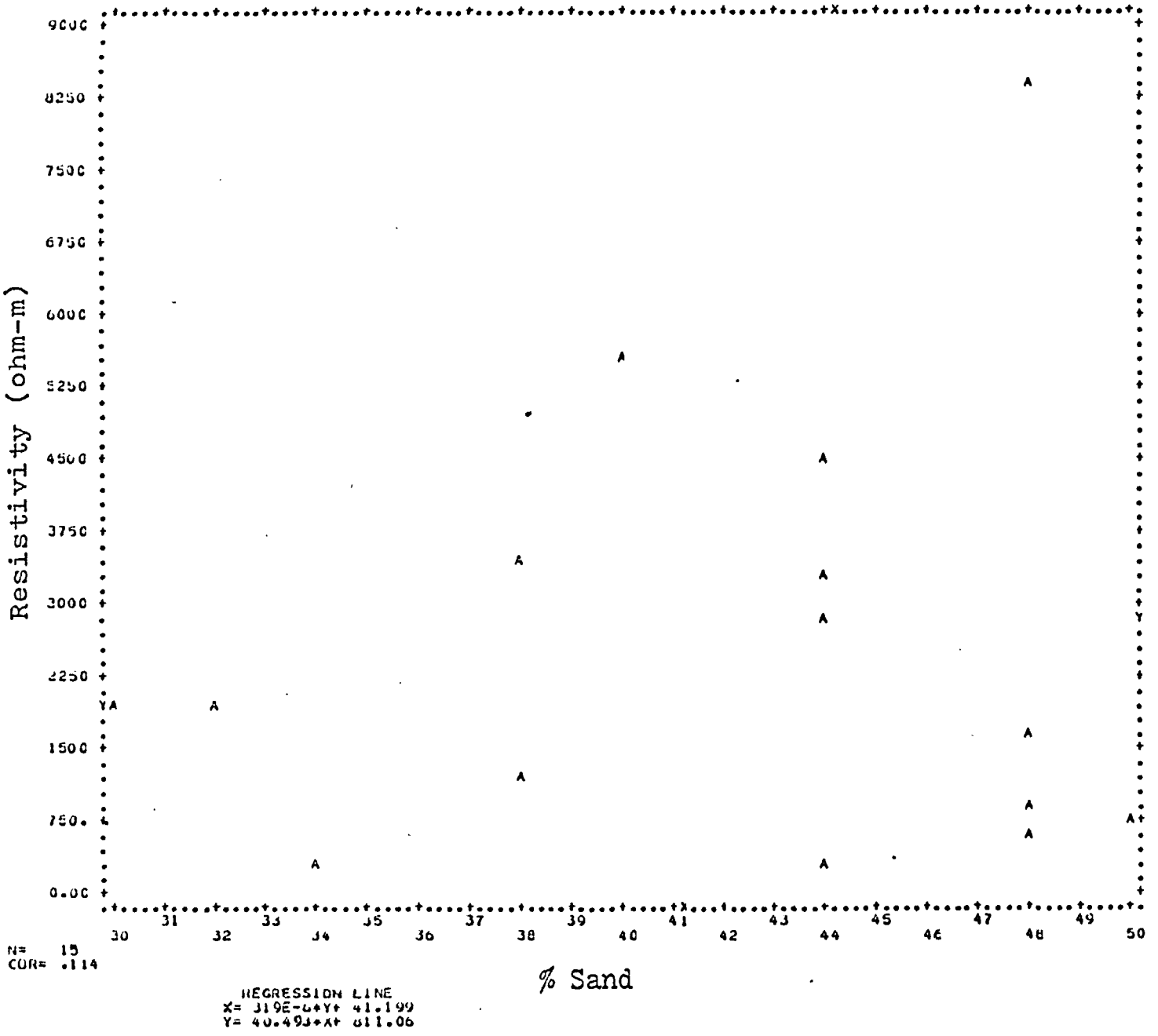

Fig. 28.10.

Site #	α	1.524	.914	.762	.609	.457	.304	.152
43	I	100	100	100	100	100	100	100
	V	295	480	570	745	950	1400	2450
	ρ_α	28.3	27.6	27.3	28.5	27.3	26.8	23.5
44	I	100	100	100	100	100	100	100
	V	120	310	420	900	1000	1600	1900
	ρ_α	11.5	17.8	20.1	21.1	28.7	30.6	18.2
45	I	100	100	100	100	100	80	50
	V	360	550	630	740	910	955	855
	ρ_α	35.0	31.6	30.2	28.3	26.2	22.9	16.4
46	I	100	100	100	100	100	100	100
	V	300	450	520	590	680	875	1200
	ρ_α	28.7	25.8	24.9	22.6	19.5	16.7	11.5
47	I	100	100	100	100	100	100	100
	V	290	490	550	670	870	1100	1600
	ρ_α	27.8	28.1	26.3	25.7	25.0	21.1	15.3
48	I	100	100	100	100	100	100	70
	V	320	460	530	630	790	920	940
	ρ_α	30.6	26.4	25.4	24.1	22.7	17.6	12.9
49	I	100	100	100	100	100	100	100
	V	310	445	500	560	690	800	1200
	ρ_α	29.7	25.6	23.9	21.5	19.8	15.3	11.5
50	I	100	100	100	100	100	100	100
	V	275	410	480	560	670	850	1300
	ρ_α	26.3	23.6	23.0	21.4	19.2	16.3	12.4

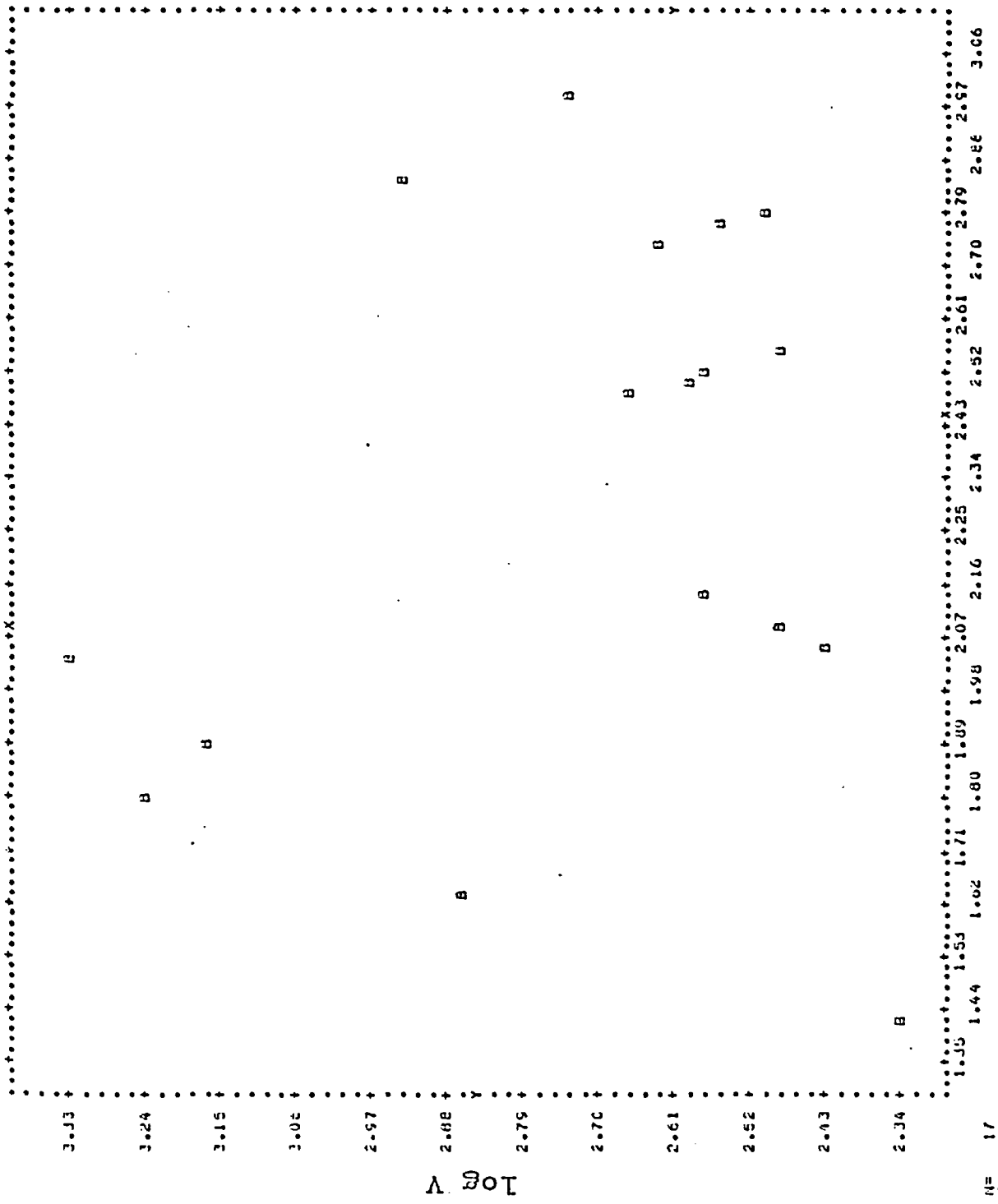

Fig. 28.11.

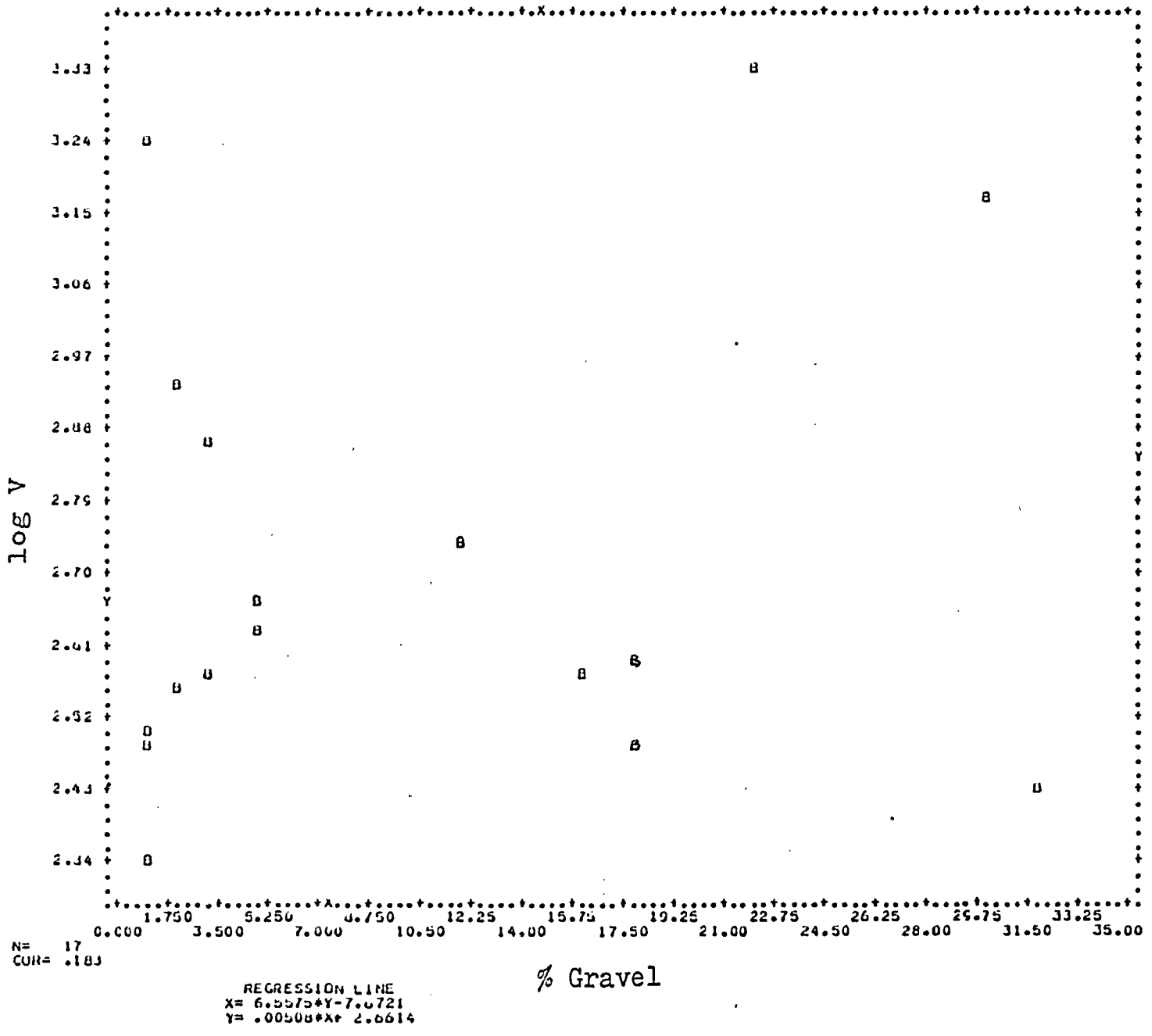

Fig. 28.12.

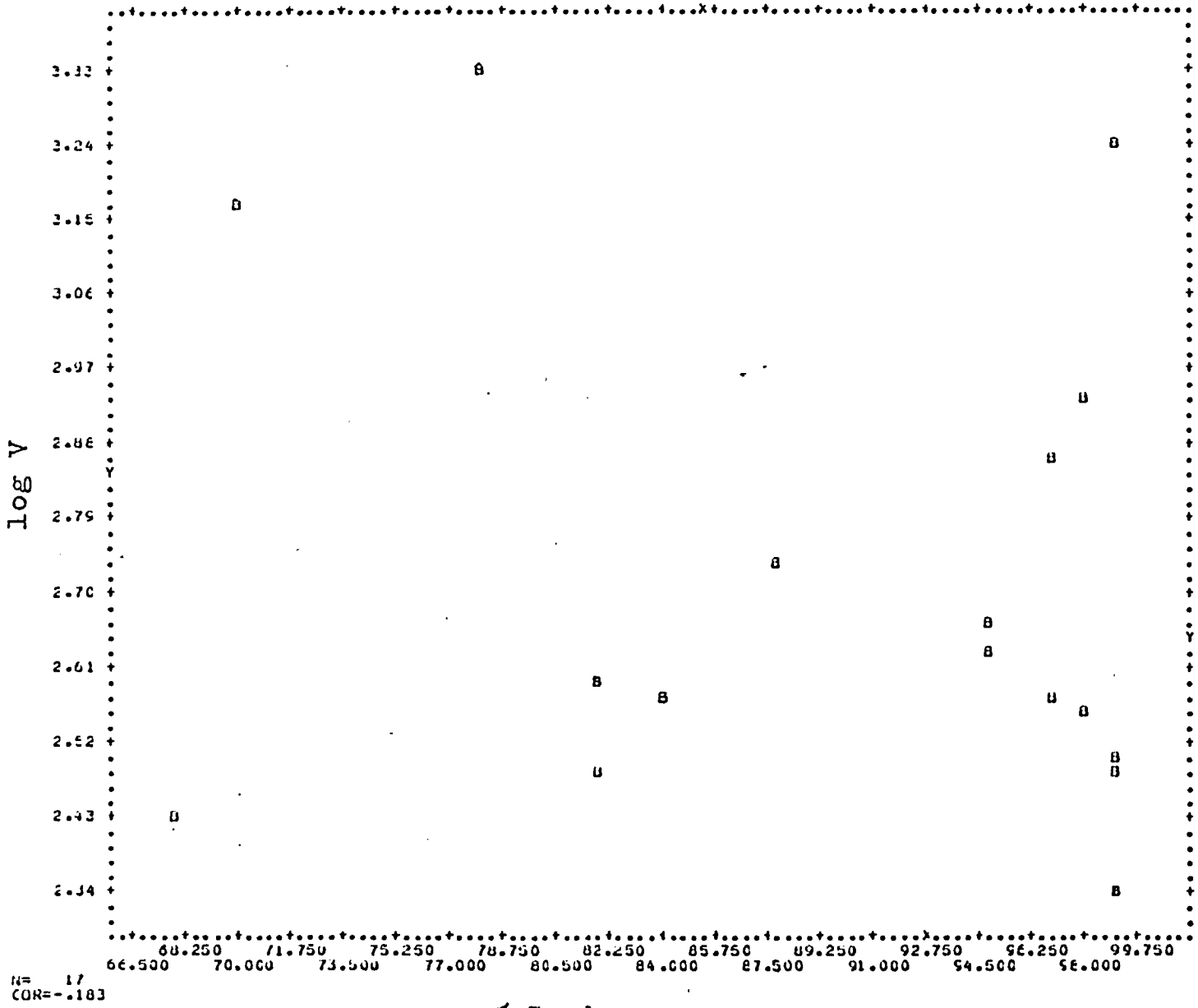

Fig. 28.13.

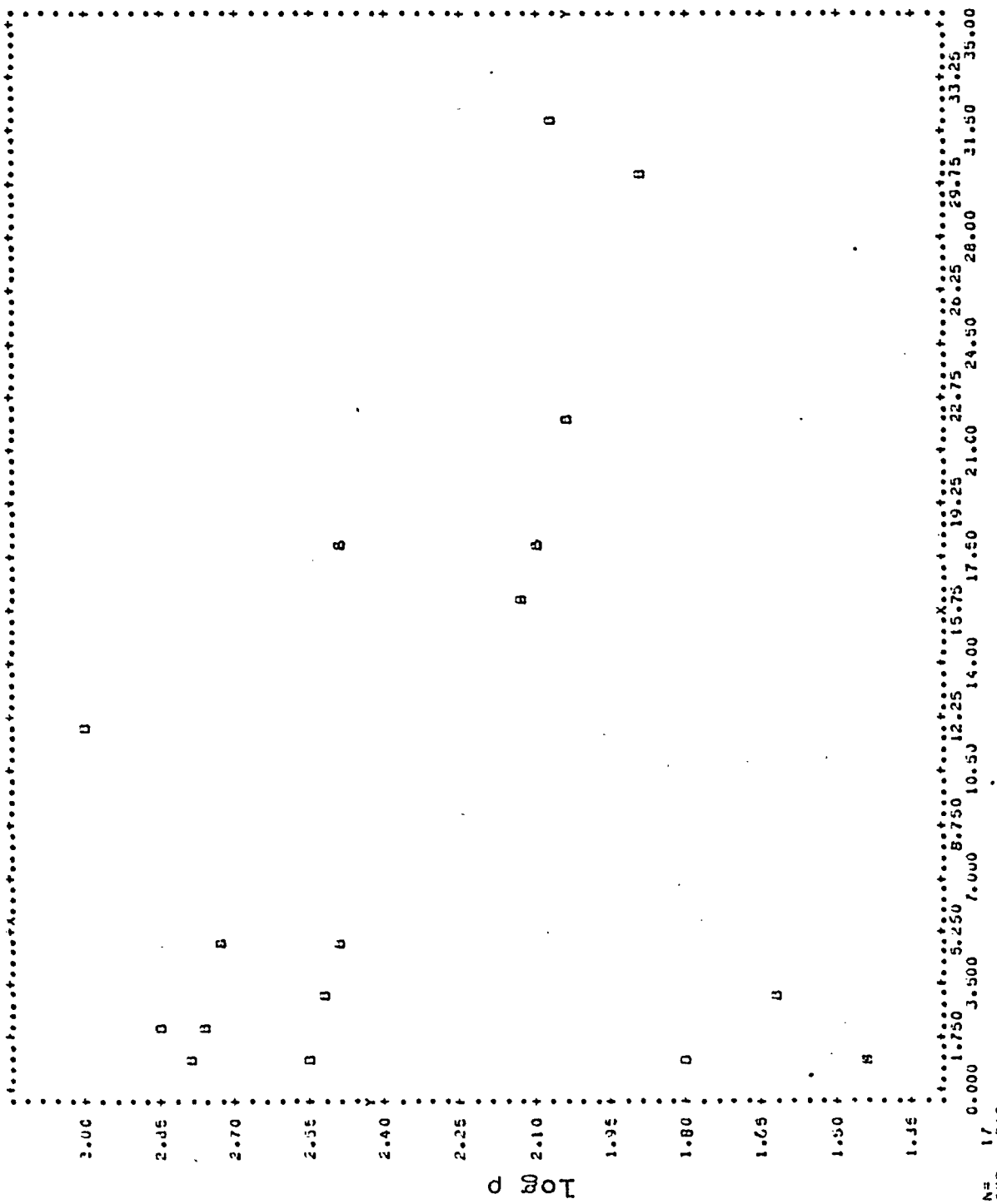

Fig. 28.14.

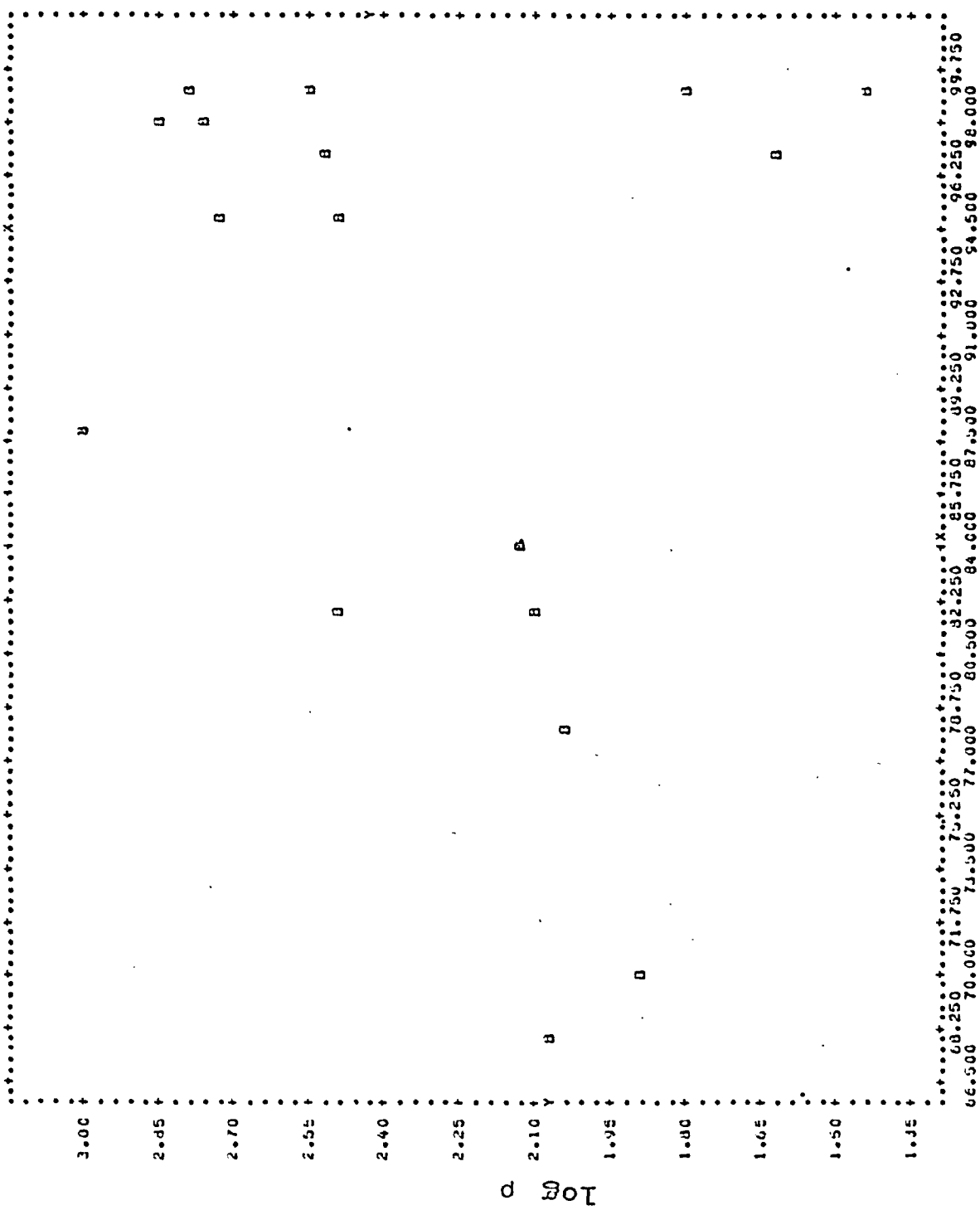

Fig. 28.15.

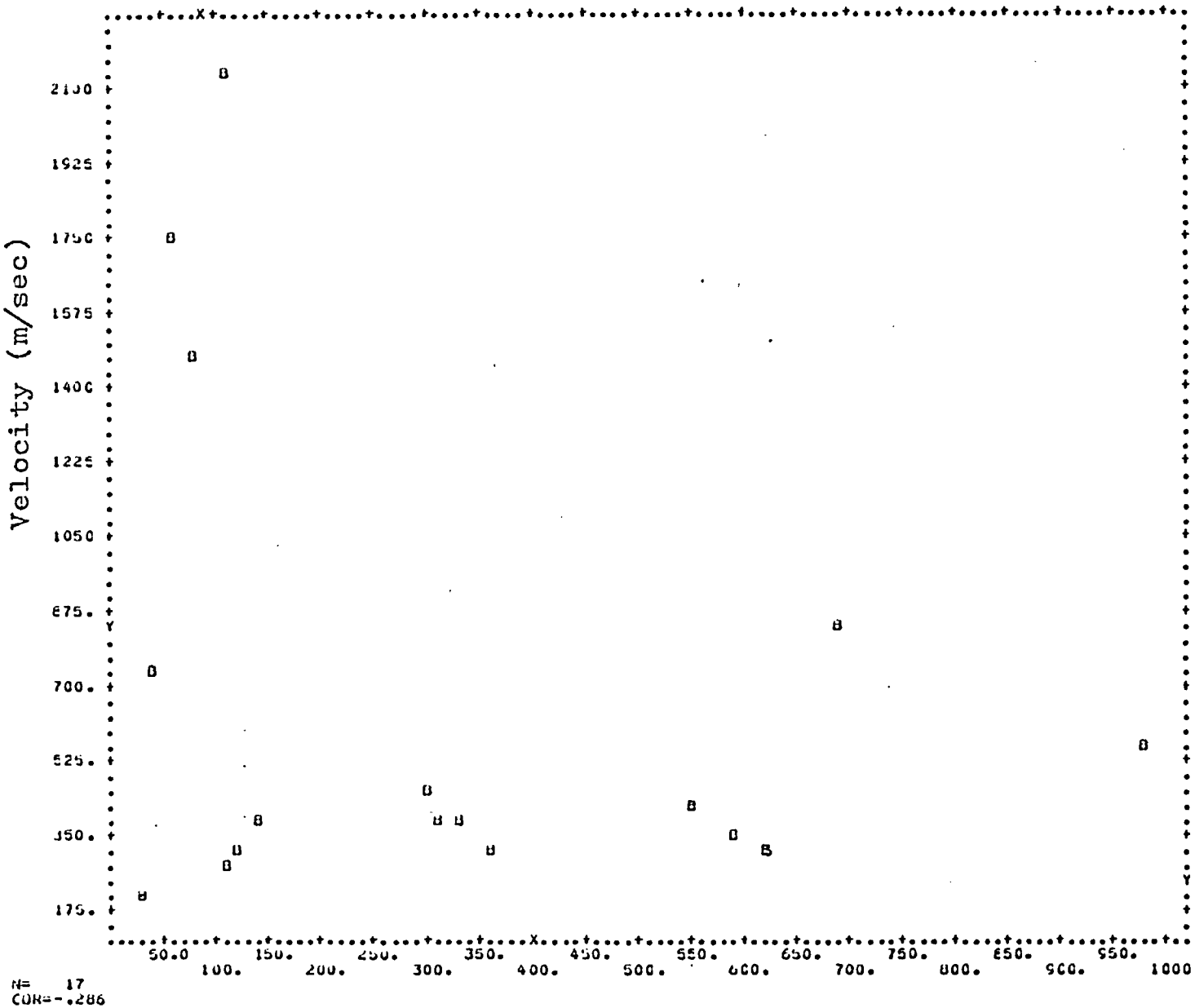

Fig. 28.16.

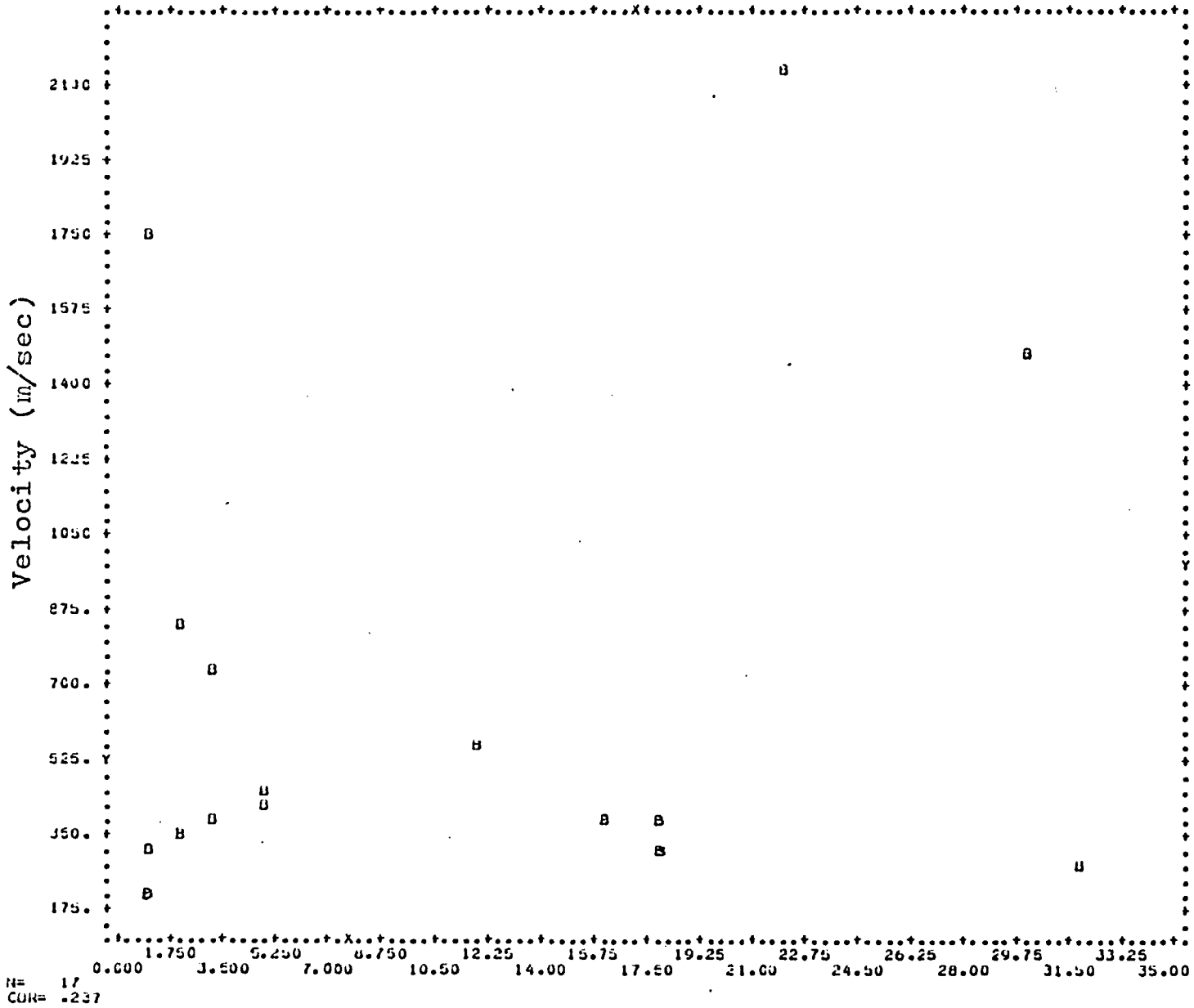

Fig. 28.17.

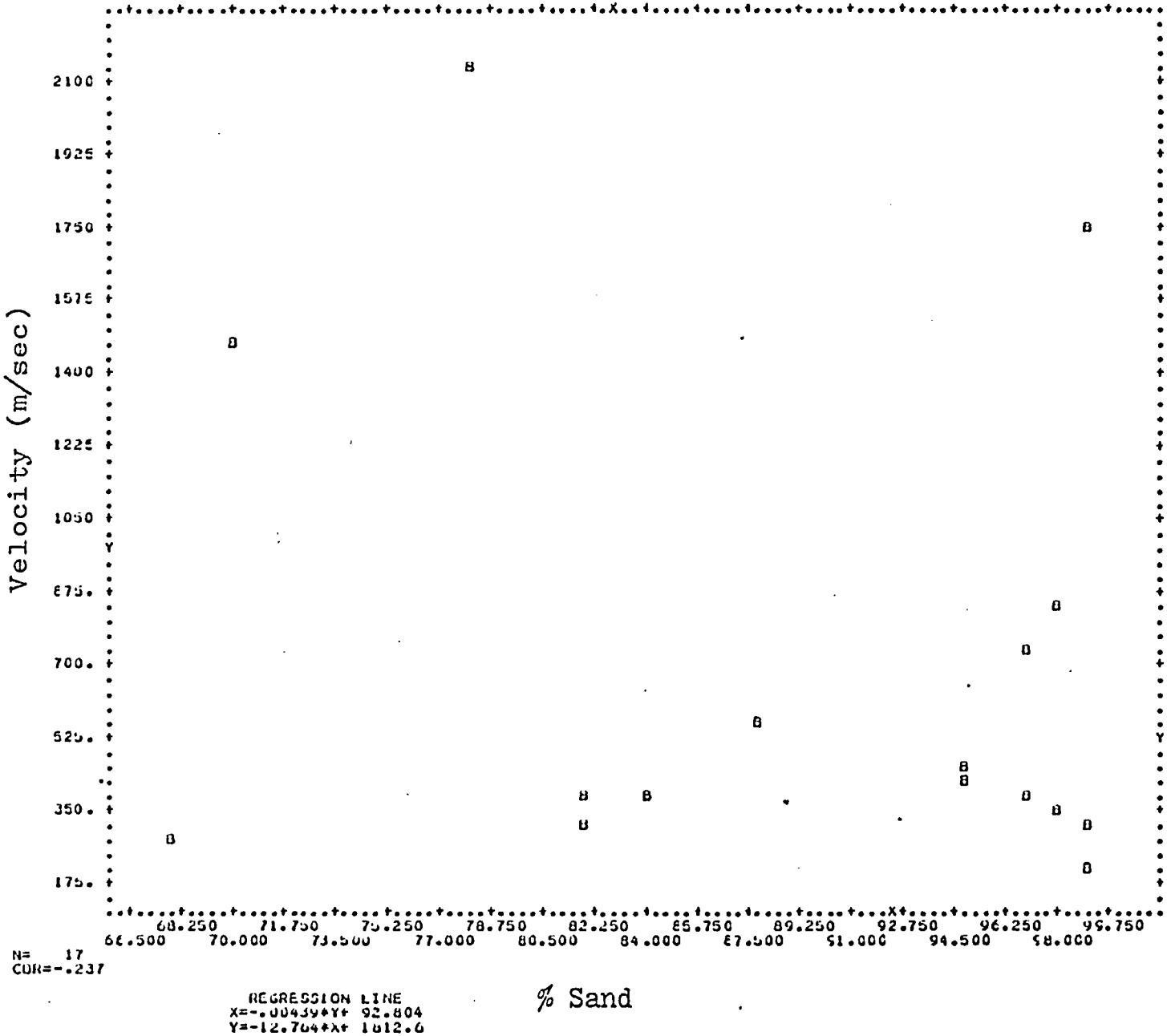

Fig. 28.18.

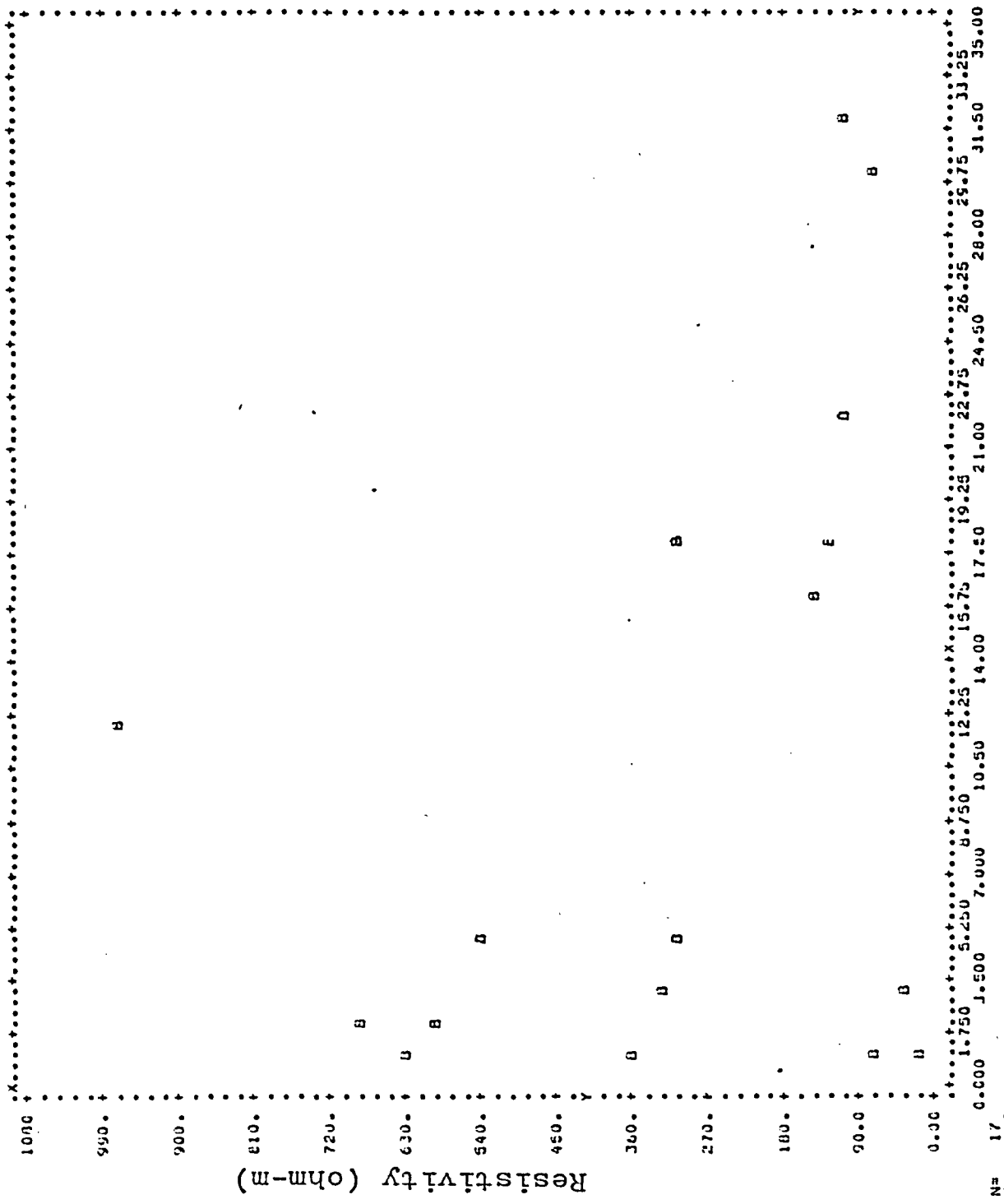

Fig. 28.19.

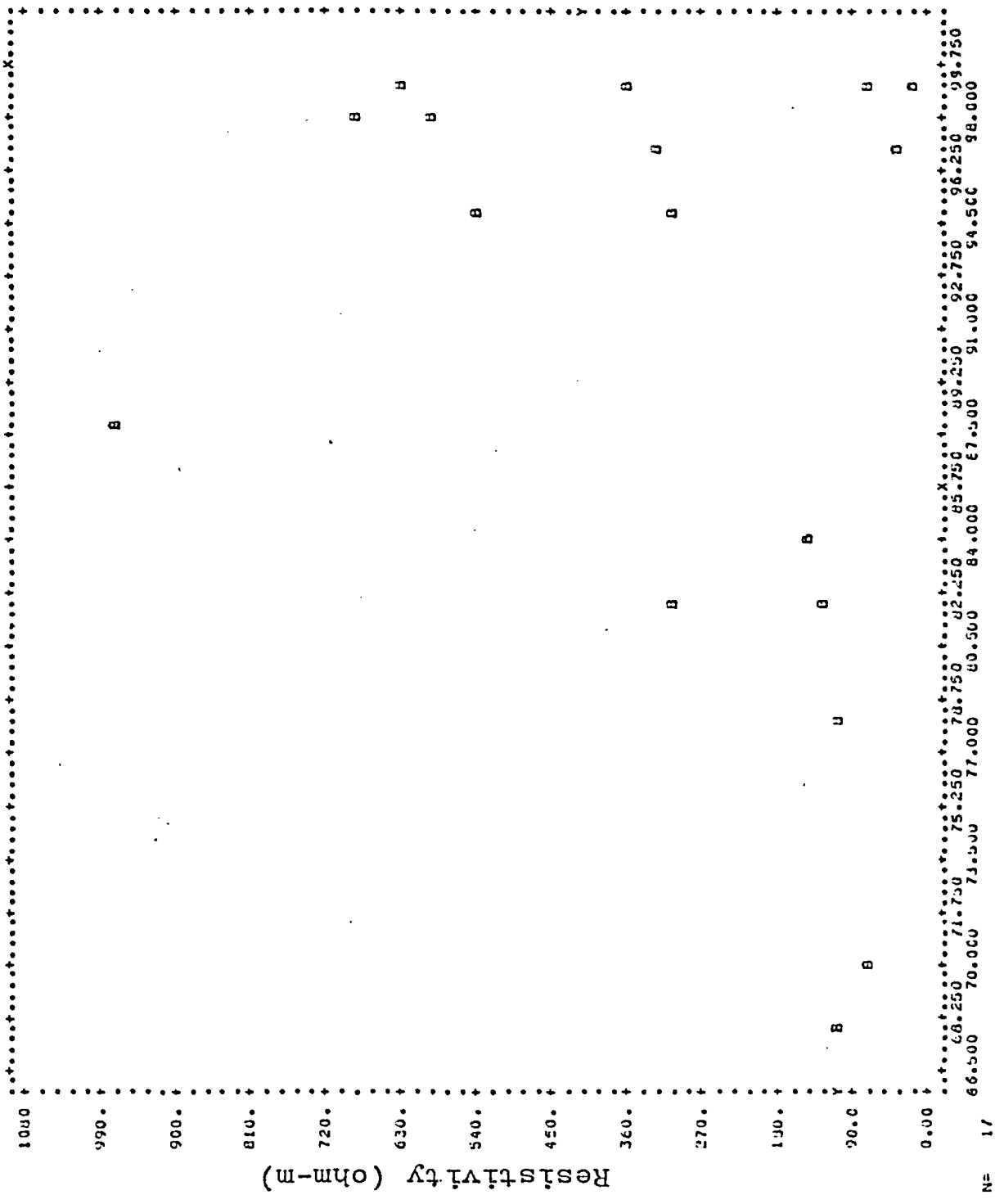

Fig. 28.20.

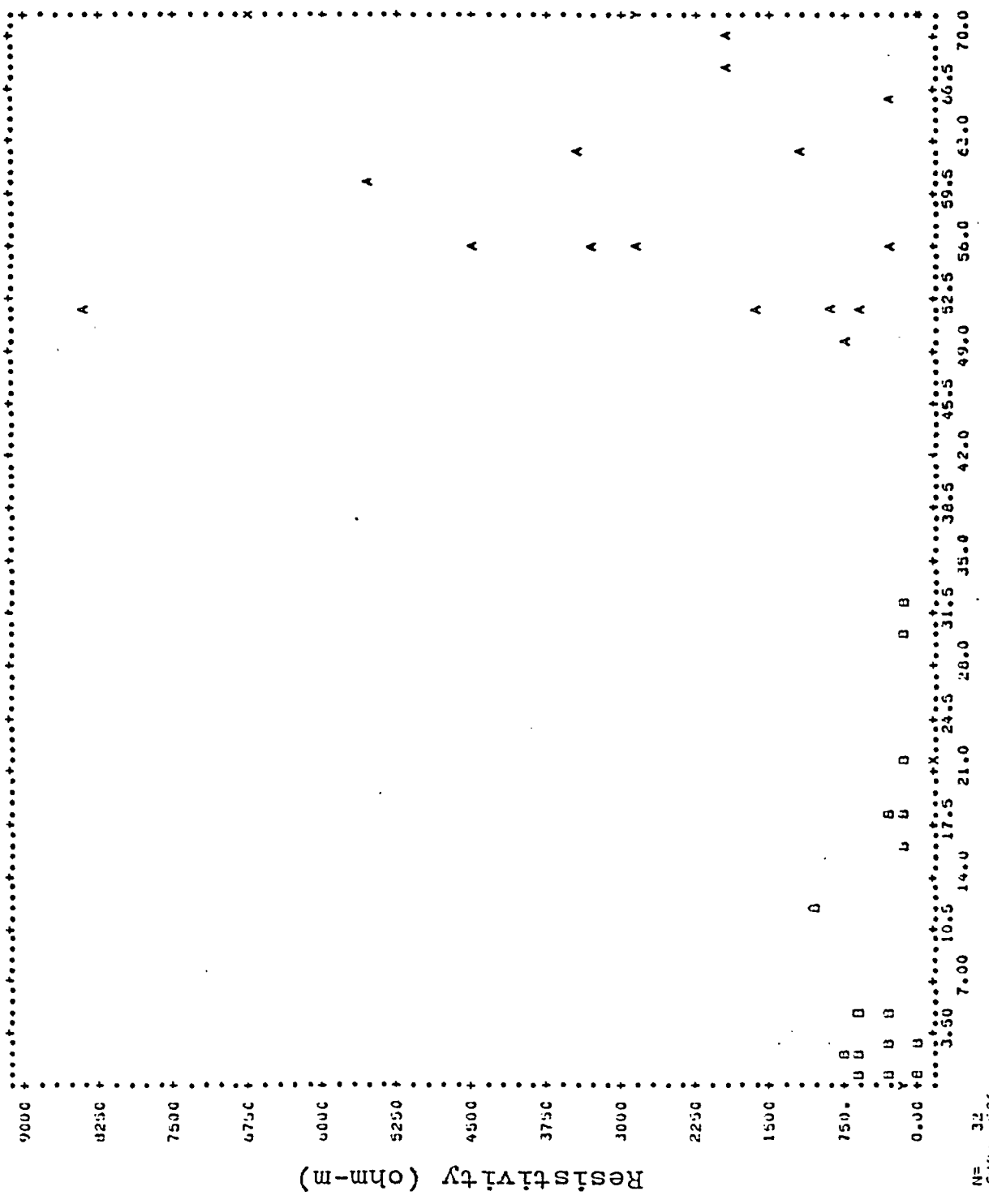

Fig. 28.21.

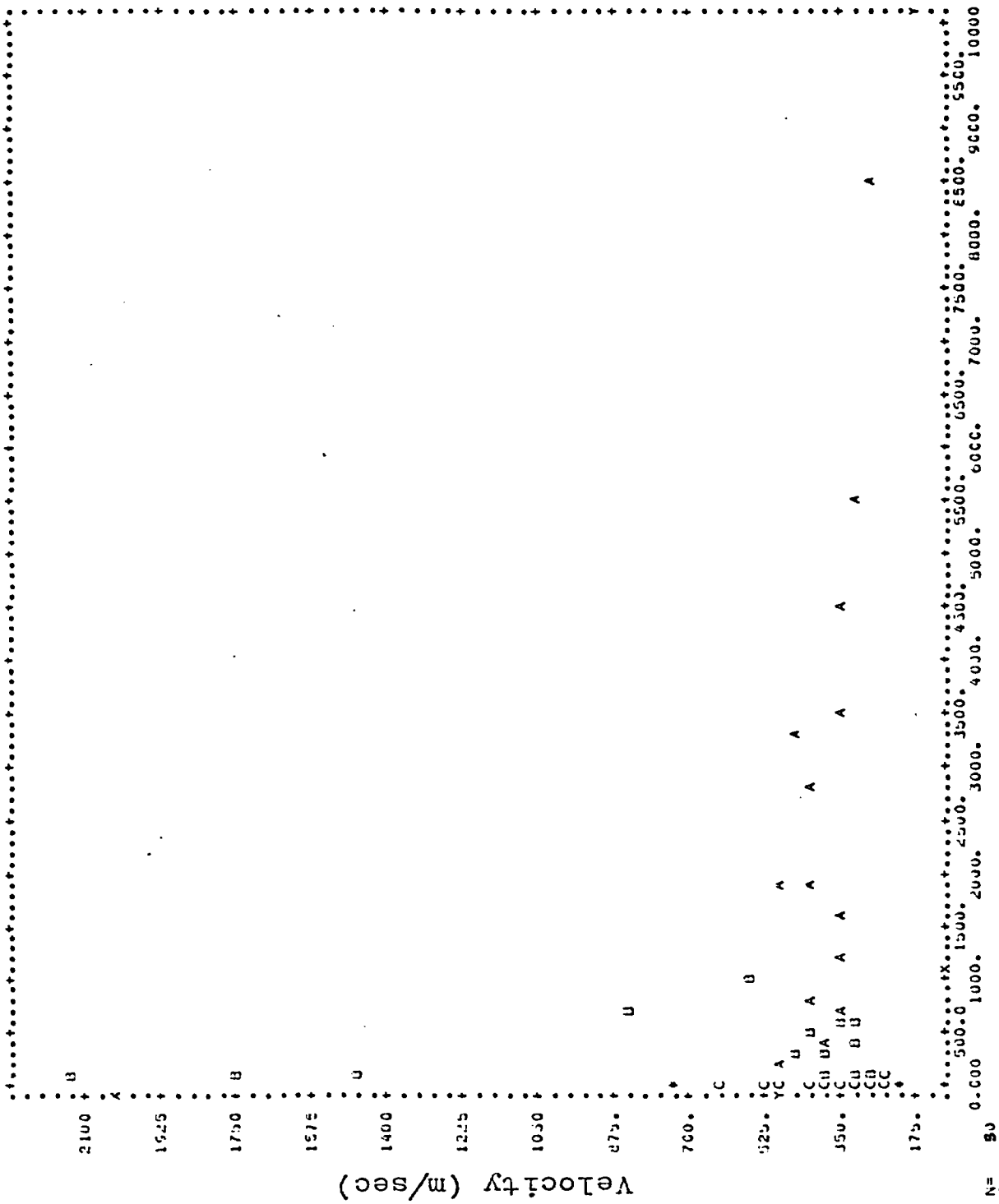

Fig. 28.22.

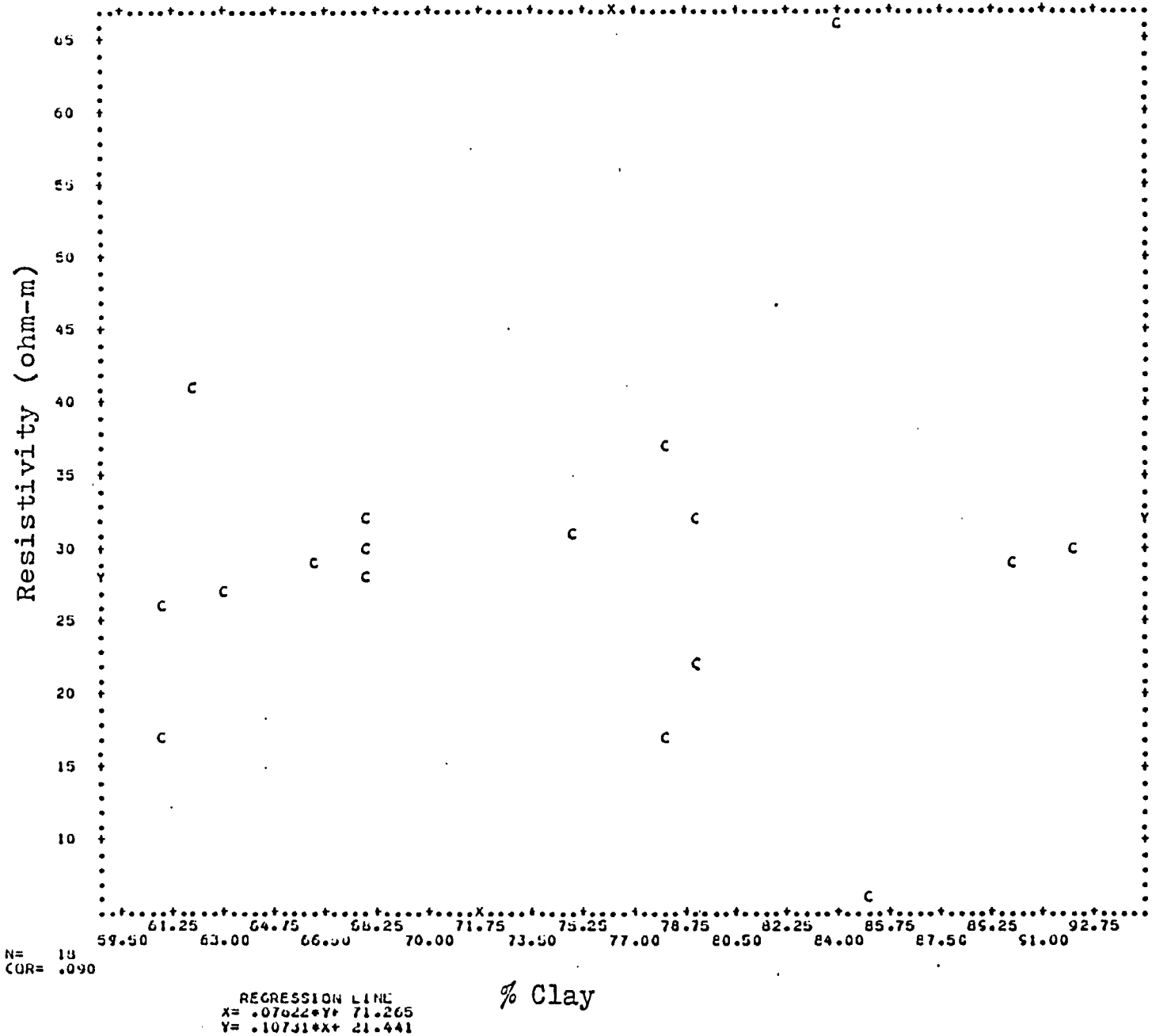

Fig. 28.23.

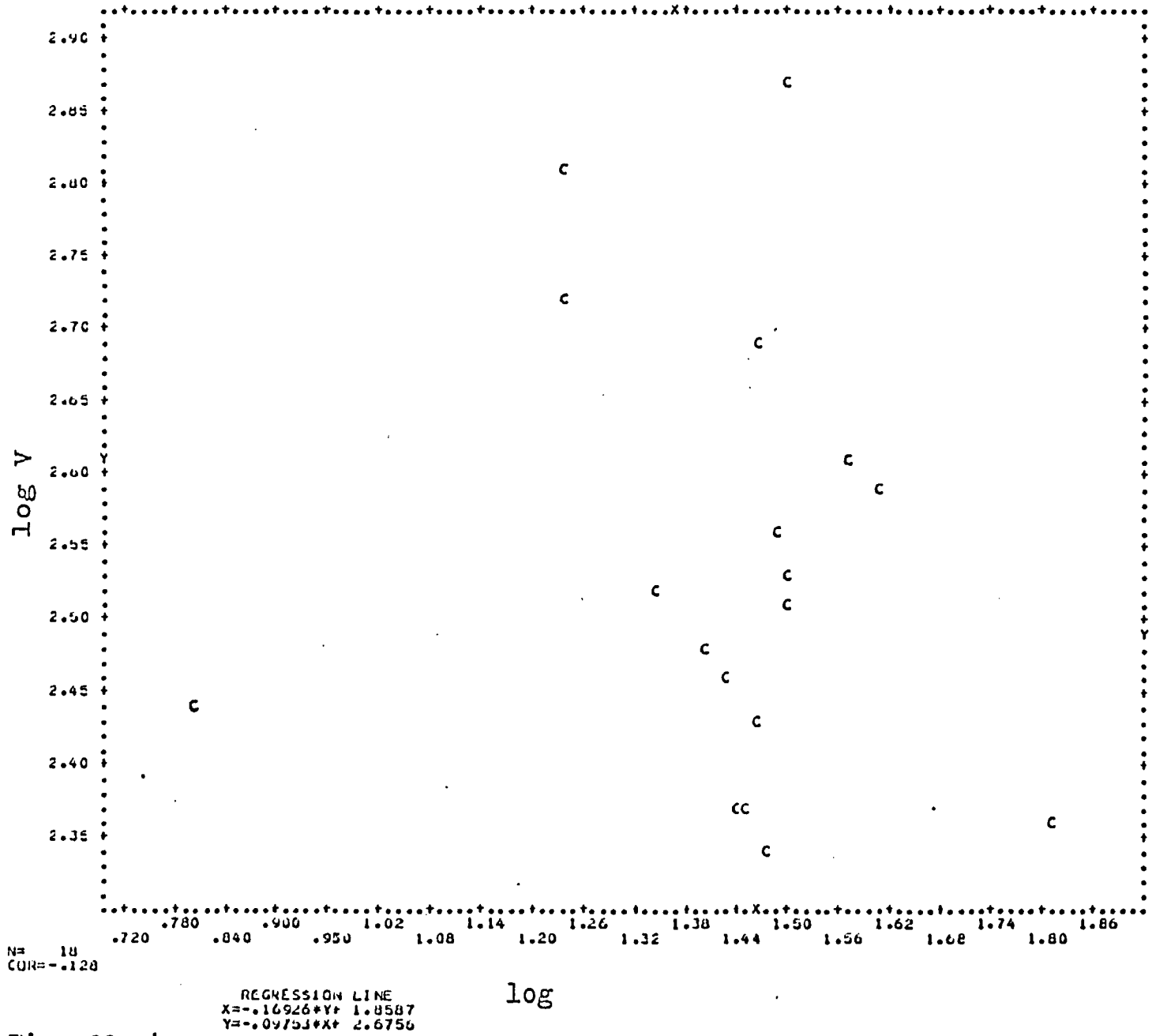

Fig. 28.24.

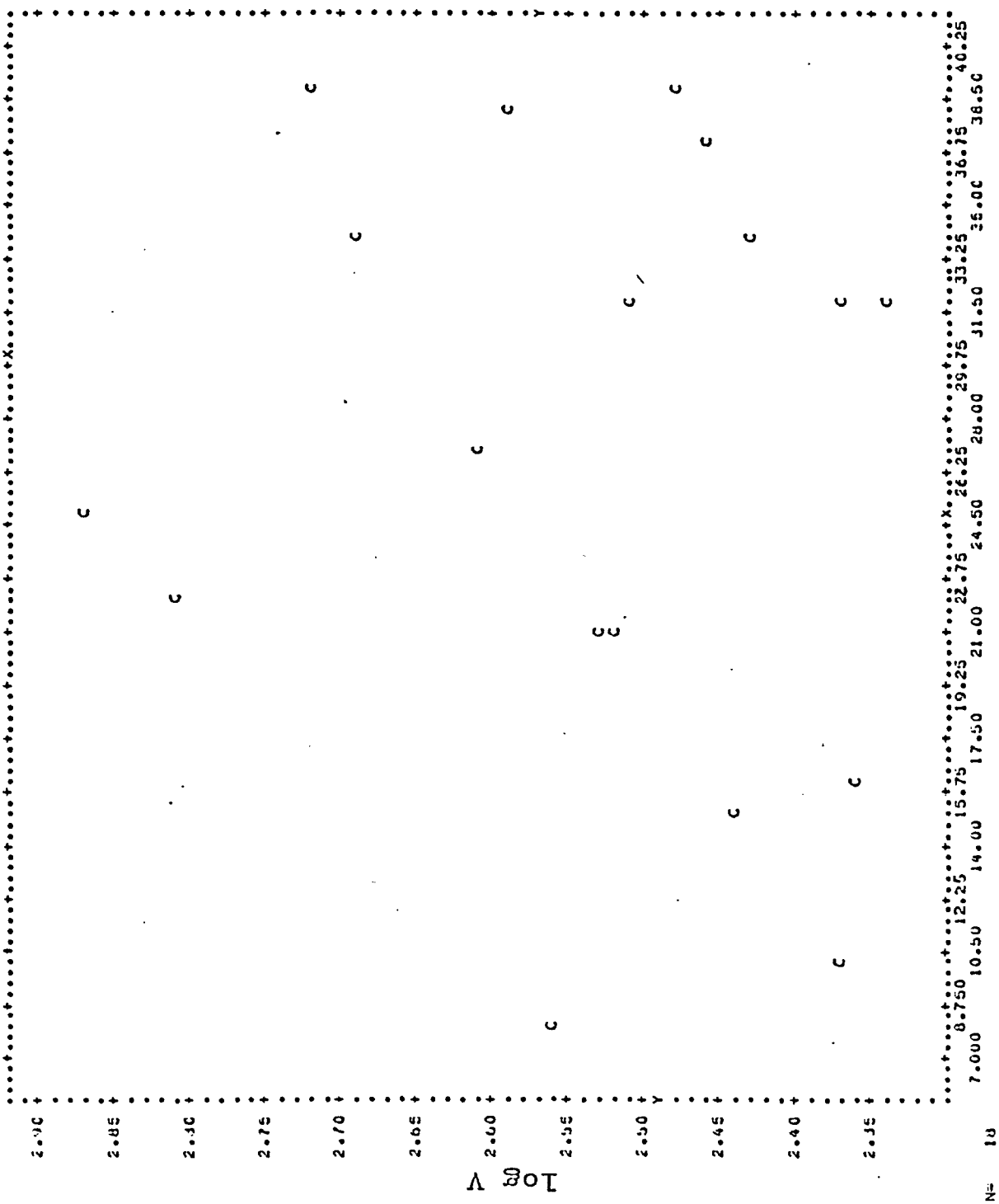

Fig. 28.25.

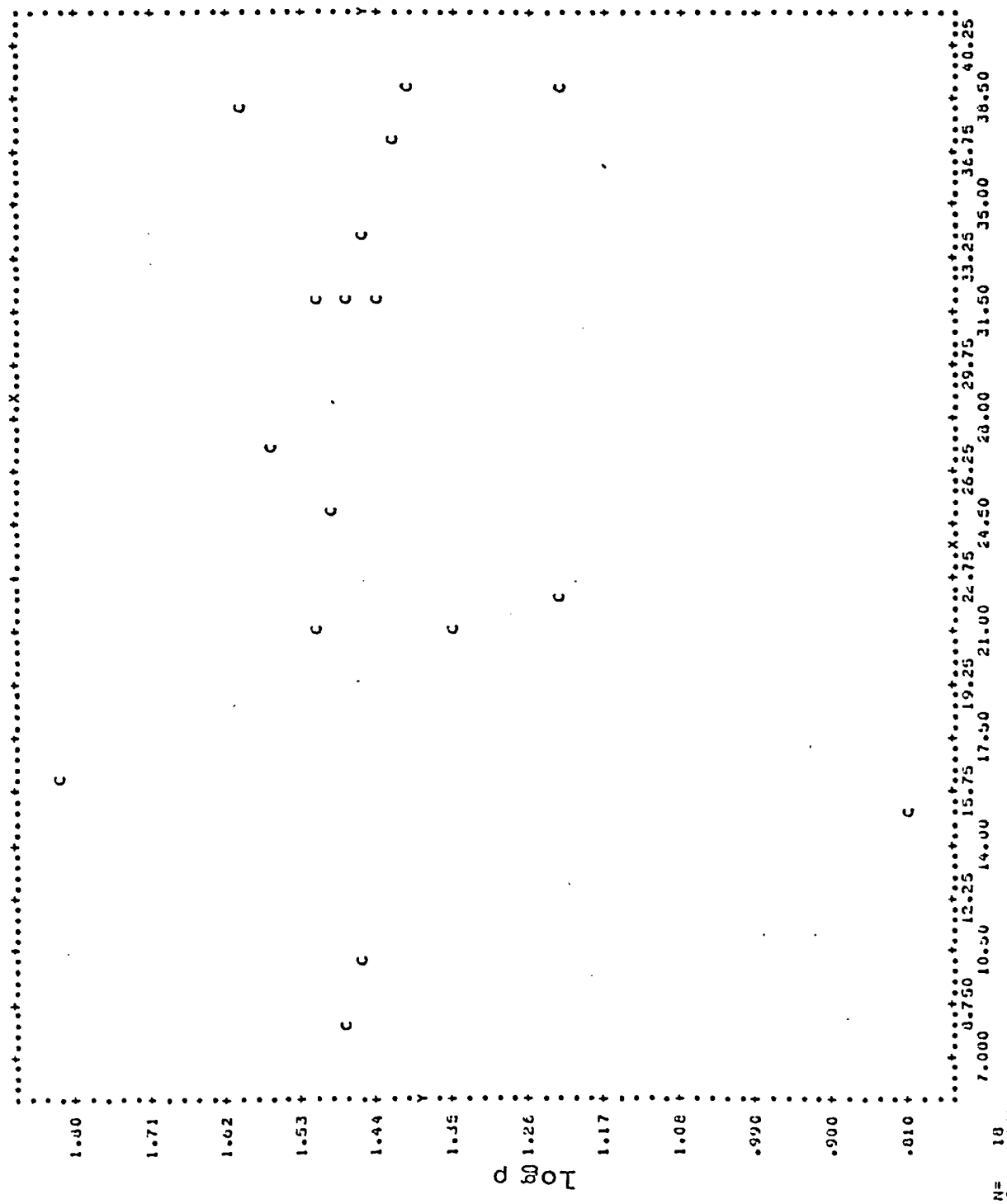

Fig. 28.26.

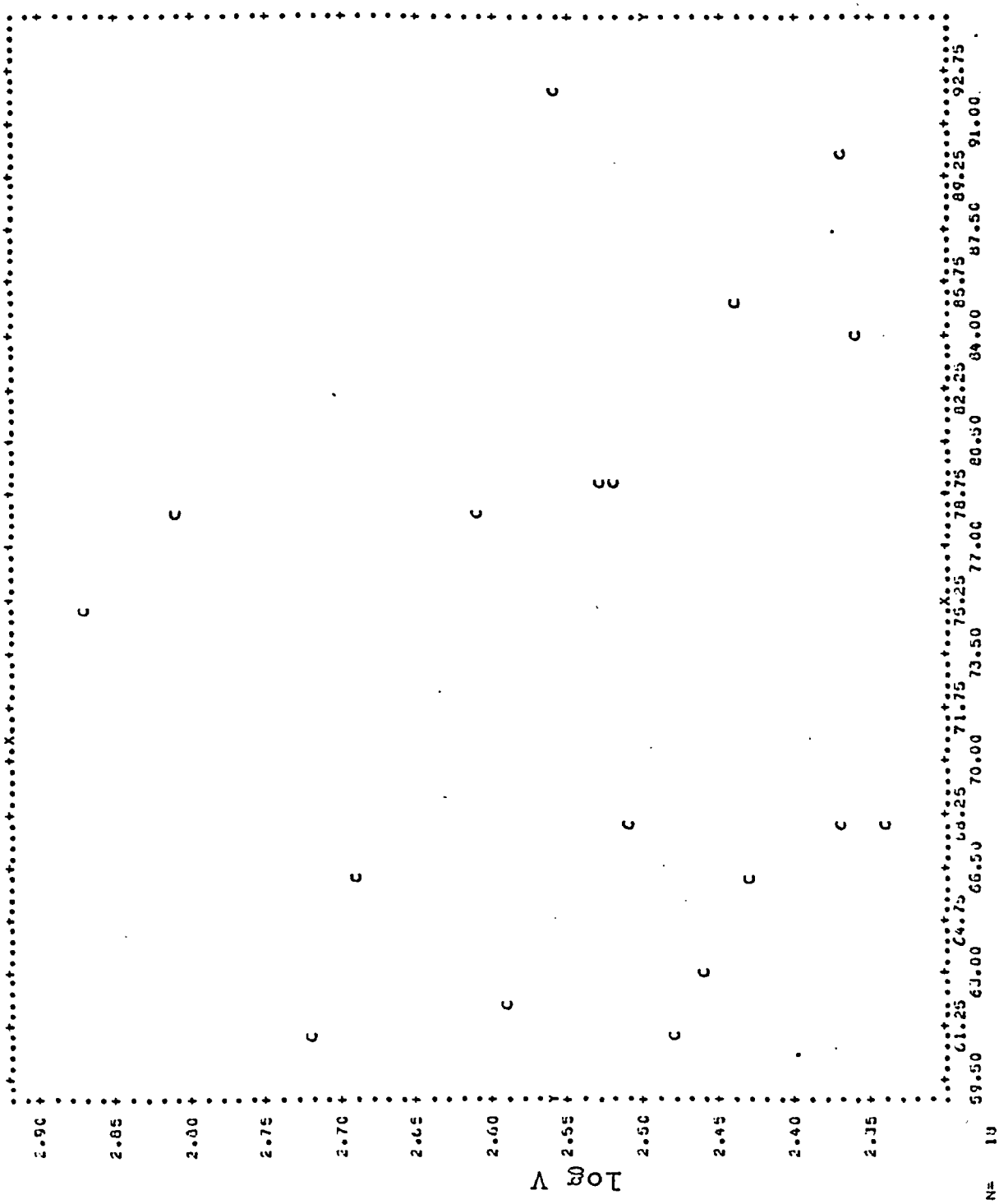

Fig. 28.27.

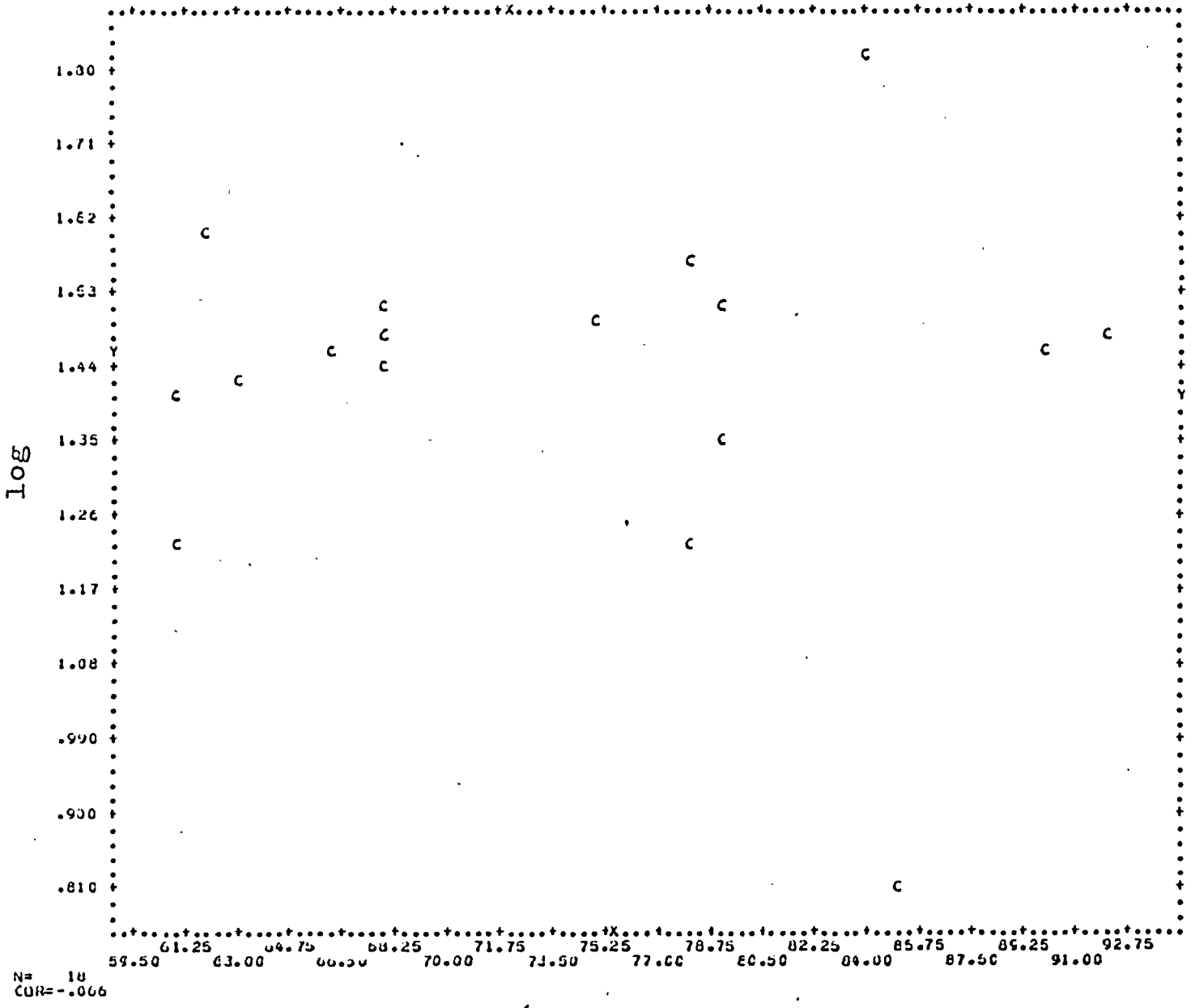

Fig. 28.28.

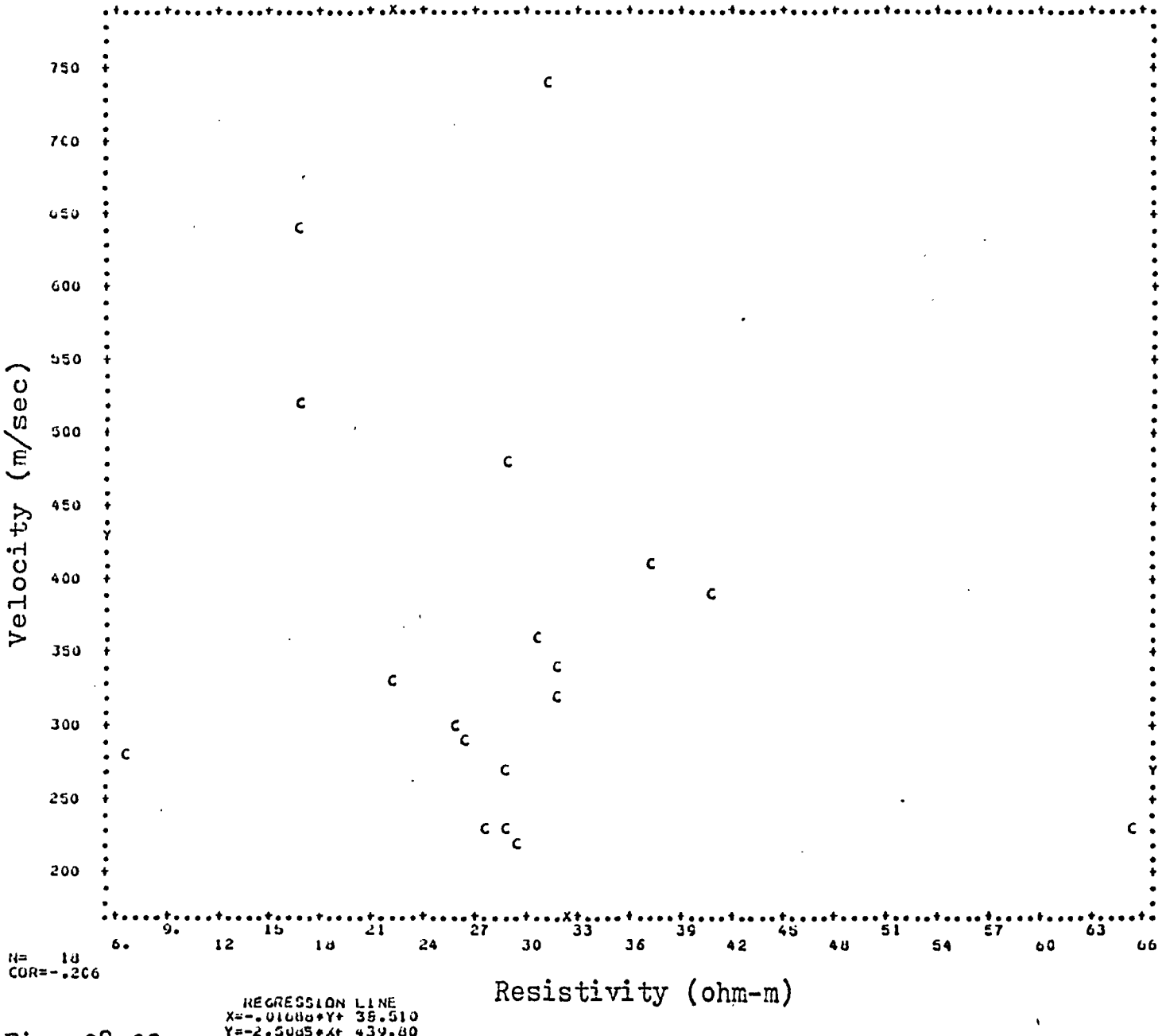

Fig. 28.29.

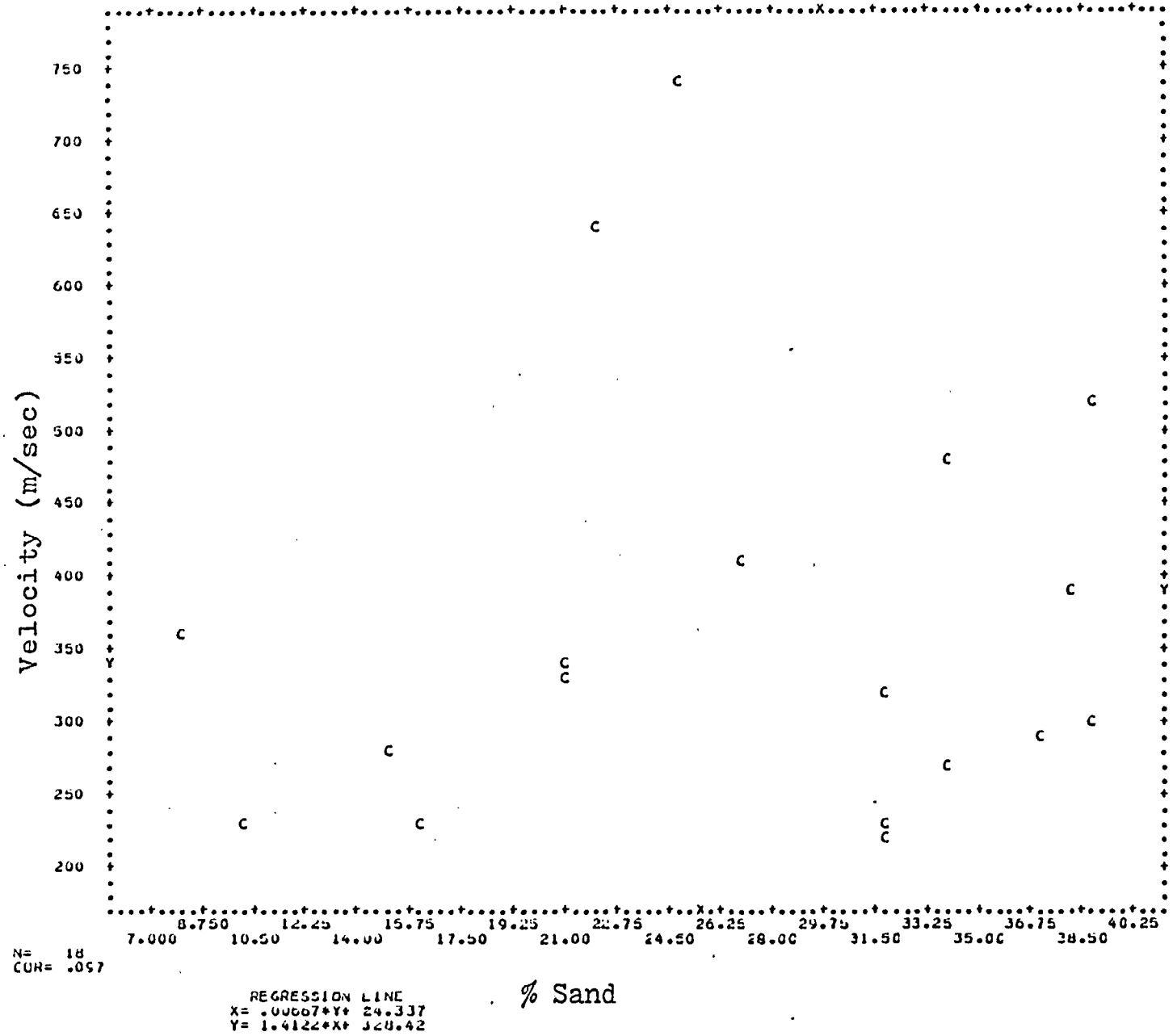

Fig. 28.30.

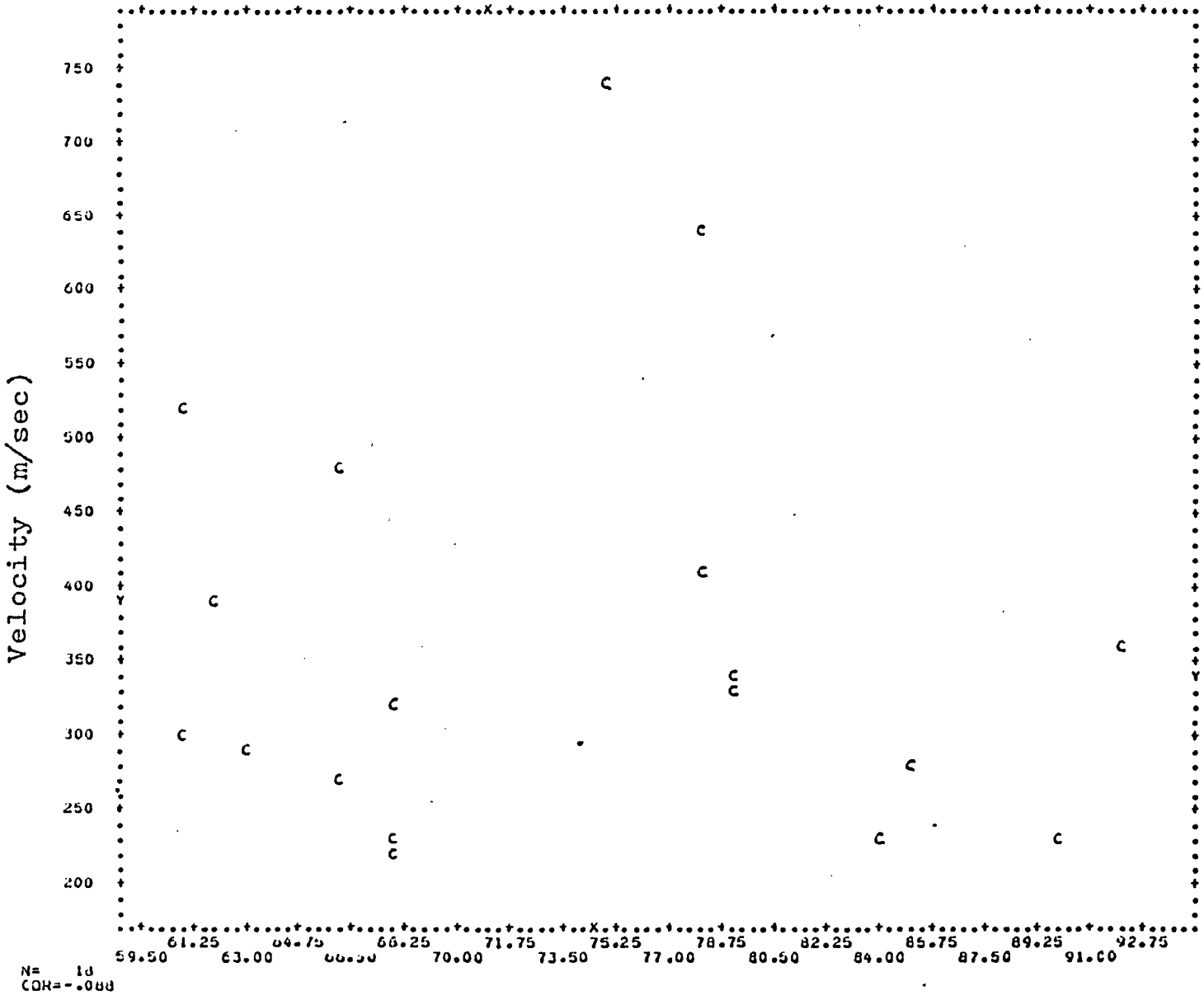

Fig. 28.31.

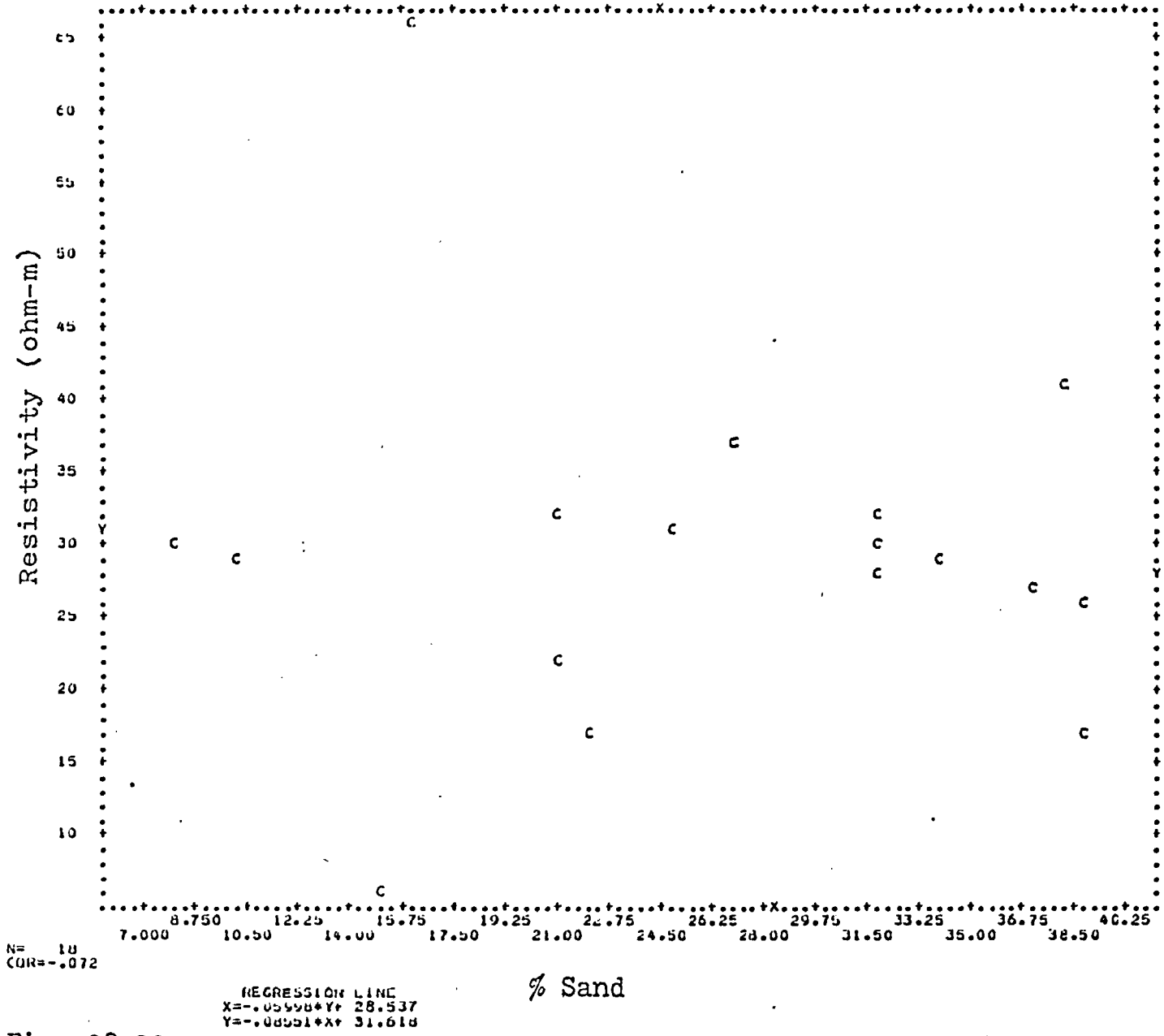

Fig. 28.32.

APPENDIX VI

INSTRUMENTS USED

FS-3 Seismograph

R-50 Resistivity unit

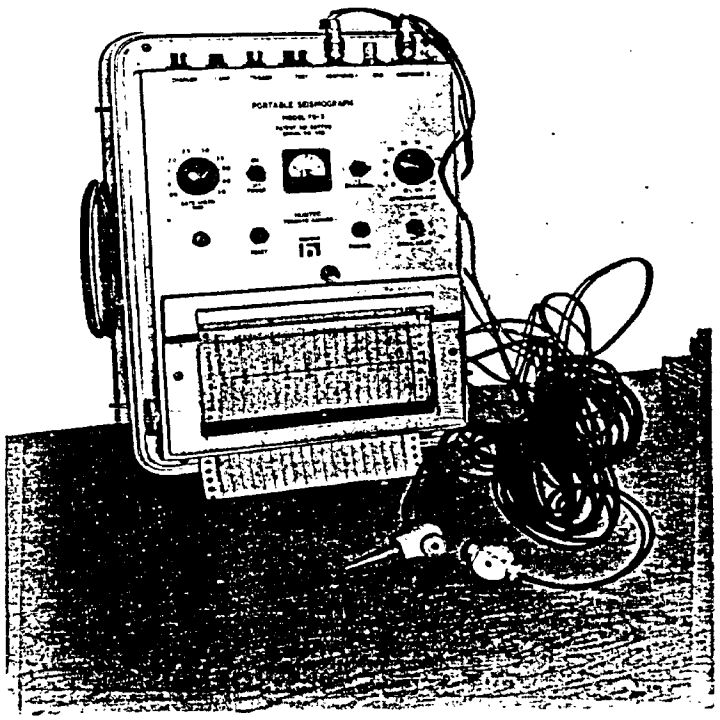

Fig. 29a. FS-3 Seismograph.

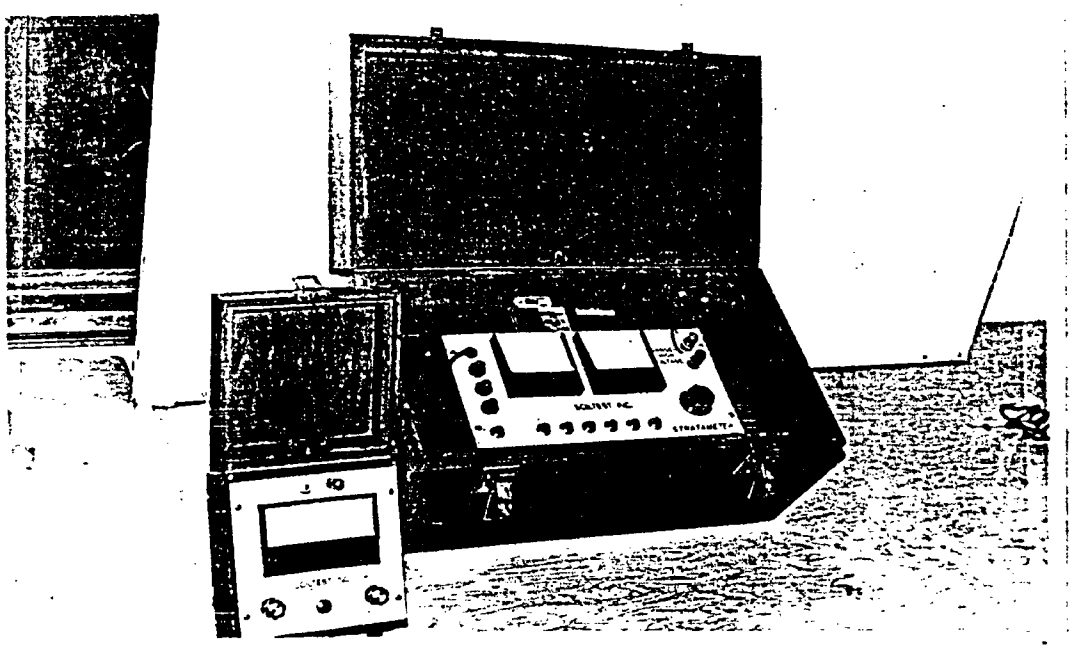

Fig. 29b. R-50 Stratameter Resitivity unit.

VITA AUCTORIS

Born: July 9, 1952, in Thesprotikon, Preveja, Greece.
Son of Mr. Theodoros and Panayota Vergos.

Education:

Secondary School:
High School of Thesprotikon, Greece.
10th High School of Athens, Athens, Greece.

University:
University of Athens, Athens, Greece.
Honour Bachelor of Science in Geology, 1975.

University of Windsor, Windsor, Ontario.
Masters of Science in Geophysics, 1979.

Working experience:

Summers of 1976, 1977, 1978 with Brinex:
Uranium exploration - geophysics.

Presently employed by New Jersey Zinc as geophysicist.

Home Address:

161 Westminster Ave.,
Toronto, Ontario. M6R 1N8
Phone: (416) 531-2117